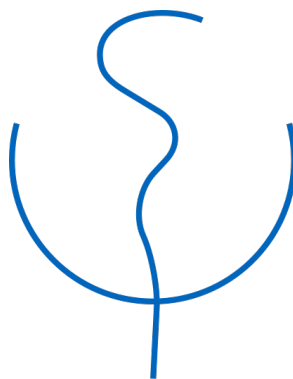




Technische Universität München

**Biophysical and Behavioral
Characterization of
Magnetoreception
in Genetic Model Organisms**

Ahne Myklatun



Fakultät für Medizin

München 2018



Technische Universität München

Fakultät für Medizin

**Biophysical and Behavioral
Characterization of Magnetoreception
in Genetic Model Organisms**

Ahne Myklatun

Vollständiger Abdruck der von der Fakultät für Medizin der Technischen Universität München zur Erlangung des akademischen Grades eines

Doktors der Naturwissenschaften

genehmigten Dissertation.

Vorsitzende: Prof. Dr. Gabriele Multhoff

Prüfende/-r der Dissertation:

1. Prof. Dr. Gil G. Westmeyer
2. Prof. Dr. Wolfgang Wurst
3. Prof. Dr. Friedrich C. Simmel

Die Dissertation wurde am 13.07.2017 bei der Technischen Universität München eingereicht und durch die Fakultät für Medizin am 02.05.2018 angenommen.

Table of contents

List of Figures

1.1	Project overview	6
1.2	The geomagnetic field	8
1.3	Orientation of birds at different wavelengths	10
1.4	True navigation	11
1.5	Radical pair hypothesis	14
1.6	Magnetite	18
1.7	Crystals in magnetotactic bacteria	19
1.8	Magnetite hypothesis	23
1.9	Magnetite particles observed in animals	26
1.10	Microfluidic magnetic separation principle	36
1.11	Theoretical magnetization curves of ferrofluids	40
2.1	Spontaneous preference assay	43
2.2	Helmholtz coils change direction of GMF	45
2.3	Directional preference of zebrafish in light	47
2.4	Swimming strategy of zebrafish in darkness	49
2.5	Swimming strategy of medaka in darkness	50
2.6	Directional preference of zebrafish in darkness	52
2.7	Directional preference of medaka in darkness	54
2.8	<i>C.elegans</i> do not perform magnetotaxis behavior in darkness	56
2.9	Rotation assay for identification of magnetic cells	58
2.10	Magnetic material observed in fishes	62
2.11	Microfluidic magnetic sorting design	65
2.12	Magnetic field simulations in microfluidic sorting system	67
2.13	Microfluidic magnetic sorting of macrophages	69
2.14	Microfluidic magnetic sorting of bioengineered cells	71
2.15	Microfluidic magnetic sorting of magnetotactic bacteria	73
2.16	Microfluidic magnetic sorting of zebrafish rosette	74
3.1	Overview of animals tested for magnetoreception	77
3.2	Spatial preference in teleost fishes	82
3.3	Rapid decrease of magnetic field gradient	98

List of figures

3.4	Alternative microfluidic designs	104
3.5	Measurement of magnetic moments	106
4.1	Summary of project outcome	111
5.1	Dissociated cells from salmon	122
A.1	Initial trajectories of zebrafish	132
A.2	Latency to first cross of virtual circle	133
B.1	Directional preference of zebrafish in light	136
B.2	Directional preference of zebrafish in darkness	137
B.3	Directional preference of medaka in darkness	138
C.1	Spatial preference of zebrafish (AB)	140
C.2	Spatial preference of medaka	141
D.1	Extracellular magnetic objects isolated from zebrafish	144
D.2	Electron microscopy of magnetic objects from zebrafish	145
D.3	Magnetic objects in salmon	146
E.1	Magnetization of feed samples	150
F.1	Juvenile zebrafish and medaka in an oscillating magnetic field	152

List of Tables

1.1	Magnetoreception studies in genetic model organisms	29
2.1	Candidate magnetoreceptor cells found in zebrafish and medaka . . .	61
2.2	Summary of microfluidic magnetic separation result	63
3.1	Diagnostic tools for mechanisms of magnetoreception	85
3.2	Continuous flow magnetic separation techniques	108
5.1	Fish used in experiments	116
5.2	Dissociation of laboratory fish	119
5.3	Dissociation conditions for adult salmon	121
5.4	Tissue dissociation conditions for salmon	123
5.5	Chemicals used for dissociation	123
5.6	Dissociation buffers	124
5.7	Magnetic nanoparticles	127
D.1	Magnetic material reported in fishes	147

List of tables

Acronyms

AFM Atomic force microscopy

BE Bearing

EDX Energy dispersive x-ray

EM Electron microscopy

FAD Flavin adenine co-factor

FEMM Finite Element Method Magnetics

FMR Ferromagnetic resonance

FPS Frames per second

GMF Geomagnetic field

HBSS Hank's balanced salt solution

HRTEM High resolution transmission electron microscopy

IR Infrared

LED Light emitting diode

LMU Ludwig-Maximilian Universität

MA Magnetic alignment

MD Multi domain

MFM Magnetic force microscopy

MRI Magnetic resonance imaging

MTB Magnetotactic bacteria

Acronyms

NE North East

NIR Near infrared

NW North West

PB Prussian Blue

PBS Phosphate buffered saline

PFA Paraformaldehyde

RCF Relative centrifugal force

RF Radio frequency

RP Radical pair

SD Single domain

SP Spatial preference

SPM Superparamagnetic

SQUID Superconducting quantum interference device

TEM Transmission electron microscopy

TRPV Transient receptor potential vanilloid

WL White light

WT Wild type

Summary

‘Magnetogenetics’ refers to a novel scientific field which aims at controlling molecular and neuronal processes via magnetic fields. In contrast to other techniques employing light or chemicals, magnetic fields travel unperturbed through biological tissues, thus enabling non-invasive manipulations also in deeper regions of the brain. However, it remains challenging to genetically bioengineer eukaryotic cells with magnetic properties that allow for interaction energies to overcome the thermal fluctuations.

On the other hand, some animals, such as migratory birds and fishes, are able to sense the Earth’s magnetic field, so-called magnetoreception. Hence, in the biomimetic approach towards magnetogenetics it would be of great advantage to find magnetosensitive genetic model organisms, such that the neuronal and molecular mechanisms of magnetoreception can be explored. The magnetite hypothesis postulates that the geomagnetic field is sensed through mechanical interaction with biogenic magnetite crystals. Alternatively, the radical pair hypothesis posits that the magnetic field influences chemical reactions, likely taking place in the cryptochromes after photon absorption.

Thus, in the first part of my PhD study, I investigated the response of established genetic model organisms to magnetic field changes in darkness to directly compare the two hypotheses of magnetoreception. Specifically, the two fish models zebrafish and medaka were tested, to assess whether they reoriented their bearing in response to an applied directional shift of the geomagnetic field. Notably, both species turned out to use the magnetic field information in absence of visible light, even after an extended period in darkness, which supports a light-independent magnetoreception pathway.

Next, I investigated whether intracellular magnetic biomineralizations were present

Summary

in the fishes. A more comprehensive understanding of putative magnetite production in a vertebrate system would be valuable for improvement of magnetogenetic techniques. To this aim, I developed a microfluidic magnetic sorting system using ferrofluids to reversibly generate the high magnetic field gradients necessary for enrichment of magnetic cells. I validated its performance with various magnetite loaded eukaryotic cells as well as magnetotactic bacteria.

In parallel, I employed rotating magnetic fields to assess magnetization of single cells from dissociated primary tissue, both from the laboratory fishes and wild salmon. However, I did not identify candidate magnetoreceptor cells in any of the fishes. Although I consistently observed magnetic material, it remains unclear whether this was part of a magnetoreceptor system. Furthermore, it is possible that the employed assay failed to detect cells containing superparamagnetic material, thus leaving open the question whether biogenic magnetite is produced in these vertebrates.

In conclusion, within my PhD work I highlighted the presence of light-independent magnetoreception in two vertebrate genetic model organisms, zebrafish and medaka. Both are optically addressable in their early stages, thus allowing for future interrogation of neural correlates and genetic machinery of magnetoreception. Hence, my PhD work offers the ground for future research aimed at understanding the interaction of magnetic fields with putative magnetically sensitive neurons in nature. Furthermore, similar microfluidic systems will be a useful complement in future searches for magnetite-based magnetoreceptor cells and for biophysical characterization of these and other magnetic cells produced in bioengineering approaches towards magnetogenetics.

Zusammenfassung

Magnetogenetik“ bezeichnet ein neues wissenschaftliches Forschungsfeld, dessen Ziel es ist molekulare und neuronale Prozesse mit Hilfe von magnetischen Feldern zu kontrollieren. Im Gegensatz zu anderen Techniken, die Licht oder aktive chemische Substanzen einsetzen, werden magnetische Felder in biologischem Gewebe nicht abgeschwächt und können somit dazu benutzt werden, um tiefer gelegene Regionen des Gehirnes nicht invasiv zu steuern. Es ist jedoch schwierig, durch genetische Veränderungen eukaryontische Zellen mit magnetischen Eigenschaften zu generieren, deren Interaktionsenergien die der thermischen Energie überschreiten.

Andererseits gibt es Tiere, wie zum Beispiel Zugvögel oder Fische, die eine Magnetorezeption besitzen und dadurch in der Lage sind das Erdmagnetfeld wahrzunehmen. Deshalb wäre es von großem Vorteil, in einem biomimetischen Ansatz der Magnetogenetik, magnetorezeptive Modelorganismen zu finden um neuronale und molekulare Mechanismen der Magnetorezeption zu erforschen. Die Magnetit-Hypothese postuliert, dass das Erdmagnetfeld durch mechanische Interaktionen durch biogene Magnetitkristalle wahrgenommen wird. Alternativ kann das auch durch eine chemische Reaktion stattfinden, in der Radikalpaare, wahrscheinlich im Protein Cryptochrom, nach Photoabsorption gebildet werden.

In dem ersten Teil meiner Doktorarbeit habe ich die Reaktionen von etablierten Modellorganismen auf Magnetfelder in Dunkelheit getestet, um diese beiden Hypothesen direkt miteinander vergleichen zu können. Es wurden die Fische Zebrafisch und Medaka untersucht, um Verhaltensmuster nach einer gerichteten Veränderung des Erdmagnetfeldes zu untersuchen. Beide Arten waren in der Lage Informationen des Magnetfeldes in der Abwesenheit von sichtbarem Licht zu benutzen, selbst nach einer längeren Zeit in Dunkelheit. Dies spricht gegen einen licht-abhängigen Magnetorezeptionspfad.

Zusammenfassung

Weitergehend habe ich untersucht, ob es Hinweise für intrazelluläre magnetische Biomineralisation in den Fischen gibt, da ein Verständnis über eine Magnetitproduktion in Vertebraten von großer Bedeutung für Magnetogenetik wäre. Um dieses Ziel zu erreichen habe ich ein mikrofluidisches magnetisches Sortierungssystem entwickelt, das reversibel mit einem Ferrofluid hohe magnetische Gradienten erzeugt und somit die Anreicherung von magnetischen Zellen ermöglicht. Ich validierte dieses System mit Magnetite-beladenen eukaryontischen Zellen und mit magnetotaktischen Bakterien.

Zusätzlich habe ich mittels rotierenden magnetischen Feldern die Magnetisierung von einzelnen Zellen aus dissoziierten Gewebeproben von Laborfischen und wilden Lachsen untersucht. Es konnten jedoch keine potenziellen magnetorezeptiven Zellen aus den untersuchten Proben identifiziert werden. Obwohl ich regelmäßig magnetisches Material finden könnte, war es nicht möglich eindeutig zu bestimmen, ob dieses Material Teil eines Magnetorezeptor ist. Es ist zudem möglich, dass die angewendete Untersuchungsmethode nicht in der Lage war superparamagnetisches Material zu detektieren. Somit bleibt die Frage offen, ob biogener Magnetit in diesen Vertebraten produziert wird, bzw in welche Zellen es produziert wird.

Zusammenfassend habe ich in meiner Doktorarbeit das Vorhandensein einer lichtunabhängigen Magnetoperzeption in den zwei genetischen Modelorganismen Zebrafisch und Medaka unterlegt. Beide Modelorganismen sind in ihren frühen Entwicklungsphasen optisch zugänglich und somit für zukünftige Untersuchungen von neuronalen Interaktionen und der genetischen Grundlage für Magnetogenetik geeignet. Meine Doktorarbeit bietet deshalb eine Basis für weitergehende Forschungsarbeiten die das Ziel verfolgen die Grundlagen der Interaktion von magnetischen Feldern mit putativ magnetisch erregbaren Neuronen zu verstehen. Vergleichbare Mikrofluidik-Systeme werden nützliche Ergänzungen in der zukünftigen Suche nach magnetitbasierenden Magnetorezeptoren sein und zusätzlich Verwendung in der biophysikalischen Charakterisierung von magnetischen Zellen finden, die durch genetische Veränderungen mit dem Ziel der Magnetogenetik durchgeführt wurden.

Chapter 1

Introduction

1.1 Magnetogenetics

The complex processes taking place in the brain is a fascinating field of research, and a large variety of imaging methods are available for the observation of these. However, in recent years there has been an increasing interest in also controlling neuronal processes in order to understand how neurons function and interact with the outside world. This has led to the rapid development of a variety of tools for interrogation of neural circuits. All of these include different approaches for selective activation upon an external stimulus. Selectivity is usually achieved through genetic expression in neuronal subpopulations of certain markers that can be specifically targeted.

For instance, a neuronal response to chemical compounds could be controlled through selective binding to genetically expressed receptors. However, this offers poor temporal precision due to the slow distribution of molecules in the body. Optogenetics, another technique rapidly emerging over the last decade, overcomes this problem by using ion channels sensitive to light in order to selectively activate neurons (Boyden et al., 2005; Fenno et al., 2011; Deisseroth, 2011). This allows for high spatial and temporal resolution of the stimulus. Although the technique is now well established, optogenetics is limited by the poor penetration of light in biological tissues, and often necessitates invasive techniques for stimulating deep brain regions. As a solution to this problem, magnetogenetics, a method to influence molecular processes non-invasively via magnetic fields and with genetic precision, has emerged

1. Introduction

as an attractive concept.

The advantage of magnetic fields is that they travel through biological tissues almost unperturbed and are therefore ideal to use for non-invasive applications. Apart from their use in magnetic resonance imaging (MRI), magnetic fields could potentially also be used to manipulate cells. However, the challenge of magnetogenetics is to genetically engineer eukaryotic cells such that their magnetic properties allow for interaction energies above the thermal energy (Meister, 2016). If achieved, this would revolutionize many fields in biomedical science. For instance, it would be valuable in the development of a gene reporter for MRI, a technique which enables whole brain imaging. It would further allow magnetically labeled cells to be remotely and non-invasively controlled with magnetic fields in order to induce an activation also in deep lying regions of the brain.

Magnetic control of neuronal signaling?

There are in fact already some reports claiming to have achieved control of neuronal signaling via magnetic fields. In order to achieve such neuronal control, there needs to be a first step of interaction that can be translated into a neuronal signal. One approach is to generate heat through relaxation of magnetic material in an oscillating magnetic field (Rosensweig, 2002). This was demonstrated by Huang et al. (2010), who used genetic targeting of magnetic nanoparticles to cells expressing a heat sensitive ion channel (TRPV), and showed that the particles could be heated in a radio frequency (RF) magnetic field. They further labeled *c.elegans* with the particles and observed behavioral responses consistent with exposure to heat when the worms were placed in the RF field (Huang et al., 2010).

This approach was recently claimed to be made fully genetic by replacing the magnetic nanoparticles with ferritin, an iron storage protein which has antiferromagnetic properties (Makhlouf et al., 1997), and linking it to the TRPV channel. By measuring the level of insulin, which gene expression was regulated by the calcium concentration in the cells, the authors demonstrated that the presence of a RF field could influence the cells. This was shown both *in vitro* and *in vivo* in mice which showed a decrease in the blood glucose upon stimulation with the magnetic fields (Stanley et al., 2015).

It is further discussed if the effect could be due to mechanosensitive properties

of the ion channel, as an aggregation of particles could induce a stress on it (see also section about the magnetite hypothesis 1.2.3). This was speculated by Stanley et al. (2015) following their observation of similar effects of a static magnetic field to what was reported in an RF field (Stanley et al., 2015). The ion channel and ferritin complex has since been optimized by Wheeler et al. (2016) for a mechanosensitive signal transduction. It was shown that a static magnetic field of 50 mT could trigger action potentials in neurons expressing the complex. This was measured by electrophysiology on brain slices and by calcium imaging in zebrafish. Young fish larvae were further shown to have an increase in their coiling behavior (escape response) in a 10 times stronger magnetic field. Finally, through control of the dopamine signaling, mice expressing the complex showed a preference for a presence of a static magnetic field (50-250 mT) (Wheeler et al., 2016).

Although the studies presenting a fully genetic approach look promising at first glance they have been heavily criticized. The magnetic properties of ferritin are not compatible with the force necessary for the effects reported in the papers (Meister, 2016; Anikeeva & Jasanoff, 2016). The interaction energy for the suggested components is several orders of magnitude lower than the thermal energy, even in magnetic fields 1000 greater than that of the Earth. Overcoming the thermal motions can be only achieved by particles with much higher magnetic moment, such as the magnetite nanoparticles used in the early studies (Huang et al., 2010). The fact that ferritin cannot be influenced by even high magnetic fields was pointed out by Kirschvink already in 1981 (Kirschvink & Gould, 1981).

Towards genetically controlled production of magnetic cells

The challenges of magnetogenetics still remains and in order to achieve a fully genetic system that can be controlled by magnetic fields, materials with much higher magnetic moments are necessary. This could potentially be achieved through a bioengineering approach, with systematic manipulation of gene expression in mammalian cells. For instance, alteration of the iron homeostasis such that the net uptake and storage of the ferromagnetic material iron is increased.

Another approach is to learn from naturally occurring biosynthetic superparamagnetic structures. In this biomimetic approach cells which are known to have specific magnetic properties are studied. One well know example is the magneto-

1. Introduction

tactic bacteria which passively align with the Earth's magnetic field due to chains of magnetite crystals (Blakemore, 1975; Frankel et al., 1979; Uebe & Schüler, 2016). However, magnetoreception, the ability to sense magnetic fields, has been demonstrated also in a large range of animals (Wiltschko & Wiltschko, 2005). The biophysical mechanism underlying this sense is still not clear, but the magnetite hypothesis predicts the presence of magnetic material in sensory cells. The hypothesis is based on mechanical forces exerted on a mechanosensitive cell through magnetic particles (see section 1.2.3) (Yorke, 1979; Kirschvink & Gould, 1981; Kirschvink et al., 2001; Winklhofer & Kirschvink, 2010). In fact, there are several reports that claim to have found magnetite in animals with magnetoreception (Kirschvink et al., 1985; Mann et al., 1988; Fleissner et al., 2003; Eder et al., 2012), although doubt has been cast over some of these findings (Treiber et al., 2012; Edelman et al., 2015).

In order to gain a deeper understanding of the biophysical and molecular mechanisms of magnetoreception, it is promising to work with genetic model organisms. These are animals for which genetic tools are available, such that candidate key genes can be studied. Ideally they are also optically addressable, allowing for investigation of neural correlates through non-invasive imaging techniques. There are some lines of evidence for magnetosensitivity in invertebrate animal models (Gegear et al., 2008; Vidal-Gadea et al., 2015), while reports of magnetoreception in vertebrate models are scarce.

Magnetoreception has been reported in the genetic model organism zebrafish, however no indication of the sensing mechanisms was included (Shcherbakov et al., 2005; Takebe et al., 2012). For medaka fish, another vertebrate genetic model organism (Wittbrodt et al., 2002), there are only indications for sensitivity to magnetic fields (Lee & Yang, 2014). Identification of vertebrate genetic model organisms that exhibit magnetoreception, would allow for studies of these to understand the mechanisms of how the geomagnetic field interacts with neurons in nature. Furthermore, if these genetic model organisms have magnetic biomineralizations, a more comprehensive understanding of the molecular production of magnetic material in a vertebrate system would be within reach.

Aims of my work

Thus, I aimed to develop some of the tools necessary for the biophysical characterization of cells potentially employable in magnetogenetics, and further lay the foundation for future research aiming to understand the interaction of magnetic fields with magnetically sensitive neurons in nature. To this end I investigated zebrafish and medaka, as well as the nematode worm *C. elegans*. Specifically, I aimed to test the magnetite hypothesis in these genetic model organisms through search for candidate magnetite-based magnetoreceptor cells. Moreover, before engaging in characterization of the cells, I validated and further explored behavioral evidence for magnetoreception in the fishes, in collaboration with Dr. Stephan Eder, Dr. Denis Shcherbakov and Dr. Antonella Lauri. In parallel I developed a microfluidic magnetic sorting system for contamination-free enrichment of magnetic cells, crucial for their downstream biophysical and chemical analysis. Thus the aims of my work were as follows:

1. Behavioral characterization of responses to magnetic field changes in genetic model organisms
2. Identify putative candidate magnetoreceptor cells
3. Develop a microfluidic magnetic sorting system for isolation and characterization of cells with intrinsic magnetic properties

1. Introduction

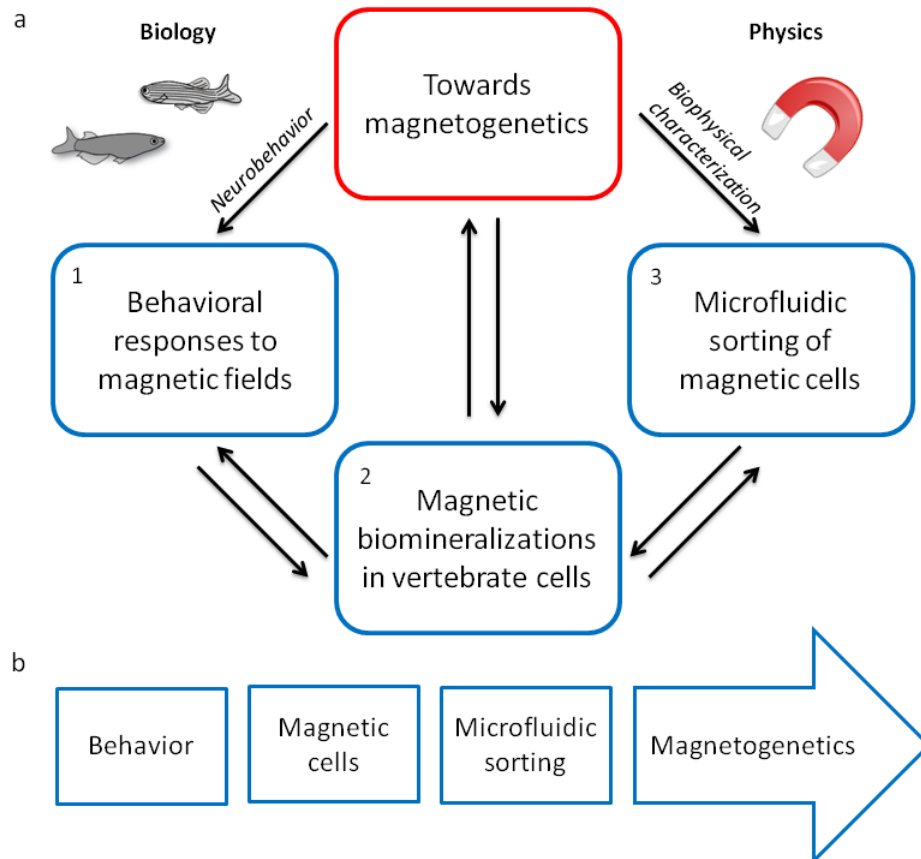


Figure 1.1: Overview of the different parts of my PhD project and how they are linked to the longterm goal of achieving magnetogenetics (a) and the workflow (b).

1.2 Magnetoreception

1.2.1 The magnetic sense

One of the remaining mysteries in nature is how birds can navigate during their seasonal migration or how salmon, after spending years in the ocean return to their native river. While we generally rely on a map and a compass to achieve such tasks, animals use geographical landmarks in combination with sun or celestial maps (Gould, 2004). However, their ability to find their way even without a clear view of such landmarks indicates the presence of an additional compass sense. The first experimental evidences for animals sensing the Earth's magnetic field, so-called magnetoreception, raised about 50 years ago, a relatively short period in comparison to the history of biosciences. Since then there has been a growing body of evidence that a large variety of animals can in fact sense the magnetic field of the Earth and use its information during long or short distance migrations as well as for choice of nest building position (Wiltschko & Wiltschko, 2005).

The Earth's magnetic field

The origin of the Earth's magnetic field arises from its viscous iron rich outer core which is in constant motion due to heat convection and the rotation of the Earth. This geomagnetic field (GMF) is similar to that of a dipole magnet with field lines going from south to north (Figure 1.2a). The magnetic north pole is tilted about 10° compared to the rotational axis of the Earth, a feature known as declination. The GMF varies systematically over the surface of the Earth and thus provides a reliable frame of reference during navigation. There are three parameters of the field that could potentially be used by animals for navigation purposes; polarity, inclination and intensity. The polarity, or direction, of the field lines is the most intuitive, as this is what we see using our mechanical compass. The inclination of the geomagnetic field, also known as the dip angle, is the angle between the Earth's surface and the magnetic field vector which varies between -90° at the south pole and 90° at the north pole. At the magnetic equator the field lines run parallel with the surface and the inclination is 0° . The magnetic field further varies in intensity across the surface, between $\sim 25\text{-}65 \mu\text{T}$, being strongest at the poles and weaker around equator.

1. Introduction

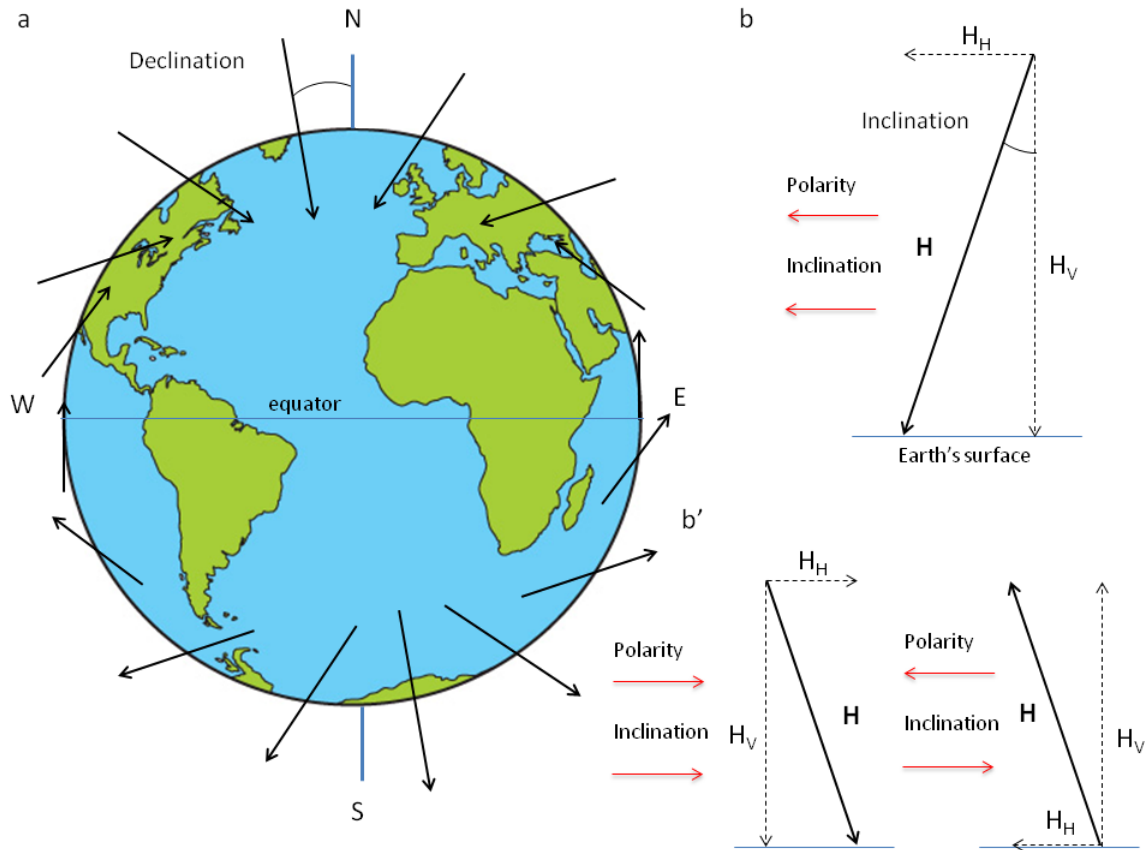


Figure 1.2: a) The geomagnetic field (black arrows) changes across the surface of the Earth, in polarity (arrowhead), intensity (vector length) and inclination (dip angle). The declination is given as the tilt angle between the rotational axis and the magnetic pole. b) Inclination is the dip angle between the magnetic field lines and the surface of the Earth. The magnetic field lines (\mathbf{H}) can be decomposed in a horizontal (H_H) and a vertical (H_V) component. Red arrows show the direction in the case of a polarity and an inclination compass. b') When the horizontal component is inverted an inversion of the direction of the two compasses is also expected. If the vertical component is inverted, the polarity is changed, but not the inclination, thus the compasses point in opposite directions. This is used as a diagnostic test for the presence of an inclination compass.

The animal compass is sensitive to polarity or inclination

Birds were early shown to possess a compass quite different from our mechanical compass; already in 1972 the magnetic information perceived by European robins was assessed (Wiltschko & Wiltschko, 1972). The birds first showed appropriate seasonal orientation in the normal GMF. As expected, when the horizontal component of the field was shifted by 180° they changed their orientation accordingly. Interestingly, when the vertical component was inverted, not changing the polarity of the field (Figure 1.2b'), the birds changed their direction (Wiltschko & Wiltschko, 1972). Thus, the robins were shown to have an inclination compass, sensitive to the angle between the GMF field lines and the surface of the Earth. Still today an inversion of the vertical component is used to verify the presence of an inclination compass, which has been demonstrated in all bird species tested (Wiltschko & Wiltschko, 1996) as well as in other animals (Phillips, 1986; Light et al., 1993).

Such an inclination compass is thought to work in combination with the vestibular system which senses the gravity. In this case the animals would be able to identify the smallest angle between the field lines and the gravity vector and thus know the direction towards the pole (Figure 1.2b', red arrows). The inclination compass is axial in its nature, meaning that only the axis of the field lines is sensed. This becomes evident when both the vertical and horizontal components are inverted and the animals again change their orientation back to the original direction (Wiltschko & Wiltschko, 1972). Thus, the two hemispheres appears identical, with decreasing inclination towards equator. In fact, animals are shown to be disoriented around equator where the inclination is 0° (Wiltschko & Wiltschko, 1972; Light et al., 1993; Schwarze et al., 2016a).

Although many animals are demonstrated to possess an inclination compass, others are insensitive to the inversion of the vertical component of the GMF (Quinn et al., 1981; Lohmann et al., 1995; Marhold et al., 1997; Wang et al., 2007). These animals respond only to a shift of the horizontal component, a behavior consistent with a polarity compass. This is a strong indication that there might be several mechanisms at play in magnetoreception (Phillips, 1986).

1. Introduction

Magnetoreception depends on light in a complex manner

Another interesting characteristic of the animal magnetic compass is its functional dependence on light. Although some animals are able to orient without trouble in darkness (Quinn et al., 1981; Light et al., 1993; Marhold et al., 1997), the magnetic sense of birds and amphibians has been shown to be dependent on light in a complex manner. In most cases the natural response to the geomagnetic field is evident only in the presence of light with certain wavelengths, usually in the blue-green range. This was first characterized in 1992 by Phillips and Borland, who observed that red-spotted newts shifted their directional preference under longer wavelengths (Phillips & Borland, 1992a). Complete loss of orientation was later observed in the absence of visible light (Phillips & Borland, 1992b).

Loss of the magnetic compass function was also observed in birds under red light illumination (Wiltschko et al., 1993). However, in other cases the light-dependency is not so straight forward. For instance, European robins are influenced by both the wavelength and the intensity of light available, navigating better under dim light conditions (Wiltschko & Wiltschko, 2001; Wiltschko et al., 2007a)(Figure 1.3). These birds further seem to regain their ability to navigate at longer wavelengths after being adapted to red light (Wiltschko et al., 2004). Conversely, robins were shown to be disoriented under green light after having been exposed to this light for one hour, although the birds usually navigate perfectly at this wavelength (Wiltschko et al., 2014). Thus, there are still open questions regarding the optimal lighting conditions for magnetoreception.

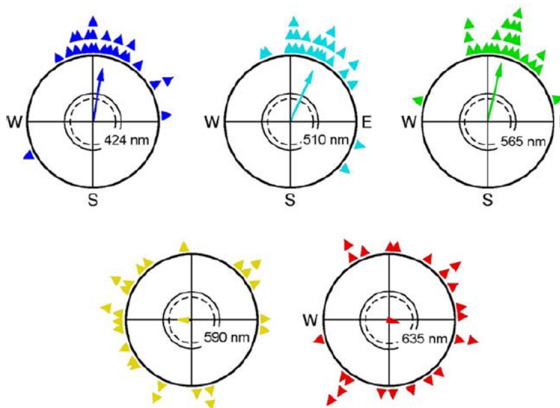


Figure 1.3: Orientation of European robins under different wavelengths. The birds are disoriented at higher wavelengths, a behavior observed also in other animals. From Wiltschko & Wiltschko (2005).

Animals with a magnetic map can perform true navigation

It is clear from the growing body of evidence that many animals possess a magnetic compass, although varied and complex in its nature. This compass is often seen in use, for instance, when birds perform their seasonal migrations. However in this case the birds know their seasonally appropriate direction and will simply need to follow their internal compass. In other cases the presence of an additional internal magnetic map has been demonstrated.

This was first shown in 2003 by Boles and Lohmann (Boles & Lohmann, 2003). They captured spiny lobsters, transported them to locations several kilometers away and released the ani-

mals. When the release site was West of the capture site the lobsters oriented towards East, and when released North-East of the capture site they navigated towards South-West. Further, to confirm that the lobsters were relying on the magnetic information during this task, the scientists then captured animals and exposed them to artificial magnetic fields corresponding to that of a location North or South of the site. Again, as seen in figure 1.4, the lobsters were significantly oriented in the direction that would take them home (Boles & Lohmann, 2003). Similar responses to virtual replacement has recently also been observed in birds (Kishkinev et al., 2015).

These are examples of what is known as true navigation; the ability to first determine a position and then select the right bearing towards a goal. This would require not only a compass, but also an internal map. These could potentially function separately through two different mechanisms, thus one not affecting the other, as demonstrated for instance in birds (Beason & Semm, 1996).

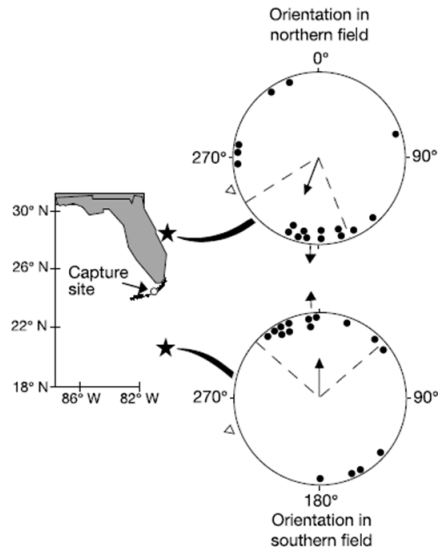


Figure 1.4: True navigation in spiny lobsters depend on the magnetic field information. From Boles & Lohmann (2003).

1. Introduction

Biophysical mechanisms of magnetoreception

The fact that some animals can sense the GMF is now proved beyond doubt. However, the underlying biophysical mechanisms still remains a mystery. There are currently two main hypothesis for how magnetoreception is achieved; through a chemical signal transduction in the radical pair hypothesis or through a mechanical mechanism in the magnetite hypothesis. These are introduced in detail below.

1.2.2 The radical pair hypothesis

Radical pairs are influenced by magnetic fields

In the radical pair (RP) hypothesis (Hore & Mouritsen, 2016), first suggested by Schulten et al. in 1978, the GMF is sensed through a magnetically sensitive chemical reaction. Specifically, it was suggested that the magnetic field could influence the spin state of a radical pair and thereby alter the ratio of reaction products (Schulten et al., 1978). A radical pair consists of two molecules (A and B, Figure 1.5a) that are radicals created by the same process. Each of the unpaired electrons have a spin angular momentum which is not canceled and thus the molecules are magnetic. The spin state of the radical pair depends on the relative alignment of the correlated unpaired electron spins, which can be either parallel or antiparallel, resulting in the triplet or the singlet state, respectively. Due to conservation of spin the radical pair will have the initial spin state equal to that of the molecules from which it was created; singlet state in the case of electron transfer.

Once the radical pair has been formed, the spin state will oscillate, known as singlet-triplet interconversion. The frequencies of these oscillations are determined by the strength of the locally effective magnetic field. The strongest interaction is due to the magnetic moment of nearby atomic nuclei, so-called hyperfine interaction. These leads to oscillations in the range of several megahertz. The Zeeman interaction between an isolated electron spin and a magnetic field causes an oscillation of the electron magnetic moment at the Larmor frequency (dependent on the field strength, 1.4 MHz at $50 \mu\text{T}$). Thus, the much weaker GMF contributes to the interconversion at a slower time scale (~ 700 ns), given that the life time of the radical pair is long enough. Furthermore, too short spin relaxation time of the radical pair would lead to loss of coherence of the two electron spins before they can be influenced by the

GMF (Hore & Mouritsen, 2016).

Due to anisotropy of the hyperfine interaction the effect of the GMF depends also on its direction relative to the radical pair. Thus, the ratio of molecules in the singlet and triplet state depends on both the intensity and axis of the GMF. After formation the RP molecules can further react in two ways; either through electron back transfer to the original molecules, A and B, or in a reaction to form a product C. The latter is possible for both the singlet and the triplet state, assumed at the same rate constant, whereas the reverse reaction can only occur from the singlet state due to spin conservation (Figure 1.5a). If the rate constants of the two reactions are similar the final yield of the reaction product C is dependent on the amount of radical pairs in the triplet state, thus forming the basis for a chemical compass (Hore & Mouritsen, 2016).

In 2000 Ritz et al. showed that magnetic fields as weak as the GMF theoretically could influence the interconversion between singlet and triplet states of a radical pair and thereby change the yields of singlet and triplet reaction products (Ritz et al., 2000). They further showed that for a given intensity of the magnetic field, the angle between the axis of the RP and the field vector influenced the triplet yield. This would result in an inclination compass, indistinguishable from the one which had been observed in birds (Wiltschko & Wiltschko, 1972).

Despite the interaction energy of the GMF with a single molecule is much smaller than the thermal energy under physiological conditions, small contributions can make an impact on a system which is far away from its equilibrium, which is the case for a radical pair. Furthermore, the signaling is likely to occur through a cascade where the first step is a conformational change of a protein. An amplification of the signal is possible in a series of subsequent chemical reactions. If the final step of the cascade is a conformational change in an ion channel in a neuron, leading to an influx of ions and thus neuronal signaling, for instance by producing a graded receptor potential or by triggering an action potential.

1. Introduction

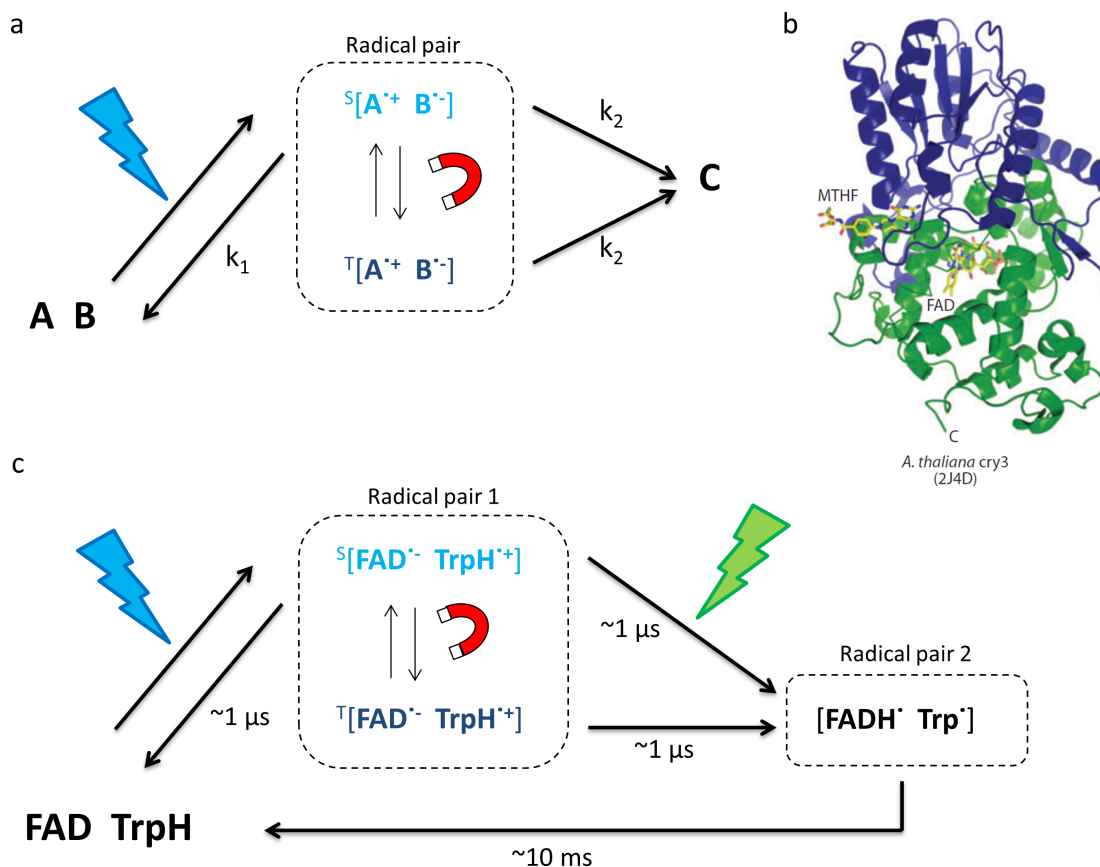


Figure 1.5: Radical pair hypothesis a) A radical pair reaction scheme, where absorption of blue light generates a radical pair [A B] in the singlet state (S). Magnetic fields influence the singlet-triplet interconversion. Both singlet (S) and triplet (T) state of the radical pair react to form product C with similar rate constants (k_2). The reverse reaction (k_1) is only possible from the singlet state. The final yield of C thus depends on the magnetic field present. b) The structure of a plant cryptochrome, from Chaves et al. (2011). c) Reaction scheme for the cryptochrome redox cycle. Radical pair 1 has spin-correlation on a time scale of $\sim 1 \mu s$, during which it can act as the magnetosensitive reaction. This can form a second radical pair, representing the reaction product, after absorption of photons with longer wavelengths.

Cryptochromes form radical pairs after photon absorption

The most likely candidate molecule for radical pair based magnetoreception is the protein cryptochrome, first suggested by Ritz et al. (2000). This is the only photoreceptor in vertebrates known to form a RP after photon absorption Chaves et al. (2011) (Figure 1.5b). Specifically, after absorbing blue light the chromophore flavin adenine co-factor (FAD) is reduced through electron transfer from a tryptophan residue, leading to the formation of the radical pair $[\text{FAD}^- \text{TrpH}^+]$.

The singlet-triplet interconversion of this radical pair can be influenced by an external magnetic field, such as the GMF. The molecules will return to the original molecules through a direct electron back transfer from the singlet state or through formation of a second radical pair (corresponding to reaction product C). Formation of the second radical pair is also dependent on light absorption of longer wavelength photons. The final electron back transfer is photon-independent (Figure 1.5c).

Evidence for the radical pair hypothesis

A mechanism involving a radical pair formed after photon absorption in the cryptochromes is consistent with reports on light-dependent magnetoreception. Most describe the necessity of short wavelength light for the compass to function (Wiltschko & Wiltschko, 2001) (Figure 1.3). Altered behavioral responses (Phillips & Borland, 1992a; Phillips & Sayeed, 1993; Muheim et al., 2002) or even complete loss of the sense have been observed for longer wavelengths (Phillips & Borland, 1992b; Wiltschko et al., 1993). Furthermore, cryptochromes are found in the retina of birds, and markers for neuronal activity (c-fos and ZENK) have been found to be co-localized with CRY1 expression in the retina of garden warblers after migratory behavior (Mouritsen et al., 2004)

However, the first direct evidence for the involvement of cryptochromes in magnetosensitivity was shown in a study comparing fruit flies (*Drosophila melanogaster*) of wildtype (WT) strains to flies where the gene encoding cryptochrome was knocked out (Gegear et al., 2008). The mutated flies, in contrast to the WT, did not show a naïve preference or avoidance of a magnetic field or the ability to learn to respond to the magnetic field. This behavior was similar to the lack of response observed in the absence of short wavelength light (<420 nm). Although magnetic field effects

1. Introduction

have been shown on circadian rhythm, which is regulated through cryptochromes (Yoshii et al., 2009), an intact circadian clock was not necessary for the flies to sense the magnetic field (Gegear et al., 2008). The magnetosensitivity was later shown to be rescued by using cryptochromes from other insect species (Gegear et al., 2010) or even humans (Foley et al., 2011). Furthermore, cryptochromes have been shown to play a role in the flies' negative geotaxis in static electromagnetic fields (Fedele et al., 2014).

Similarly, a recent study showed the involvement of cryptochromes in cockroaches' response to alterations of the GMF (Bazalova et al., 2016). The insects showed an increased restlessness when the horizontal component of the magnetic field was oscillating at low frequencies, however only in animals with intact cryptochromes. Thus, these seemed to mediate the magnetic field dependent stress response.

The disorientation observed for animals in radio frequency (RF) magnetic fields is considered a strong evidence for the radical pair hypothesis (Ritz et al., 2004; Wiltschko et al., 2015; Nießner & Winklhofer, 2017). Such a magnetic field oscillations are expected to resonate with the precession of electron spins in the RPs. This in turn should affect the singlet-triplet interconversion and consequently the magnetic field sensory information. Thus, an RF magnetic field has been used as a diagnostic tool to distinguish a mechanism involving a radical pair from one based on magnetic particles.

1.2.3 The magnetite hypothesis

Magnetite particles can interact with the geomagnetic field

Another well established hypothesis for magnetoreception is postulated in the magnetite hypothesis, which could provide basis for the first step in a magnetomechanical signal transduction pathway. The mechanical interaction of magnetic particles with the GMF would enable a sensor independent of the light conditions. The most probable material for this purpose is magnetite, an iron oxide crystal (Fe_3O_4). With its inverse spinel structure and ferrimagnetic properties, magnetite is one of the most strongly magnetic minerals that occurs naturally (Figure 1.6a). In fact, due to its tendency to align in the North-South axis of the Earth, it was used in the first

man-made compasses.

As with all ferro- and ferrimagnetic materials the properties of magnetite depend on the size of the crystal, which in turn influence the magnetic domain structure (Figure 1.6c). A magnetic domain is a volume of the crystal that has a homogeneous magnetization, referred to as spontaneous magnetization. Single domain (SD) magnetite is a crystal in the size range 30-100 nm, depending on the aspect ratio and shape of the crystal. It is the most stable form of a magnet as it is small enough to develop only one magnetic domain, thus maximizing the magnetic moment of the crystal. In contrast, a larger multi-domain (MD) magnet will consist of several magnetic domains of various sizes and different directions of their magnetic moments.

If the magnetite particles are smaller than about 30 nm, they will be in the superparamagnetic (SPM) regime. In this case the crystal still consists of one domain like for a SD, however the magnetic moments are not strictly fixed in the crystal and will randomly flip their direction (Neel relaxation). Thus, in the absence of an external magnetic field the net magnetic moment of a population of particles is zero. However, SPM crystals have a high magnetic susceptibility and in the presence of an external magnetic field the magnetic moments will align with the magnetic field resulting in a strong response (see also section 1.3.2 on Ferrofluids).

1. Introduction

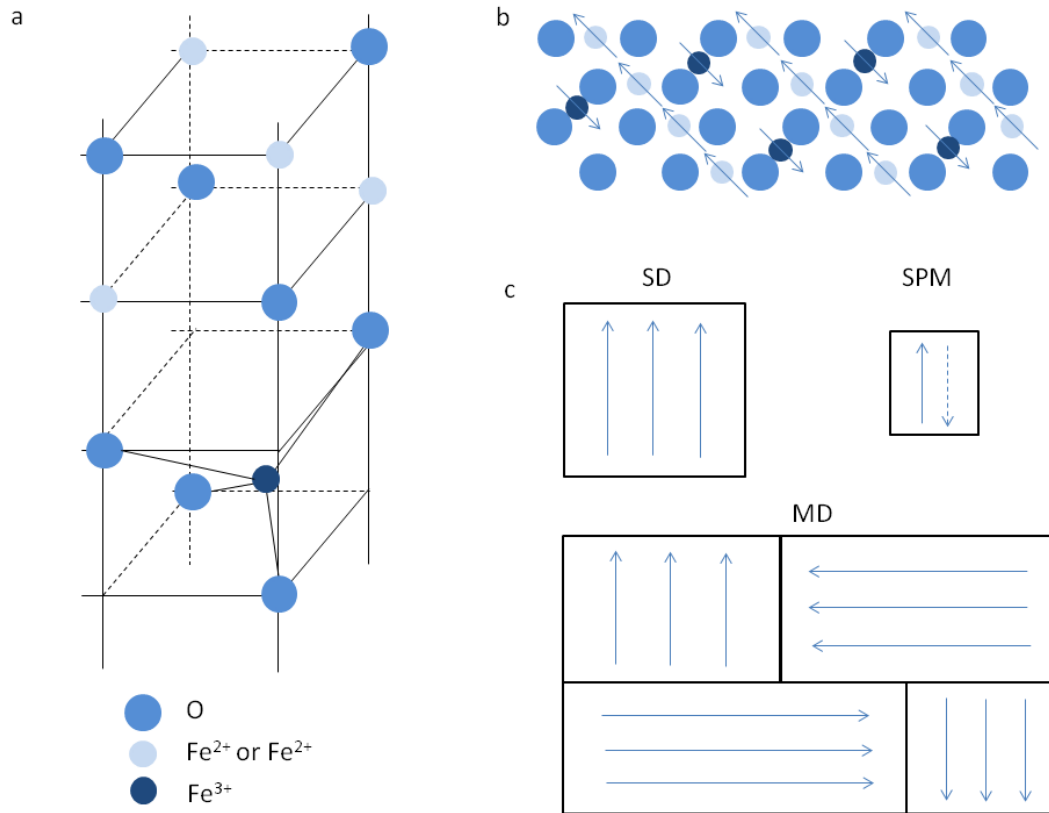


Figure 1.6: a) The inverse spinel structure of a magnetite crystal. Octahedral sites (light blue) can be occupied by Fe²⁺ or Fe²⁺, while in tetrahedral sites there will only be Fe³⁺. b) The difference between the two magnetic sublattices gives the ferrimagnetic crystal its net magnetic properties, in the case of magnetite the iron ions in the octahedral sites. c) A single domain (SD) crystal will have all the spins in the crystal aligned in one direction. The same is true for a superparamagnetic (SPM) crystal, but the orientation of the magnetization will be unstable. A multi domain (MD) crystal will consist of several domains of different shapes and sizes, all with their magnetization pointing in random directions.

Magnetotactic bacteria passively align with the GMF lines

Around the same time as it was starting to emerge that certain animals can sense magnetic fields, and scientists were wondering about the underlying mechanisms, a small organism acting as a compass needle was discovered. Magnetotactic bacteria (MTB) were first described by Blakemore in 1975. He observed that these bacteria contain chains of permanently magnetized material which passively align the bacterium with the GMF (Blakemore, 1975).

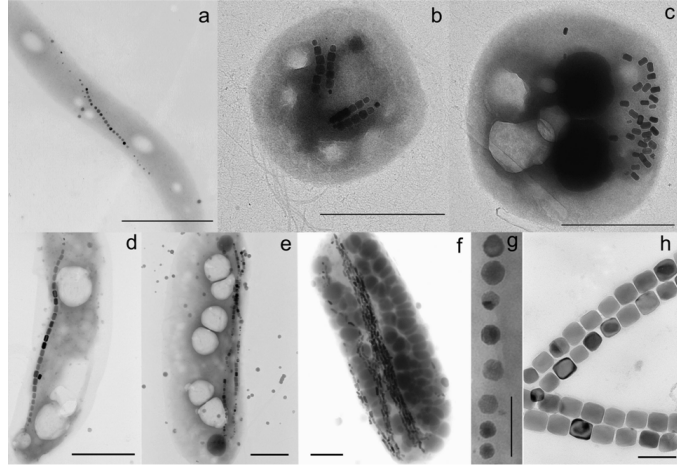


Figure 1.7: Variation of magnetic crystals in magnetotactic bacteria. From Faivre & Schüler (2008).

Blakemore showed that the particles were rich in iron, and the material of the magnetic chains was later shown to be single domain magnetite (Frankel et al., 1979). Many species of MTB have been discovered since then, all of them having one or more of the characteristic chain of magnetic crystals (Figure 1.7, (Faivre & Schüler, 2008)).

Following the discovery of (MTB), a similar mechanism for magnetoreception in other organisms was first suggested in 1978 when Gould et al measured magnetic remanence in bees (Gould et al., 1978). Yorke performed theoretical analysis on the forces and response time of such a chain of magnetic particles (Yorke, 1979), and since then extensive theoretical considerations have found the so-called magnetite hypothesis to be plausible (Kirschvink & Gould, 1981; Davila et al., 2003; Winklhofer & Kirschvink, 2010).

SD magnetite crystals could open mechanosensitive ion channels

According to the magnetite hypothesis movement of magnetic particles in the GMF leads to activation of neurons and a subsequent signal transduction. However, the

1. Introduction

details of this mechanism remains unknown. Signaling would most easily be realized in a cell where magnetite particles of sufficient size (*i.e.* in the SD region) are attached to mechanosensitive ion channels. Due to the permanent magnetic moment (μ) of a SD magnet a change in the direction of an external magnetic field (\mathbf{H}) relative to the particles will induce a torque ($\tau = \mu \times \mathbf{H}$), in order to realign the magnetic moment of the particles with the external field. Such a torque could potentially lead to opening of an ion channel if the particles are connected directly to the gating mechanism or to the membrane close to a stress-activated channel (Winklhofer & Kirschvink, 2010) (Figure 1.8a).

To achieve the forces necessary the torque can be enhanced by making a chain of magnetite particles or even several parallel coherently polarized chains, thus summing up the magnetic moments of the particles. This is for instance observed in magnetotactic bacteria ((Hanzlik et al., 1996), Figure 1.7). A torque sensor based on single domain particles could be sensitive to the polarity of the magnetic field if the mechanism could transmit the full rotation of the particles. However, if only the magnitude of the torque could be transmitted this would be consistent with the inclination compass. In either case, the fluctuations of the particle position (variance) could be a measure for the magnetic field intensity as the torque is proportional to this and thus a stronger alignment response is expected for higher field intensities (Winklhofer & Kirschvink, 2010).

Another possible mechanism, which has received little attention, would be to combine the magnetic torque with the high electrical conductivity of magnetite ($2 \cdot 10^4$ S/m) in the so-called membrane short model (Kirschvink & Gould, 1981). If a partially insulated single domain particle was left free to rotate within the membrane of a sensory cell, alignment with the GMF in a certain direction would let magnetite make contact on both intra- and extracellular side of the membrane and lead to a depolarization (Figure 1.8b). Such an electrical sensor would not be sensitive to the polarity of the magnetic field due to symmetry. However, since the size of SD magnetite crystals (>30 nm) is large compared to an average cell membrane (10 nm) this model is considered unlikely. Thus, a similar concept where a large magnetite crystal is influencing the orientation of nearby crystals of much smaller size, so-called sympathetic satellites located in the membrane, has also been suggested (Kirschvink & Gould, 1981).

1.2.3 The magnetite hypothesis

As for the RP hypothesis (section 1.2.2), most accurate information about the field direction could be obtained if several sensory cells are organized in an orthogonal fashion. In this case the nervous system could integrate the information from cells with different orientations relative to the magnetic field.

Clusters of SPM particles can be influenced by magnetic fields

SD magnetite was considered the most likely candidate to convert the magnetic information into a mechanical stimulus, also due to their existence in MTB. However, mechanosensitive ion channels could also be opened by a population (cluster or chain) of smaller SPM particles. A torque-based sensor could be possible with these particles due to their high magnetic susceptibility, however only if this is anisotropic. This can be achieved if the particles form a collective with shape anisotropy, such as a chain, where the magnetization will be induced in its long axis. In fact, a collective of smaller SPM particles will tend to self-organize into a chain even in weak magnetic fields (Davila et al., 2005). In this case the torque will be given by $\tau = V(\chi \cdot \mathbf{H}) \times \mathbf{H}$, where V is the volume and χ is the apparent susceptibility of the particle collective and \mathbf{H} the external magnetic field. In contrast to the torque produced on SD particles, the rotation of a SPM chain is due to magnetostatic interactions between particles. If the chain is located at a mechanosensitive free nerve ending even small movements of the chain will induce a stress on the membrane and lead to a nervous signal (Davila et al., 2005).

Other SPM-based mechanisms have also been suggested. For instance, several clusters of magnetite particles could interact in the presence of a magnetic field. If the distance between SPM clusters is small movement of the clusters would arise from attraction or repulsion between these resulting from the induced magnetization (Davila et al., 2003). When the external magnetic field is parallel to the alignment of the particles such that these are magnetized head to tail in the north-south axis, they attract each other and reduce the distance. On the other hand, when the field is oriented perpendicular to the axis of alignment, the particles will have their north south magnetization side by side, thus resulting in a repulsion and consequently an increased distance (Figure 1.8c). Although these movements are small they could still significantly influence nearby stress-sensitive ion channels (Davila et al., 2003).

The small crystals could also be organized in a lattice with spins parallel and an-

1. Introduction

tiparallel to mimic the structure of a ferrimagnet (Kirschvink & Gould, 1981). More likely however, is a suspension of SPM particles (a ferrofluid) enclosed by a membrane which could function as a magnetoreceptor (Shcherbakov & Winklhofer, 1999; Winklhofer et al., 2001). Such a ferovesicle would change its shape, from spherical to elongated, due to alignment of the single particles with the external field, and thus induce a stress on a mechanosensitive cell (Figure 1.8d). Furthermore, the ferovesicle could also influence the osmotic pressure in a cell as the magnetically induced shape change is counterbalanced. Thus signaling does not necessarily depend on a mechanoreceptive cell to initiate the signal transduction (Shcherbakov & Winklhofer, 1999).

Due to the axial nature of the SPM cluster response to directional changes in the magnetic field, a magnetoreceptor based on these principles would be an axial compass. SPM clusters is thus consistent with the inclination compass, similar to the RP hypothesis. Because of this the observation of an axial behavioral response cannot be used to distinguish the two hypotheses.

Evidence for the magnetite hypothesis

As the light-dependency of magnetoreception in certain animals argues for the radical pair hypothesis, the fact that some animals can use their magnetic sense in darkness provides evidence for a light-independent magnetoreception pathway. Thus, the magnetite hypothesis remains as a likely candidate. A fully functional magnetic compass in darkness has been reported for a variety of animals, such as salmon (Quinn et al., 1981), sea turtles (Light et al., 1993; Lohmann & Lohmann, 1993), lobsters (Lohmann et al., 1995) and mole rats (Marhold et al., 1997; Kimchi et al., 2004).

In contrast to radical pairs, the magnetite particles are not expected to be influenced by magnetic fields oscillating in the MHz range (Ritz et al., 2004). However, the function of the magnetic particles could be altered by a strong and short magnetic pulse (~ 0.5 T over a few milliseconds). This would either remagnetize, rotate or disrupt the chain of particles, depending on the particle size and the angle between the chain and the axis of the applied magnetic field (Davila et al., 2005). Indeed, experienced migratory birds have been shown to change their orientation for a few days after treatment with a magnetic pulse (Beason et al., 1995; Wiltschko et al.,

1.2.3 The magnetite hypothesis

1998). Similar effects have also been demonstrated in sea turtles (Irwin & Lohmann, 2005) and spiny lobsters, which gained a preferred orientation after exposure to a magnetic pulse (Ernst & Lohmann, 2016).

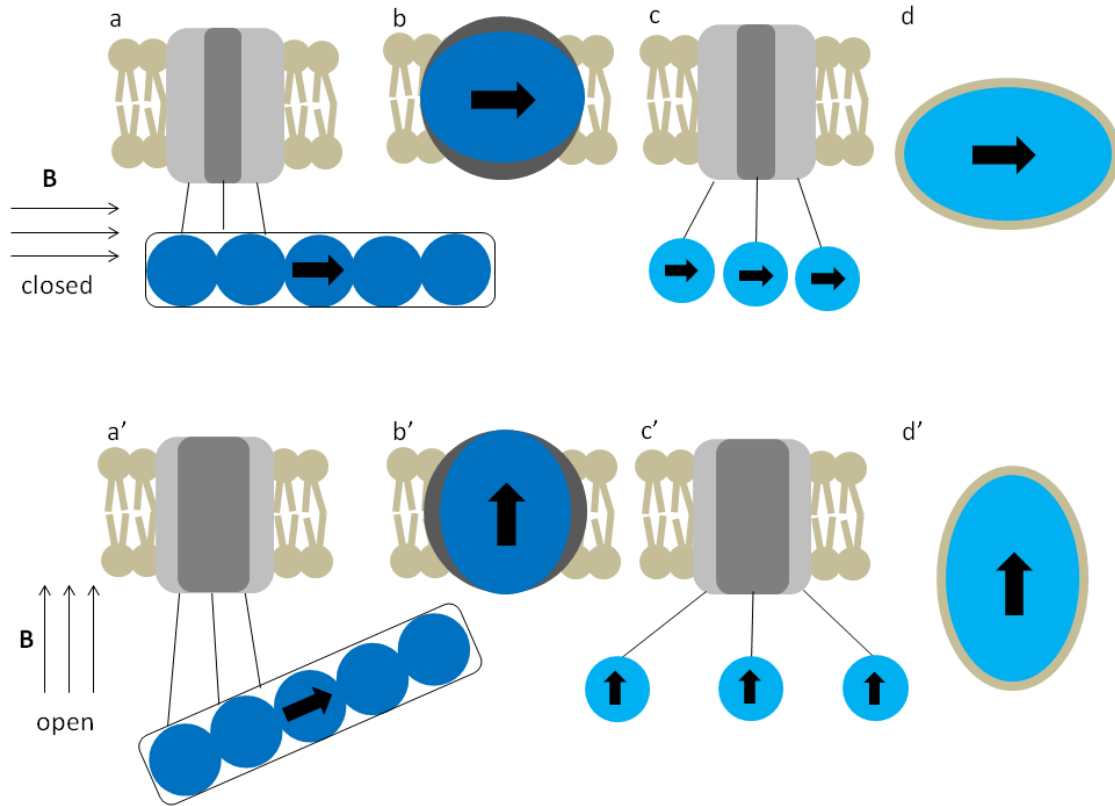


Figure 1.8: Examples of the possible initial steps in signal transduction mechanisms according to the magnetite hypothesis. a,a') SD particles (dark blue) in a chain, similar to the ones found in MTB can produce a torque on mechanosensitive ion channels when aligning with the magnetic field. A similar mechanism is possible with clusters of SPM particles. b,b') According to the membrane short model the high conductivity of magnetite will result in a depolarization of the cell when the SD crystal in the membrane rotates and the magnetite is exposed to both intra- and extracellular sides (Kirschvink & Gould, 1981). c,c') Clusters of SPM magnetite (light blue) can interact due to rotation of the induced magnetization (black arrows) and thus produce attractive (c) or repulsive (c') forces, resulting a stress on mechanosensitive structures (Davila et al., 2003). d,d') A cluster of SPM particles enclosed by a membrane (a ferrovessicle) will change its shape upon a directional change in the external magnetic field and can thus be used in a magnetoreceptor (Shcherbakov & Winklhofer, 1999)

1. Introduction

The existence of MTB is in itself evidence that a living organism can produce magnetic particles of sufficient magnetic moment to interact with the GMF. Although the bacteria are well studied and the understanding of how these can produce magnetite is increasing (Schüler, 2008; Uebe & Schüler, 2016), it is not clear if the same mechanisms could be realized in animals. Specifically, the low oxygen conditions under which these bacteria live and magnetite is produced, would prove challenging for a vertebrate system. However, magnetic material, putatively magnetite, has been reported in a variety of animals, including birds (Fleissner et al., 2003), insects (Kuterbach et al., 1982) and several fish species (Mann et al., 1988; Eder et al., 2012). These studies thus form the basis for the search for candidate magnetoreceptor cells.

1.2.4 Candidate magnetoreceptor cells

Observing putative magnetoreceptors

There is a growing body of behavioral evidence for the presence of a magnetic sense in a variety of animals. And after the discovery of MTB (Blakemore, 1975) and the following suggestions for similar processes in other organisms (Yorke, 1979) the search for magnetoreceptor cells began (Kirschvink, 1989). To this day, how information from the GMF can be sensed by an organism remains a mystery. However there must exist some cells acting as magnetoreceptors which are initializing a signal transduction from the magnetic field input. Specifically, if the magnetite hypothesis holds true it should be possible to find the magnetoreceptor cells mediating the magnetic sense as these should contain magnetic material such as magnetite.

There are a number of techniques that can be applied in the search for candidate magnetoreceptor cells, that can generally be divided in two categories; direct and indirect observations (Shaw et al., 2015). Techniques directly observing magnetic particles, using the properties of these, such as reflection, structure, high density or chemical content, include optical and electron beam methods. Indirect techniques on the other hand observe the presence of magnetic signal in a sample without directly observing the source of a signal, and include measurements with a superconducting quantum interference device (SQUID) and ferromagnetic resonance (FMR). Some more recent techniques are also able to combine the two observation paradigms

1.2.4 Candidate magnetoreceptor cells

by employing optical imaging of magnetic fields Le Sage et al. (2013). However a general limitation of direct observation techniques is the small sample size that can be assessed with such methodologies, thus making these unsuitable for larger scale screening applications.

Magnetite is found in animals exhibiting magnetoreception

Many techniques have been employed in the search for a magnetic sensor, and this has led to magnetic material being found in several organisms that exhibit magnetoreception. Already in 1979 SQUID, electron microscopy (EM) and optical microscopy was employed when Walcott et al. found implications for the presence of SD magnetite particles in the head of pigeons (Walcott et al., 1979). Conversely, a study employing Prussian Blue (PB) staining, a histochemical method for detecting Fe^{3+} , and transmission electron microscopy TEM, later concluded that the pigeons have SPM ($< 5\text{nm}$ grains) magnetite clusters at six specific locations in the upper beak (Hanzlik et al., 2000). Further analysis of the clusters identified SPM magnetite in nerve endings (Fleissner et al., 2003). These studies triggered the models for magnetoreception based on SPM clusters (Winklhofer et al., 2001; Davila et al., 2003) (see section on magnetite hypothesis 1.2.3). The magnetite clusters in the beak of pigeons were long considered a candidate for magnetoreception, however this has later been brought into question (Treiber et al., 2012).

In the meantime chains of magnetite crystals, remarkably similar to the ones found in magnetotactic bacteria, were isolated by mechanical and chemical extraction from ethmoid tissue samples from sockeye salmon (*Oncorhynchus nerka*) and observed with high resolution transmission electron microscopy (HRTEM) (Mann et al., 1988). The chains of particles were estimated to have sufficient magnetic moments for interaction with the GMF to overcome the thermal energy ($2\text{-}10 k_B T$). Similar particles have also been identified in other species of salmon (Kirschvink et al., 1985; Moore et al., 1990), as well as in other fishes, such as yellowfin tuna (Walker et al., 1984) and rainbow trout (Walker et al., 1997). While some studies only localized and characterized the magnetite with sensitive magnetometers, such as SQUID (Walker et al., 1988), many combine these measurements with extraction and subsequent characterization of magnetic particles. See Table D for an overview of magnetic material reported in fishes.

1. Introduction

The presence of SD and SPM magnetite has since been reported in a variety of organisms, ranging from insects to humans (see the review by Shaw et al. (2015) and figure 1.9 for an overview) The uniform size distribution of magnetite particles found in several species indicates a biological origin of these. Theoretical considerations of the magnetic moments of the chains observed argue that the particles could be part of a magnetoreceptor system (Winklhofer et al., 2001; Davila et al., 2003), while others claim that these are simply a result of contaminations (Treiber et al., 2012; Edelman et al., 2015).

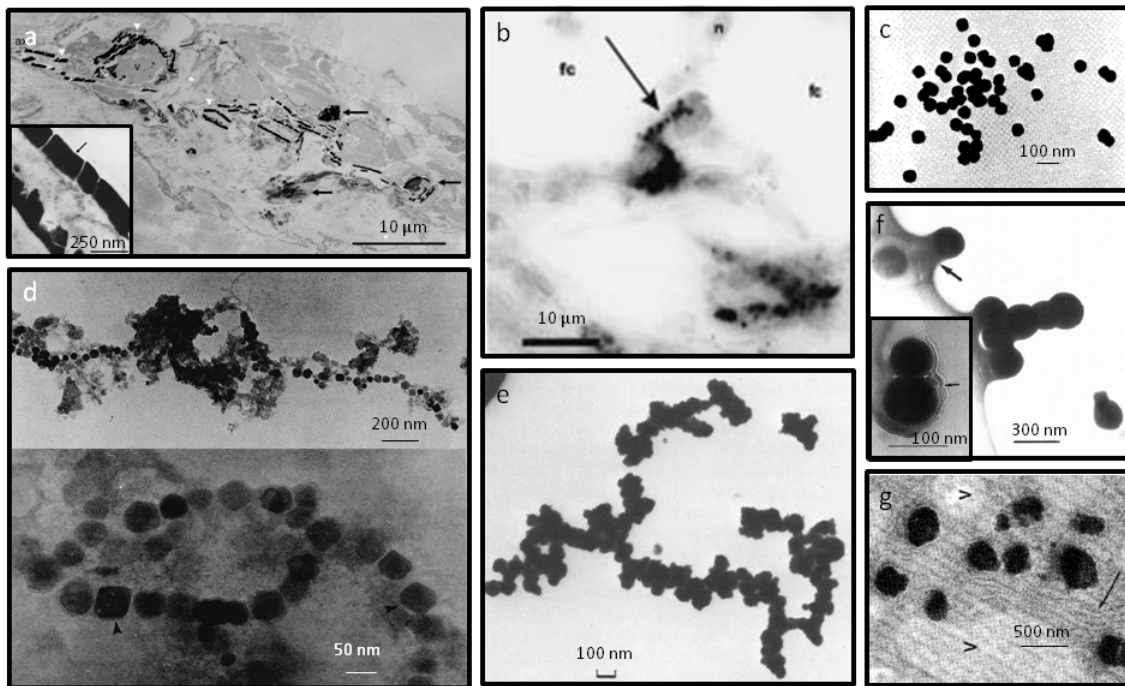


Figure 1.9: Magnetite particles observed in animals exhibiting magnetoreception. (a) Pigeon, beak (Fleissner et al., 2003) (b) Pigeon, beak (Hanzlik et al., 2000) (c) Yellowfin tuna, head and skull (Walker et al., 1984) (d) Sockeye salmon, ethmoid region (Mann et al., 1988) (e) Chinook salmon, dermethmoid tissue (Kirschvink et al., 1985) (f) Atlantic salmon, lateral line region (Moore et al., 1990) (g) Honey bee, abdomen (Kuterbach et al., 1982)

Identifying candidate magnetoreceptors

Techniques independent of the assumed mechanism of magnetoreception has also been employed when investigating the magnetic sense. For instance candidate nerves have been interrogated with extracellular recordings during magnetic field stimuli. Through this technique Beason and Semm (1987) found that the ophthalmic branch of trigeminal nerve in birds, as well as photoreceptors of the optic tectum and pineal gland, responds to changes in the direction of the horizontal or vertical component of the GMF (Beason & Semm, 1987). The trigeminal nerve was further shown to respond also to small changes in the magnetic field intensity (Semm & Beason, 1990), and was demonstrated to potentially be associated with magnetized material, in line with the magnetite hypothesis (Beason & Semm, 1996).

In 1997 Walker et al. combined behavioral studies and extracellular electrophysiological recordings in rainbow trout and found that the rostral V branch of the trigeminal nerve responded to changes in the magnetic field direction or intensity. Reflection microscopy and electron microscopy revealed iron-rich reflective crystals, similar to magnetite in magnetotactic bacteria, in the lamina propria layer in the olfactory rosettes. These were further shown to be linked to the rostral V nerve (Walker et al., 1997). In a subsequent study the reflective crystals were shown with magnetic force microscopy to be magnetic with properties consistent with single domain magnetite (Diebel et al., 2000).

The candidate magnetoreceptor cells identified in the olfactory rosettes of rainbow trout have later been isolated and characterized from dissociated tissue samples through a rotation assay developed by Eder et al. (2012) (see also Figure 2.9). The assay, using a rotating magnetic field, was used to screen samples of dissociated tissue for single cells with magnetic properties. Specifically, cells with permanently magnetized material, such as SD magnetite, anchored to its membrane or cytoskeleton would experience a torque in the changing magnetic field and thus rotate with the same frequency. Other iron rich cells with induced magnetic moments would in general only change their internal magnetization in the field without a movement of the cell being observed (Figure 2.9a). They found iron-rich and reflective inclusions in cells that could be manipulated by a rotating magnetic field of moderate intensity (2 mT), indicating a permanently magnetized structure. The magnetic moments of the isolated candidate magnetoreceptor cells were in the order of 4 - 100 fAm² (Eder

1. Introduction

et al., 2012).

Despite the large number of studies reporting magnetite crystals suitable for magnetoreception across several species, other studies claim that magnetic material found in these animals is likely to be result of contaminations. Quinn et al. (1981) could not detect magnetic material in 26 of 30 of the sockeye salmon fry were they observed magnetic orientation. Treiber et al. (2012) showed that the majority of the iron rich cells found in the beak of the pigeons, described by Fleissner et al. (2003), were macrophages. And candidate magnetoreceptor cells found in pigeons and rainbow trout have been argued to be contaminations due to the fact that these cells are rare and vary in size, magnetic moment and elemental composition (Edelman et al., 2015).

Even with the many studies searching for candidate magnetoreceptor cells there are few replications of experiments and the proper controls are often lacking (Shaw et al., 2015). It therefore remains unclear whether magnetic material found in animals is part of magnetoreceptor system or not. Hence, if one is able to isolate candidate magnetoreceptor cells from genetic model organisms, one could potentially gain deeper understanding of the identity of these cells.

1.2.5 Genetic model organisms

Genetic model organisms for magnetoreception studies

Although some of the mysteries around magnetoreception have been revealed, the molecular mechanisms underlying the magnetic sense are still not well understood. In order to investigate these further and to gain a more comprehensive understanding of magnetoreception, it is useful to work with genetic model organism which are suitable to whole-organism laboratory manipulations. Specifically, these are genetically addressable, such that candidate key genes could be interrogated. Furthermore, the model should be optically addressable, such that neural correlates of magnetoreception could be investigated employing non-invasive imaging techniques. Finally, and most importantly, a good model for magnetoreception studies should show robust and easily quantifiable behavioral responses to modulations of the GMF, ideally throughout the year, as opposed to the seasonally dependent behavior in birds. Table 1.1 summarizes the behavioral evidence for magnetoreception in genetic model

1.2.5 Genetic model organisms

organisms reported so far.

Table 1.1: Magnetoreception studies in genetic model organisms

Organism	Experimental test	Field	Reference
Invertebrates:			
<i>Drosophila</i>	Trained preference	GMF	Phillips & Sayeed 1993
	Trained preference	500 μ T	Gegear et al. 2008
	Trained preference	GMF	Dommer et al. 2008
	Spontaneous preference	GMF	Painter et al. 2013
<i>C.elegans</i>	Spontaneous preference	GMF	Vidal-Gadea et al. 2015
Vertebrates:			
Zebrafish	Conditioned response	100 μ T	Shcherbakov et al. 2005
	Spontaneous preference	GMF	Takebe et al. 2012
	Spatial preference	GMF	Osipova et al. 2016
	Spontaneous preference	GMF	Krylov et al. 2016
	Spontaneous preference	GMF	Myklatun, Lauri et al. 2018
Medaka	Spontaneous preference	GMF	Myklatun, Lauri et al. 2018
Mice	Trained preference	GMF	Muheim et al. 2006

Invertebrate genetic model organisms show responses to magnetic fields

Invertebrate genetic model organisms are often used as they have fast and well understood development and are easily bred and maintained in the laboratory. Genetic manipulation is easy allowing for genes of interest to be investigated. Among the most popular invertebrate model organisms are the fruit fly, *Drosophila melanogaster*, and the nematode worm *Caenorhabditis elegans*, and evidence for magnetosensitivity has been reported for both.

As described in the section about the RP hypothesis (1.2.2), magnetosensitivity with implications of the involvement of cryptochromes has been shown in *Drosophila melanogaster* (Gegear et al., 2008; Yoshii et al., 2009; Gegear et al., 2010; Foley et al., 2011). However, compass orientation of the flies were first shown in 1993 when Phillips and Sayeed trained *Drosophila* to a directional preference in a magnetic field using their natural preference for light (Phillips & Sayeed, 1993). Similar learning has also been observed in larval stages of *Drosophila* (Dommer et al., 2008), which has also been shown to exhibit spontaneous quadrumodal directional preference in

1. Introduction

the GMF (Painter et al., 2013). Naïve preference or avoidance towards a magnetic field stronger than that of the Earth was shown in WT flies when tested in a binary choice assay Gegeer et al. (2008). The flies could further be trained to prefer the magnetic arm of the arena when rewarded with sugar in this area, whereas mutated flies lacking functional cryptochromes were not able to perform in the same tests (Gegeer et al., 2008).

Magnetoreception has only recently been reported in *C. elegans* (Vidal-Gadea et al., 2015). In a vertical burrowing assay worms migrated with a certain angle relative to the GMF inclination, likely in order to optimize the vertical translation. They further found that the direction of migration depended on the feeding state of the worms. In order to more easily assess magnetic behavior in different strains of *C. elegans* a magnetotaxis assay was established. Similar to the assay in *Drosophila* the worms showed a preference for the presence of a permanent magnet when evaluated for a binary choice (Vidal-Gadea et al., 2015).

Although responses to magnetic fields has been explored in invertebrate genetic model organisms, their behavior is still not well characterized. Further, some of the tests performed involved high magnetic fields, up to 10 times GMF (Gegeer et al., 2008). Interestingly however, while it was indicated that cryptochromes are involved in the sensitivity to magnetic field of *Drosophila*, *C. elegans* seemed able to employ the magnetic information in darkness (Vidal-Gadea et al., 2015). However, this would have to be confirmed by independent studies (see also section 2.1.4). Further, to gain a better understanding of magnetoreception and the mechanisms, studies of vertebrate genetic model organisms are of high value.

Zebrafish (*Danio rerio*) respond to changes in GMF

Zebrafish (*Danio rerio*) is a genetic model organism commonly used in laboratories, both for behavioral and neurobiology studies. It is a shoaling freshwater fish belonging to the teleost family, with its natural habitat in rivers, small streams, rice paddies and other slow moving waters in India and southern Asia (Engeszer et al., 2007). The zebrafish genome has been fully sequenced, which makes it useful in research as a vertebrate genetic model organism. Other advantages include the fast and well understood development, in addition to the transparent larval stages which makes them easy to study with optical methods.

However, concerns arose that zebrafish exhibit strong inter-strain and inter-individual genetic and behavioral variabilities also in the commonly used domesticated strains (Guryev et al., 2006; Drew et al., 2012; Wilson et al., 2014). Such variability presents a challenge for behavioral studies as fish might react differently, for instance when introduced to novel environments (Sackerman et al., 2010). On the individual level, reactive fish are considered shy and will be cautious when exploring a new arena, or even freeze, whereas proactive fish are considered bold and will often show more exploratory behaviors (Rey et al., 2013).

The first evidence for magnetoreception in zebrafish was presented in 2005, when Shcherbakov et al. trained fish to respond to directional inversions of an applied magnetic field (Shcherbakov et al., 2005). Since zebrafish are shoaling they were tested in groups of four in the conditioning experiment, where the fish were trained to change compartment upon magnetic field change. If the fish failed to cross the midline after field change they were punished with a mild electric shock. Although the study concluded that zebrafish respond to magnetic fields, it has been criticized for using magnetic fields stronger than the GMF and for the close proximity of the coils producing the magnetic field to the test arena.

In order to address these issues Takebe et al. (2012) designed an experiment where a spontaneous magnetic orientation in the GMF could be tested in zebrafish, as opposed to a conditioned response. In these experiments the arena, illuminated with white light (WL) from above, was placed far away from the three pairs of Helmholtz coils which shifted the GMF to either north, east, south or west. Individual fish, of the WT strain EKK, were released from the center of a circular arena, triggering an escape response which served as motivation for a spontaneous directional preference choice. Analysis of the bearing for each fish when they first crossed a virtual line demonstrated that the zebrafish had directional preference consistent with the axis of the applied magnetic field. However, the response was shown to be group dependent, with fish from different parent couples having distinct directional preferences. This was most likely due to the similar genetic background, as the preference did not seem to depend on age or gender of the fish (Takebe et al., 2012).

The axial preference was recently confirmed both in a circular release assay (Krylov et al., 2016), and in a cross maze (Osipova et al., 2016). The latter study

1. Introduction

found that the fish of the WT strain AB preferred the arms in east and west direction. However, this was changed to the north and south arms when the horizontal component of the geomagnetic field was shifted 90°. Other modifications of the magnetic field, such as inverting the vertical or horizontal component, did not change the behavior of the fish (Osipova et al., 2016).

While these studies address magnetoreception, other studies present effects of unnatural stimuli such as strong magnetic fields altering swimming behavior through a disturbed vestibular system (Ward et al., 2014) or moderate oscillating fields delaying development (Skauli et al., 2000). However, none of the studies in zebrafish aim towards a mechanistic understanding of the magnetic sensitivity, thus not using the full potential of this genetic model organism.

Magnetoreception is unexplored in Medaka (*Oryzias latipes*)

Medaka (*Oryzias latipes*) is another freshwater teleost fish which is gaining popularity as a genetic model organism. In the wild this small fish is primarily found in Japan, but also in Korea and the eastern part of China, where they prefer the habitat of the rice fields. Medaka is similar to zebrafish in terms of husbandry, and the two species can be kept alongside each other in the same facility. Most techniques used for zebrafish can also be applied for medaka (Furutani-Seiki & Wittbrodt, 2004), and more techniques are being developed (Wittbrodt et al., 2002).

Unlike zebrafish however, medaka can be taken from the wild and be inbred, meaning that a group of fish is genetically homozygous, and a large selection of lines is available (Wittbrodt et al., 2002). Thus medaka presents less genetic differences between individuals. Further, whereas zebrafish are likely to move between streams and nearby rice paddies (Engeszer et al., 2007), medaka also migrate between freshwater and brackish waters in the wild. Although there is evidence that high frequency weak electromagnetic fields can influence their development and result in an increased anxiety behavior (Lee & Yang, 2014), until now magnetoreception has remained unexplored in medaka. Thus, I set out to investigate medaka and compare their response to directional changes of the GMF to those of zebrafish. Taken together, both these fishes could potentially be very attractive model organisms for studying the underlying mechanisms of magnetoreception.

1.3 Microfluidic magnetic sorting

1.3.1 Magnetic separation of cells

In working towards magnetogenetics, biophysical characterization of the magnetic properties of cells is of high value. And in the search for potential candidate magnetoreceptor cells good isolation techniques are essential. It is natural to think of a magnetic sorting system for separation and enrichment of magnetic cells from dissociated tissue samples. Traditionally, magnetic material was isolated from biological samples using a permanent magnet close to the test tube was used. However, now more sophisticated methods have been developed.

For the subsequent characterization of a sample it is crucial to avoid introduction of magnetic contaminants. There are three main sources of contaminations when isolating candidate magnetoreceptor cells that need to be taken into consideration: 1) Contamination from external material during the preparation process must be avoided by using non-magnetic material, and 2) a magnetic sorting system which avoids contact between the magnetic material and the sample is crucial. Finally, 3) the high abundance of iron in biological tissues can make the identification of the real magnetoreceptor cells challenging.

There are commercial magnetic sorting systems, for example from companies such as Miltenyi Biotec GmbH. Their magnetic columns for separation of magnetically labeled cells use strong magnetic gradients produced by a mesh of magnetic particles which the cells travel through (Miltenyi et al., 1990). This system is well established for magnetically labeled cells, however, the risk of contamination is high since the sample comes into contact with superparamagnetic material in the column. This makes it unsuitable for isolation of candidate magnetoreceptor cells. The risk of contamination can be avoided by using an array of permanent magnets, such as a quadrupole, to create a force towards the wall from the center of the magnets (Zborowski et al., 1999). However, the disadvantage of both these systems is the lack of visual control and the limited ability to tune the system parameters.

An attractive alternative for magnetic sorting of cells is to use a system combining continuous flow microfluidics with strong magnetic field gradients (Pamme, 2006; Hejazian et al., 2015). Such a system could allow for manipulation of single cells with tunable parameters under visual monitoring, and potentially without risk of

1. Introduction

contamination. Thus, in this work I aimed to establish a microfluidic magnetic sorting system for isolation and potential characterization of cells with intrinsic magnetic properties.

1.3.2 Microfluidic systems for magnetic cell sorting

Microfluidic systems

In fluid mechanics the ratio between the inertial forces due to momentum changes (acceleration) of a fluid element ($\mathbf{F}_i \sim \rho v^2/L$) and viscous forces resulting from gradients in viscous stress ($\mathbf{F}_v \sim \eta v/L^2$) in a system is known as the Reynolds number (Re) and is given by

$$Re = \rho v L / \eta, \quad (1.1)$$

where ρ is the density of the fluid, v is the velocity, η is the viscosity of the fluid and L is the characteristic length of the system, typically the diameter of a channel. Turbulent fluid flow, which is chaotic and difficult to predict, is a part of many macroscopic and everyday systems, such as rivers or fluids in industrial pipes.

On the other hand, when the viscous forces dominate the system, in the low Reynolds number regime ($Re < 1$), laminar flow can be observed. Laminar flows are predictable and the time scale necessary to establish steady flow is found by balancing the inertial and viscous force densities, and is typically in the order of milliseconds in a microfluidic system. Furthermore, the lack of lateral mixing, meaning that two fluids running in parallel will not mix other than by diffusion, is advantageous for more precise control over fluid manipulation. As seen from equation 1.1, a low Reynolds number can be achieved by decreasing the velocity, increasing the viscosity of the fluid or by reducing the dimensions of the system.

In microfluidic systems laminar flow is achieved by manipulating fluids in channels of small dimensions, typically in the micrometer size range. This allows for precise control of the fluids and can be employed in a number of designs for separation of samples (Hejazian et al., 2015). A simple sorting device has two inlets and two outlets and a manipulation force to move samples from one to the other outlet (Figure 1.10). In the case of a cell sorter the sample containing single cells would be injected into one inlet and a buffer solution in the other. The laminar

1.3.2 Microfluidic systems for magnetic cell sorting

flow would keep the cells separated from the buffer and the two solutions would exit the microfluidic channel separately through the two outlets, unless a force is pulling the cells out of the flow. Opposing this movement is the drag force (\mathbf{F}_d), given by Stokes law

$$\mathbf{F}_d = -6\pi r\eta(v_f - v_c), \quad (1.2)$$

where r is the radius of the cell, η is the dynamic viscosity of the fluid and v_f and v_c is the velocity of the surrounding flow and the cell, respectively.

In order to reduce the effect of diffusion of cells into the buffer, the respective flow rates of the two fluids can be adjusted. The fluid with the higher velocity (buffer in this case) would take up more volume in the channel and thus have the broadest flow. The viscosity of the fluids is also influencing the flow behavior and can be used to further decrease the Reynolds number in order to achieve laminar flow.

A magnetic force will deflect magnetic cells from their trajectory

In a microfluidic system, as depicted in Figure 1.10, a force orthogonal to the flow direction will displace the target cells (blue) into the buffer flow. This will result in a separation of the sample. In order to separate cells containing magnetic material from the dissociated sample a magnetic field intensity gradient is necessary to generate a translational force, since homogeneous magnetic fields can only generate a torque. The translational force acting on a cell with magnetic moment \mathbf{m} is given by

$$\mathbf{F}_m = \mathbf{m}\nabla\mathbf{B} = \frac{V\Delta\chi}{\mu_0}\mathbf{B}\nabla\mathbf{B} \quad (1.3)$$

where \mathbf{B} is the magnetic field intensity and $\nabla\mathbf{B}$ is the magnetic field intensity gradient. V is the volume of each magnetic cell, $\Delta\chi$ is the difference in magnetic susceptibility between the cell and the surrounding medium and μ_0 is the permeability of free space. The force on the cell will attract it in the direction of the increasing magnetic field gradient. This is used in the microfluidic device in order to move cells with sufficient magnetic moment from the sample flow into the buffer flow, and thereby a separation is achieved (Figure 1.10).

1. Introduction

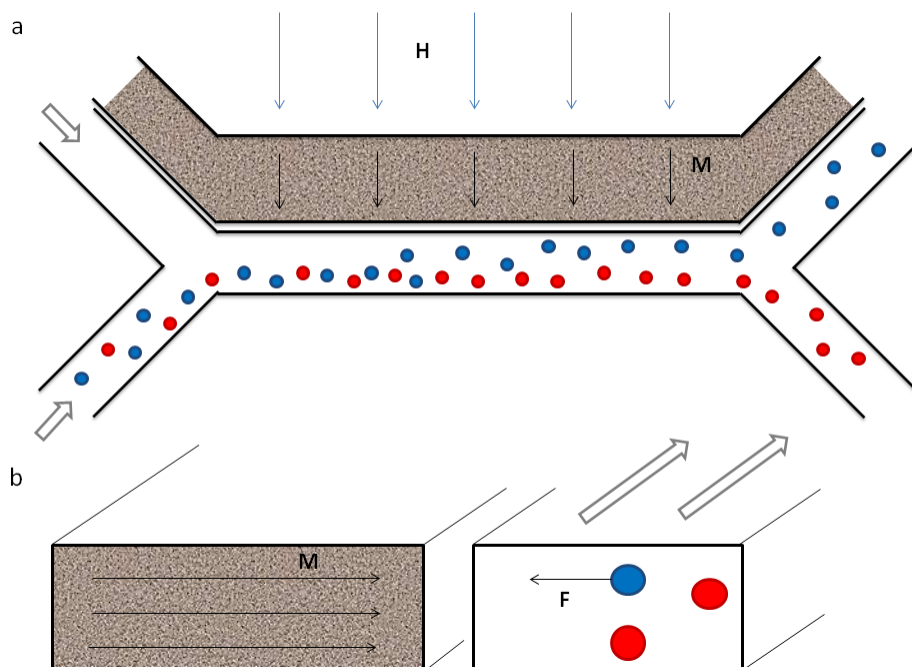


Figure 1.10: Microfluidic magnetic separation principle. The microfluidic channels seen from above (a) and through a cross section (b). The sample is introduced into the sorting channel on the side opposite of the ferrofluid. A buffer is injected at the second inlet. An external magnetic field (H) will magnetize the ferrofluid (M) and create a gradient orthogonal to the flow direction. Cells with magnetic moments will experience a force and be pulled into the buffer flow, and a separation is achieved.

In order to optimize the force acting on the cells there are a few approaches that can be used. One way is to increase the susceptibility mismatch between the cell and the medium. This is often achieved by binding magnetic particles through antibodies on target cells (Miltenyi et al., 1990; Adams et al., 2008). However, for separation of intrinsically magnetic cells this is not possible. Thus, to achieve efficient separation in microfluidic magnetic sorting systems an additional increase of the magnetic field gradient is necessary.

Optimizing the translational force

There are several ways of creating a magnetic field gradient in such a microfluidic system. For instance, Siegel et al. (2006) used a wire parallel to the sorting channel

1.3.2 Microfluidic systems for magnetic cell sorting

to create an electromagnet and thus a magnetic gradient when current was passed through it. Likewise, electromagnets have been used to generate a traveling magnetic field gradient (Liu et al., 2007). These designs allow for great control by tuning of the gradient field through changing the current. However, the strength of the gradient that can be achieved is limited due to small dimensions and the associated heat generated by the current in the system.

A more common approach, which usually also generate higher magnetic field gradients, is to introduce a ferromagnetic structure in close proximity to the sample. For instance, Adams et al. (2008) used strips of nickel on the bottom of the sorting channel, which proved to be effective for separating cells with different magnetic moments. A recent study showed that similar strips consisting of embedded ferromagnetic particles inside the microfluidic channel can be used to trap magnetically labeled cells in the presence of an external magnetic field (Sun et al., 2016). This concept is also similar to the magnetic columns presented by Miltenyi et al. (1990), and although visual control is added, the risk of contaminations is still present in both these designs.

In order to avoid risk of contaminations through contact between the sample and ferromagnetic material the magnetic field enhancers need to be placed outside of the microfluidic channel. This presents a challenge due to the rapid decrease of a magnetic gradient with distance. In order to have a stronger gradient the magnetic field lines of a permanent magnet can be concentrated by a sharp object of a material of high magnetic permeability, for instance with a comb-like structure (Xia et al., 2006).

The idea of using ferromagnetic particles to concentrate the magnetic field lines was first presented by Lin et al. (2007). They used a permanent magnet in combination with nickel microparticles immersed in silicon oil to achieve a high magnetic gradient across the sorting channel. The microparticles were filled in a parallel channel in close proximity to the sorting channel, resulting in a magnetic force on the cells which was 3.3 times higher compared to the presence of a permanent magnet alone (Lin et al., 2007).

The particle based approach was recently further developed by Zhou & Wang (2016). They demonstrated through magnetic simulations and experiments with magnetic particles that there are three main factors that need to be optimized

1. Introduction

in such a system. First, the particle concentration will influence how much the magnetic field gradient is enhanced. Next, the distance between the sample and the magnetic structure or particles, thus the width of a sorting channel, must be as small as possible. Finally, the shape of the magnetic structure will influence the interaction time of the magnetic force on the sample (Zhou & Wang, 2016).

Ferrofluids for increased magnetic gradient

The magnetic field gradient can also be created by filling the side channel with a ferrofluid. A ferrofluid is a dispersion of superparamagnetic nanoparticles in oil, which is known to retain phase stability (Scherer & Figueiredo Neto, 2005). The particles are usually made of iron or an iron containing material, such as magnetite. Typical values for the size are in the order of 10 nm, at a particle concentration of about 5%, however commercial ferrofluids with a particle concentration above 15% are also available.

Ferrofluids have a strong response to magnetic fields, depending on the material and concentration of particles. In the absence of an external magnetic field the SPM ferrofluid will not have any net magnetization due to the random orientation of the magnetic moments within the single SPM particles. However, in the presence of an external magnetic field, e.g. from a permanent magnet, the magnetic moments of the particles align with the magnetic field creating a net magnetization of the ferrofluid. This reversible magnetization (M) of a ferrofluid can in general be estimated by the Langevin function which is given by

$$M_L(H) = n\mu(\coth(\frac{\mu_0 H \mu}{k_B T}) - \frac{1}{\frac{\mu_0 H \mu}{k_B T}}), \quad (1.4)$$

where H is the magnetizing field, n is number of nanoparticles per unit volume in the ferrofluid and μ is the magnetic moment of each nanoparticle, μ_0 is the permeability of free space, k_B is the Boltzmann constant and T is the absolute temperature.

In dense ferrofluids, where the particle concentration exceeds ca. 10% of the volume, interactions between particles would lead to an additional significant contribution to the magnetization. Specifically, the formation of chain structures would increase the initial susceptibility of the ferrofluid. These interparticle correlations can be taken into consideration by introducing an effective magnetizing field (H_e)

1.3.2 Microfluidic systems for magnetic cell sorting

with a contribution also from the surrounding particles (Ivanov & Kuznetsova, 2001). The effective field is given by

$$H_e = H + \frac{4\pi}{3}M_L(H) + \frac{(4\pi)^2}{144}M_L(H)\frac{\Delta M_L(H)}{\Delta H}, \quad (1.5)$$

where M_L is the Langevin magnetization given by equation 1.4 for the applied magnetizing field H . The magnetization of a ferrofluid can then be estimated by the Langevin function using the effective magnetizing field ($M_L(H_e)$). Figure 1.11 shows the magnetization curve for ferrofluids containing different concentrations of 10 nm magnetite particles.

The reversible magnetization of the ferrofluid in a microfluidic channel would generate a strong gradient close to it as the resulting magnetic field intensity decays with the distance. Furthermore, this design enables one to conveniently switch on and off the magnetic gradient in the sorting system by moving in and out external permanent magnets, respectively, such that proper control of flow conditions can be achieved prior to starting the separation process. Thus, I developed a microfluidic sorting system for separation of intrinsically magnetic cells where I used a ferrofluid to generate high magnetic gradients.

1. Introduction

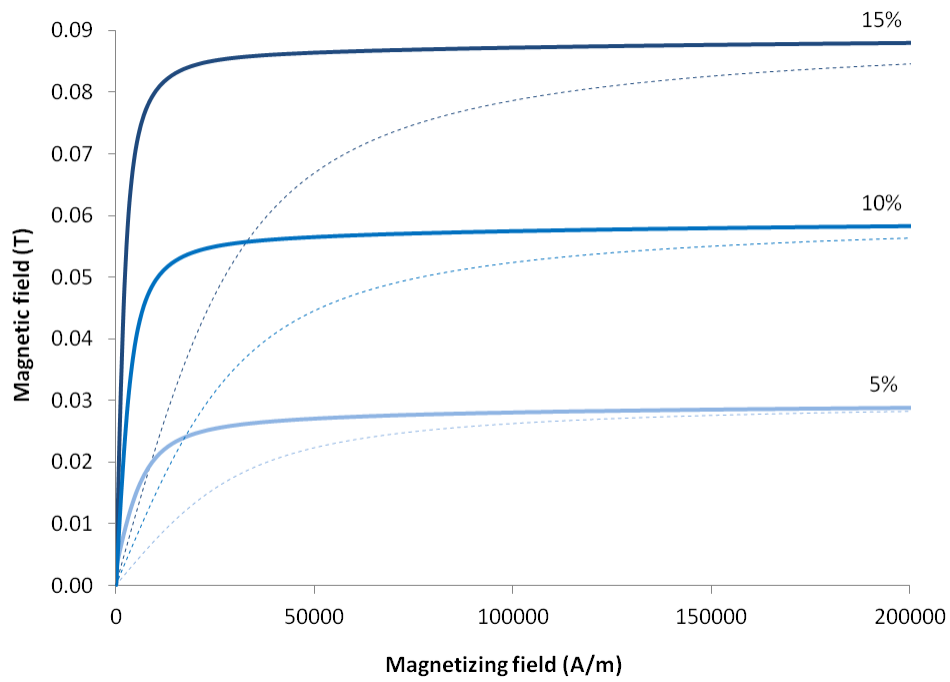


Figure 1.11: Theoretical magnetization curves of ferrofluids consisting of different concentrations of 10 nm magnetite particles. The dotted lines represents the magnetization according to the Langevin function, while the solid line shows the effective magnetization when the interparticle correlations are taken into consideration. Adapted from Myklatun et al. (2017)

Chapter 2

Results

2.1 Magnetoreception in genetic model organisms

Magnetogenetics is a novel scientific field aiming at selectively controlling neuronal processes via application of magnetic field, for instance through heating of genetically expressed particles in the cell membrane. It is hypothesized that some animals are able to produce magnetite particles that can interact with the geomagnetic field (GMF), and employ these during navigation. The understanding of putative magnetite production in higher organisms and the interaction of these particles with weak magnetic fields would be of great value for magnetogenetics (Meister, 2016). Such knowledge could potentially be gained from genetic model organisms, for which a variety of genetic tools for investigation of candidate key genes are available. Thus, I set out to investigate behavioral responses to magnetic field changes, and directly test the magnetite hypothesis, in three genetic model organisms; the teleost fishes zebrafish and medaka, and the nematode worm *C. elegans*.

In close collaboration with Dr. Stephan Eder and Dr. Antonella Lauri, we aimed at assessing spontaneous directional preference in the two vertebrates, zebrafish and medaka. We found it necessary to improve the existing behavioral assay which has been described for zebrafish (Takebe et al., 2012). The assay was first optimized in order to reduce variability in behavioral responses. We then employed this assay in order to investigate whether the putative magnetosensitivity was present also in darkness, as predicted by the magnetite hypothesis (see section 1.2.3).

Furthermore, magnetosensitivity has recently been reported in *C. elegans* (Vidal-

2. Results

Gadea et al., 2015). This simple invertebrate would be attractive for studying the molecular mechanisms of magnetoreception. Thus, in order to more broadly investigate magnetoreception in genetic model organisms, I aimed to validate the described behavior of *C. elegans* in a simple magnetic field preference assay in darkness.

2.1.1 A spontaneous directional preference assay

Magnetosensitivity is not well characterized in the teleost fishes zebrafish and medaka, which are widely employed as vertebrate genetic model organisms. Thus, together with Dr. Stephan Eder, we set up an assay that assessed whether the fish showed directional preference in the GMF. The behavioral test was based on the experiments presented by Takebe et al. (2012), where individual zebrafish were released from the center of a circular arena after the direction of the magnetic field was changed (Figure 2.1). In order to evaluate the spontaneous directional preference of the fish the initial crossing of a virtual circle after release was analyzed. The bearing of each fish was then defined as the angle between North and the crossing point, with vertex at the center of the arena (Figure 2.1b) (Takebe et al., 2012). The preferred direction could then be assessed by comparing the bearings for groups of fish with the direction of the shifted horizontal component of the magnetic field.

Similarly, in our experiments we tested zebrafish in a release assay and assessed their initial bearing. The fish were placed in the a transparent cylinder at the center of a circular arena and then released through an automated lifting mechanism. In addition to evaluating the response of the fishes in white light (WL) illumination from above, we also assessed the fish under infrared (IR, 1060 nm) light (Figure 2.1a). The IR illumination has been shown not to be perceived by zebrafish (Shcherbakov et al., 2013), and thus allowed us to investigate the directional preference also in darkness. This was done with individual fish acclimated either in light or in darkness (Figure 2.1c).

However, we believed that further improvements were necessary for a more reliable behavioral assessment of magnetosensitivity. Specifically, we reduced the electromagnetic noise in the set up. In addition, we adapted an intra-subjective approach in order to cope with the large variability between zebrafish individuals (Sackerman et al., 2010; Rey et al., 2013). Finally, together with Dr. Antonella Lauri, we employed the behavioral assay to assess also medaka, for which magne-

2.1.1 A spontaneous directional preference assay

toreception had so far remained unexplored. To this end, the assay was further adapted as medaka showed a different swimming behavior as compared to zebrafish.

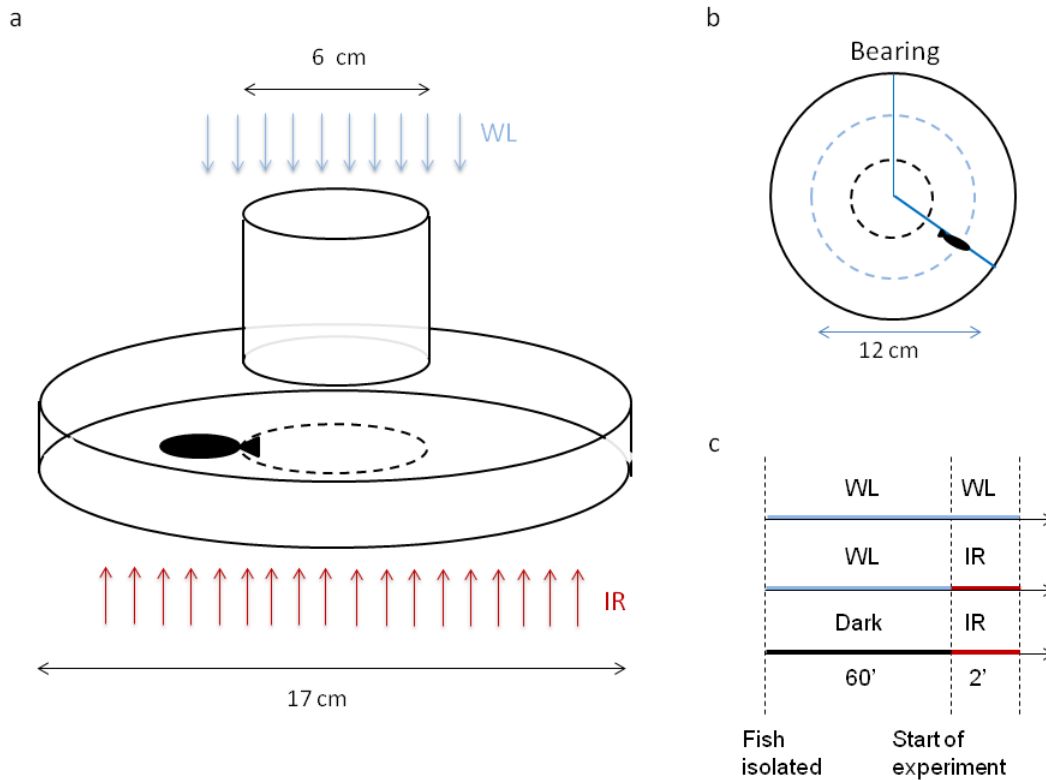


Figure 2.1: Spontaneous directional preference assay. a) Individual fish were released from the center of a circular arena with an automated lifting mechanism. The arena was illuminated from below with IR (1060 nm) or from above with a circular WL source. b) The bearing, defined at the point where the fish was first crossing a virtual line (blue), was assessed. c) Schematics of the experimental procedure. Zebrafish were tested in WL or in IR after 60 minutes acclimation in WL or in darkness.

Reducing electromagnetic noise in the set up

In order to accurately control both the direction and intensity of the GMF horizontal component, we decided to use two pairs of Helmholtz coils, in which the distance between a pair of coils was equal to their radius. This configuration generated a homogeneous field at the center of the coils, where the test arena was placed (Figure 2.2a). However, the current running through coils when generating electromagnetic

2. Results

fields can also be a source of heating and vibrations in the system. Thus, it was important to also control for unspecific effects due to the presence of current when assessing animal magnetoreceptive behavior. This way the results from the behavioral tests could be confidently attributed to the shift of the magnetic field direction as opposed to a response due electromagnetic noise.

In order to simultaneously control for the direction of the GMF and the presence of current we applied a magnetic field in the East-West axis of the GMF. This allowed us to shift the direction of the magnetic field by 45° towards either North-East (NE) or North-West (NW). In this way the same amount of current was flowing in the two conditions, however in opposite directions (Figure 2.2a,b). The intensity of the resulting magnetic field was adjusted by applying another field in the North-South direction using the second pair of coils, such that it was equal to the intensity of the GMF (Figure 2.2b). The current in this second pair of coils remained constant throughout all the experiments.

This design allowed the fish to experience a total magnetic field shift of 90° in two subsequent trials. Thus, we could assess their reorientation, as described below. With this shift a directional preference in the GMF would be evident also if fish showed an axial distribution, as has been previously reported for zebrafish (Takebe et al., 2012).

2.1.1 A spontaneous directional preference assay

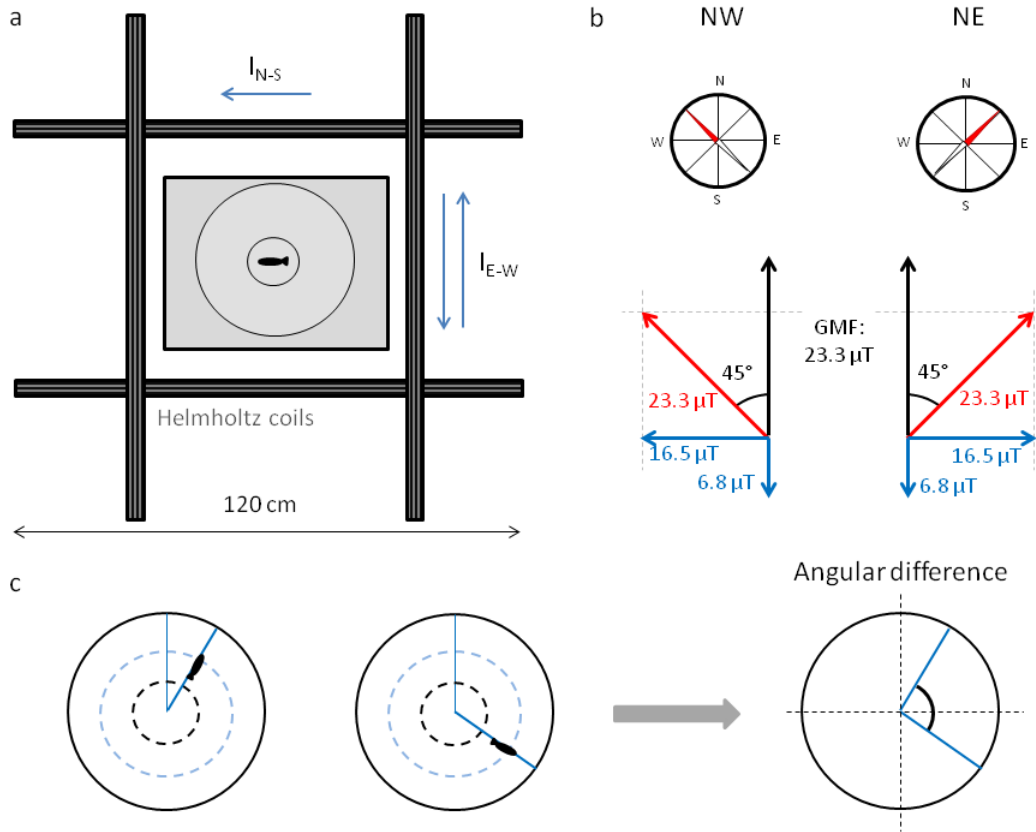


Figure 2.2: Helmholtz coils used to change the direction of the GMF. a) The arena was placed on top of an IR illumination table in the center of two pairs of square Helmholtz coils, which was used to shift the horizontal component of the GMF by applying a current (I , blue arrows). b) The horizontal component of the GMF (black arrow) was changed by applying a magnetic field (blue arrows) induced by current of opposite directions in one pair of coils (I_{E-W}), while the field from the other coil pair (I_{N-S}) remained constant. The resulting magnetic field (red arrows) was thus shifted 45° with the same intensity as GMF c) The bearing, defined at the point where the fish was first crossing a virtual line, was assessed with the GMF shifted 45° towards West (NW) and East (NE). Thus, the reorientation, defined as angular difference between bearings in the two conditions, could be calculated for each fish and their distribution compared to the expected mean of 90° .

Assessing reorientation of individual fish

The directional preference previously reported in zebrafish was specific for groups originating from a single parent couple (Takebe et al., 2012). Thus, all the groups of

2. Results

fish tested in our experiments were from single genetic cohorts. However, zebrafish are known to also exhibit high inter-individual differences, even within single cohorts (Guryev et al., 2006; Rey et al., 2013). In order to overcome these differences we developed an intra-subjective approach, where each individual fish was tested twice, once in each of the two magnetic field directions (NW and NE).

In addition to comparing the same group of fish in the two magnetic conditions, this allowed for analysis of the reorientation performed by individual fish. To this end we calculated the angular difference between the bearings obtained for the two magnetic conditions (Figure 2.2c). This was done for each individual fish. From the shift of the applied magnetic field we expected that the fish, if they had a preference for a certain magnetic direction, would change their bearing by 90° . Thus, by performing a V-test (Batschelet, 1981), the angular differences could be directly tested for a uniform distribution with the alternative hypothesis of a non-uniform distribution with a mean of 90° . This change in bearing of individual fish would be evident even if the groups did not show a common preference.

Indeed, when we tested a cohort of zebrafish (AB) under white light (WL) illumination after the fish had been isolated and acclimated in light (Figure 2.1b), we observed a significant reorientation of the fish. The directional preference was evident for individual fish when the angular differences of the bearings were investigated. The axial distribution of these reorientations was non-uniform and compatible with the 90° shift of the applied magnetic field ($n = 12$, mean = $109/289^\circ$, V-test(90°): $p = 0.01$, Figure 2.3). The fish did not seem to differentiate in which direction the change occurred, i.e. clockwise or anticlockwise, resulting in the axial response. This was consistent with what has previously been reported for zebrafish (Takebe et al., 2012; Osipova et al., 2016; Krylov et al., 2016). Notably, in contrast to what has been reported for another WT strain (EKK) (Takebe et al., 2012), the zebrafish in our test did not show a group directional preference. Although belonging to the same cohort, their bearings, measured as the crossing of the 6 cm radial line, was uniformly distributed in both magnetic conditions (NW: $n = 13$, mean = $136/316^\circ$, Rayleigh test: $p = 0.46$; NE: $n = 15$, mean = $74/254^\circ$, Rayleigh test: $p = 0.75$, Figure 2.3). This showcases the strength of the intra-subjective approach also for small groups of fish.

2.1.2 Altered swimming patterns of zebrafish and medaka in darkness

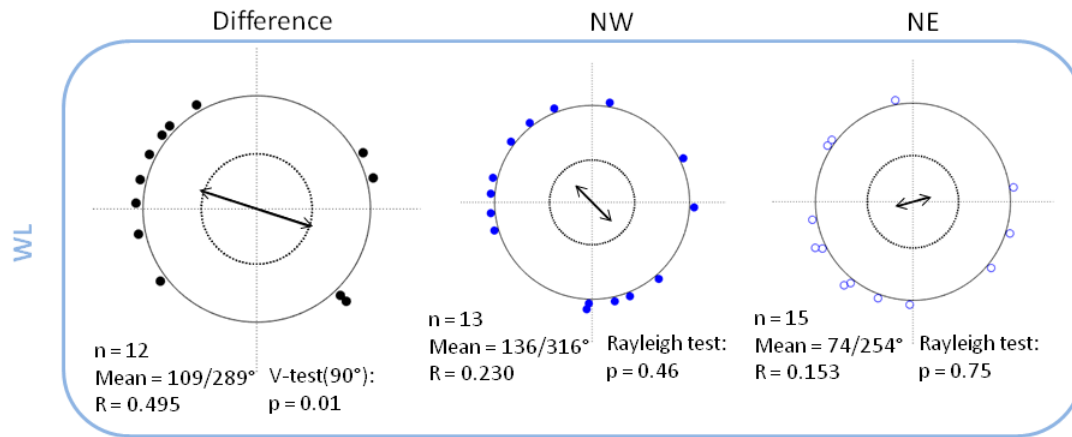


Figure 2.3: Directional preference of zebrafish tested under WL illumination. Zebrafish showed a significant reorientation of their bearings (Difference, black dots), however no group preference was observed in the two magnetic conditions (NW, closed dots; NE, open dots). For all plots each dot represents the bearing (blue) or the angular difference in bearings (black) for a single fish. The central black line represents the mean vector and the inner dotted circle represents the significance threshold for the Rayleigh test ($p < 0.05$). The values are given underneath each plot.

2.1.2 Altered swimming patterns of zebrafish and medaka in darkness

To gain potential insights into the mechanism of magnetoreception, we tested the fishes also under infrared (IR) illumination (1060 nm). This wavelength is not perceived by several fish species, including zebrafish (Shcherbakov et al., 2013). These tests aimed to differentiate the mechanical magnetite hypothesis from the light dependent radical pair hypothesis, as the wavelength is much longer than those known to activate cryptochromes (Chaves et al., 2011). Thus, we assessed groups of zebrafish in the release assay under IR illumination. Together with Dr. Antonella Lauri we expanded the behavioral assay to also include medaka, for which magnetoreception was unexplored. However, we first observed that both fish species showed different behaviors in darkness compared to in light.

2. Results

Zebrafish increased thigmotaxis in darkness

When we observed the behavior of the zebrafish during the first trial under IR illumination we noted that they swam differently compared to the behavior of the fish that were tested in light. Specifically, the group of zebrafish ($n = 16$) tested in IR spent $63.4 \pm 4.1\%$ of the time during the first minute of exploration along the wall, so-called thigmotaxis. This was significantly higher compared to $37.1 \pm 6.6\%$ for the group of fish which were allowed to explore the arena in white light ($n = 16$, Mann-Whitney test: $p = 0.0066$, Figure 2.4).

Despite their thigmotactic behavior, the fish that were released in darkness showed a rather linear initial swimming trajectory towards the perimeter of the arena before they started circling along the wall. Thus, in our analysis, the choice of a different crossing radius did not affect the result for the IR group of zebrafish. On the contrary, the group of fish tested in WL did not exhibit such linear initial trajectories, resulting in differently defined bearings depending on the chosen radius, demonstrating an added value of testing the fish in darkness (see Appendix A and B for details).

Medaka exhibited looping behavior in darkness

In contrast to the rather linear initial swimming trajectory observed for zebrafish in darkness, medaka (CAB) showed an immediate looping behavior upon release in the circular arena. This characteristic behavior was recognized by the fish swimming in small circles, sometimes drifting from the center of the arena, in great contrast to the thigmotaxis observed for zebrafish (Figure 2.4).

In order to confirm that this behavior only occurred in absence of visible light, fish were allowed to explore a circular arena for two minutes under both lighting conditions. Indeed, the number of continuous turns, measured by the number of two complete turns sequentially (720° continuous turn), was significantly increased. Specifically, when the fish were exploring the arena for two minutes in light they performed on average 0.36 ± 0.25 continuous turns, compared to 5.5 ± 1.9 turns in darkness ($n = 11$, Wilcoxon signed rank test: $p = 0.016$, Figure 2.5a,c). We further noted that this increase was not due to difference in activity, since the distance traveled by the fish did not significantly differ between the two lighting conditions,

2.1.2 Altered swimming patterns of zebrafish and medaka in darkness

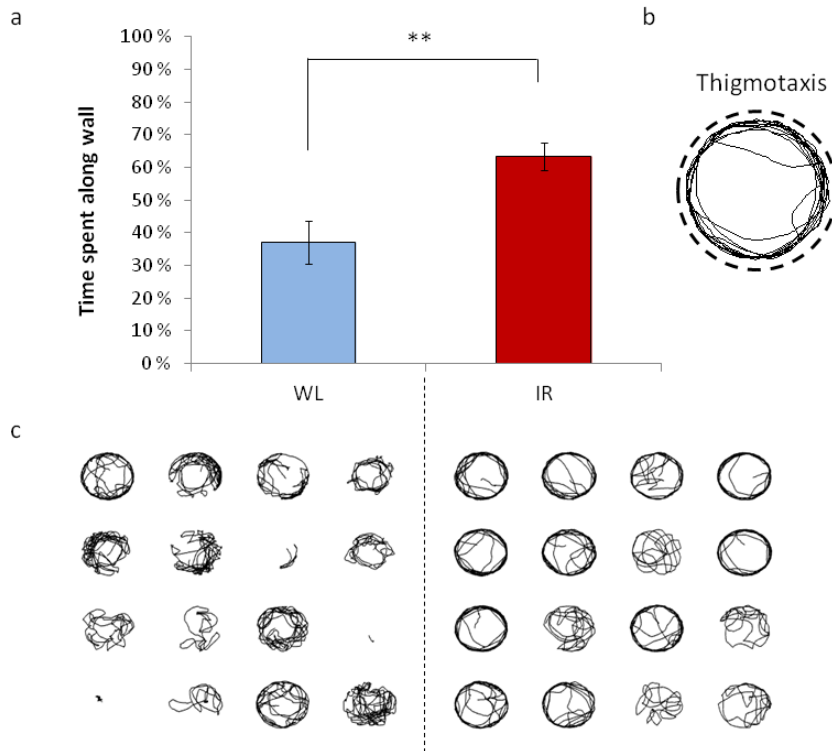


Figure 2.4: Zebrafish changed their swimming strategy in darkness. a) The fish showed an increased thigmotaxis behavior under IR illumination compared to in white light (WL). The time spent along the tank wall for the group under IR illumination was on average $63.4 \pm 4.1\%$, significantly more time than the group in white light ($37.1 \pm 6.6\%$, t-test: $p = 0.0016$). b) Example of thigmotactic behavior. c) Swimming trajectories during one minute for zebrafish in IR and in WL. Adapted from Myklatun, Lauri et al. (2018)

with 154.3 ± 31.4 cm and 189.8 ± 31.9 cm covered in light and dark, respectively (Wilcoxon signed rank test: $p = 0.37$, Figure 2.5b).

The observed looping behavior in medaka made the crossing of the virtual line unsuitable to assess their bearing. However, we could observe that the fish after a while stopped circling and eventually made specific and recognizable contacts with the wall of the arena. Thus, we expanded the radius of the virtual circle to the wall such that the point of this initial contact to the wall could be assessed as their chosen bearing.

2. Results

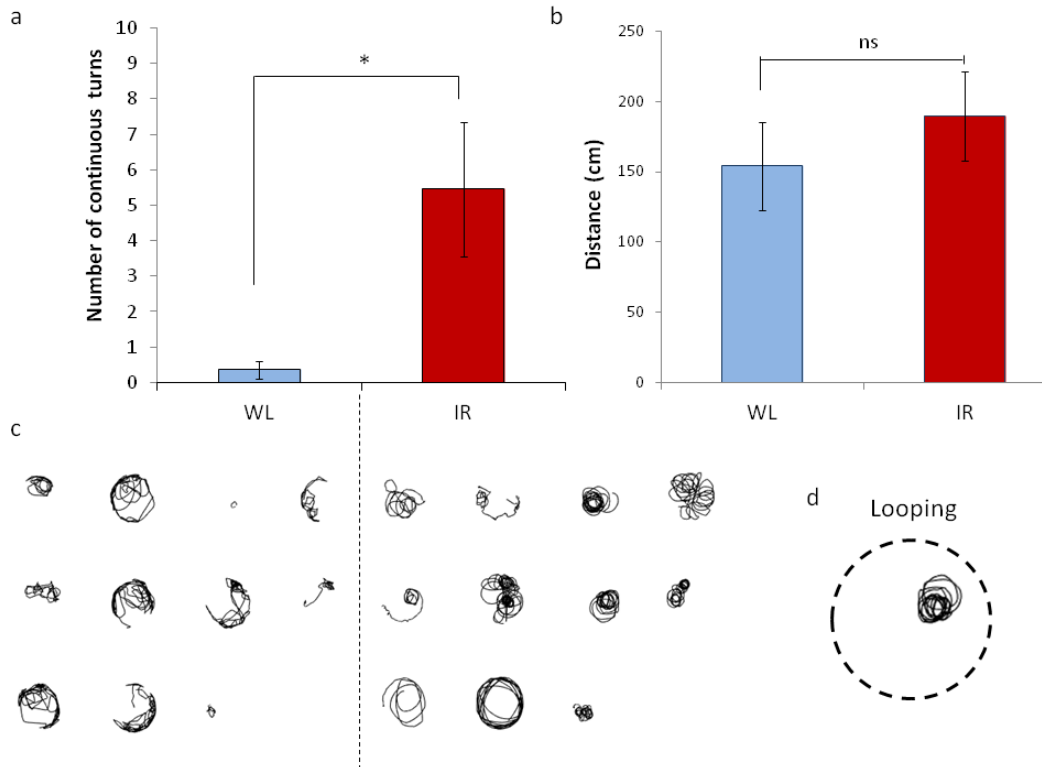


Figure 2.5: Swimming strategy of medaka in darkness. a) Medaka (CAB) showed significantly increased looping behavior in darkness, assessed by the number of continuous turns, defined as two complete turns sequentially. b) The distance traveled was not significantly different between the two lighting conditions. The bar graphs represent mean with SEM and the significance level of the non-parametric Wilcoxon signed rank test (* $p < 0.05$). c) Swimming trajectories for the fish during the two minutes of exploration in WL and IR d) Example of looping behavior. Adapted from Myklatun, Lauri et al. (2018)

2.1.3 Directional preference in the GMF of zebrafish and medaka in darkness

In order to better characterize the magnetoreceptive behavior of zebrafish and medaka, we analyzed their directional preference in the GMF under IR illumination. Furthermore, a response to the altered magnetic field direction in this condition could indicate a light-independent mechanism for magnetoreception, *i.e.* provide evidence for the magnetite hypothesis.

2.1.3 Directional preference in the GMF of zebrafish and medaka in darkness

Zebrafish reoriented according to GMF also in darkness

First, we tested a group of zebrafish belonging to the same cohort as those tested in light (Figure 2.3). This group was kept individually in the presence of light prior to the experiment and then tested under IR illumination (Figure 2.1c). These fish showed a significant axial distribution of their angular differences of bearings ($n = 16$, mean = $64/244^\circ$, V-test(90°): $p = 0.047$; Figure 2.6a). Furthermore, and similar to the case in WL, we did not observe that the group of fish was significantly oriented in their bearing in any of the two conditions (NW: $n = 16$, mean = $96/276^\circ$, Rayleigh test: $p = 0.60$; NE: $n = 16$, mean = $94/274^\circ$, Rayleigh test: $p = 0.38$; Figure 2.6a). Thus, the fish tested in darkness exhibited the same axial response to the shift of the magnetic field direction as we observed in light.

A concern has been raised, that prolonged activation of cryptochromes could still be responsible for the magnetoreceptive mechanism also in darkness, as reported for birds (Nießner et al., 2014; Wiltschko et al., 2014). To this end, we next tested a group of zebrafish from a second genetic cohort under IR illumination, however only after the fish had been kept isolated for one hour in darkness (Figure 2.1c). Also this time we did not observe significant group preferences for any of the two magnetic conditions (NW: $n = 24$, mean = 184° , Rayleigh test: $p = 0.052$; NE: $n = 24$, mean = 324° , Rayleigh test: $p = 0.75$; Figure 2.6b). However, the distribution of reorientation angles of individual fish showed a significant non-uniform distribution with a mean of 125° ($n = 24$, V-test(90°): $p = 0.024$; Figure 2.6b). Thus, the zebrafish of the AB strain seemed able to use the magnetic field information also after an extended period in darkness. Our results thus indicate that these fish likely employ a light-independent mechanism for magnetoreception.

2. Results

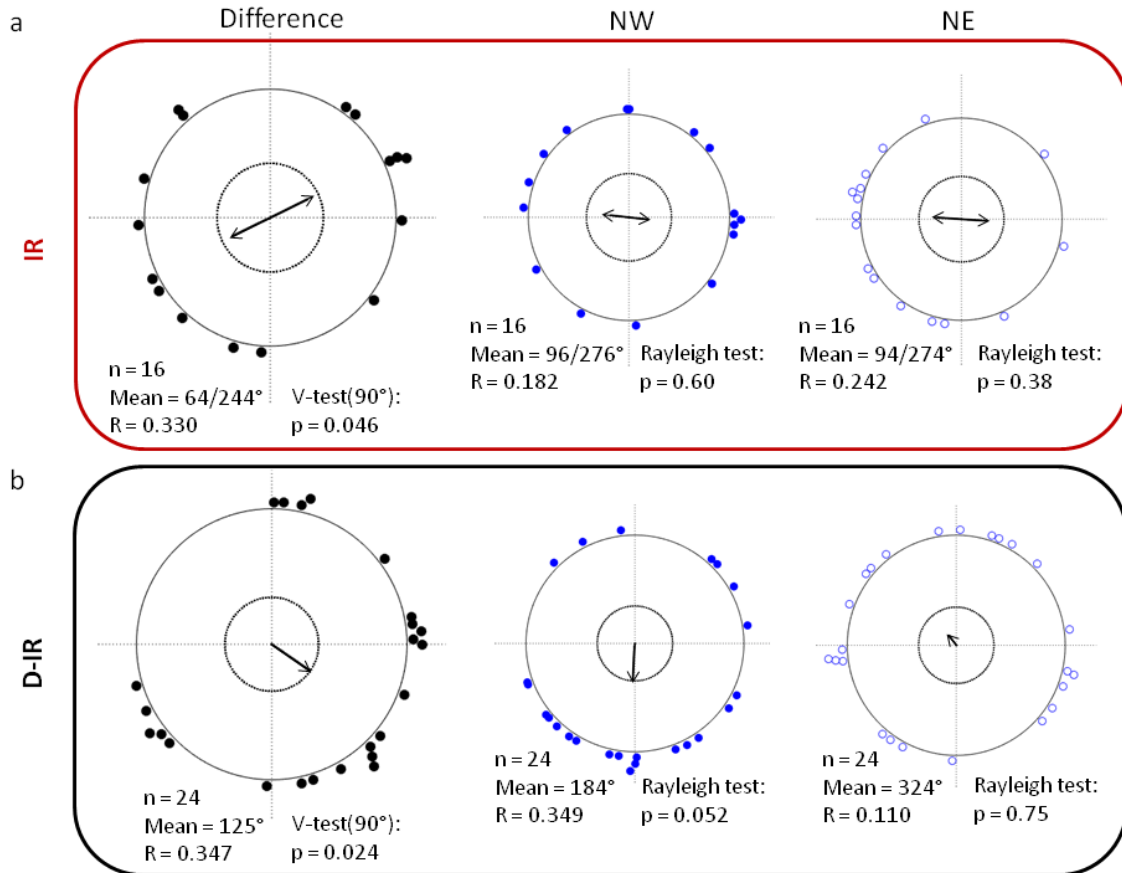


Figure 2.6: Directional preference of zebrafish tested under IR illumination. a) After being kept in light prior to the experiment (IR) zebrafish showed a difference in their bearing with a significant axial distribution (Difference, black dots). A group preference was not observed in the NE condition (NE, open dots), or in NW (NW, closed dots). b) After having been acclimated to darkness before the start of the experiment (D-IR), the fish showed a significant difference in their bearing (Difference, black dots), however no group preference was observed. For all plots each dot represents the bearing (blue) or the angular difference in bearings (black) for a single fish. The central black arrow represents the mean vector and the inner dotted circle represents the significance threshold for the Rayleigh test ($p < 0.05$). The values are given underneath each plot.

2.1.3 Directional preference in the GMF of zebrafish and medaka in darkness

Medaka showed GMF directional preference in darkness

In order to more broadly assess magnetic sensitivity in genetic model fishes, we tested a cohort of sexually mature medaka of the CAB strain in the GMF directional preference assay under IR illumination. Due to their looping behavior in darkness (Figure 2.5), we assessed their initial contact with the wall through an increase of the crossing diameter (8.5 cm). We observed that individual fish significantly changed their bearing between the two magnetic conditions. The reorientation of the bearings showed a significant non-uniform distribution with a mean of 99° ($n = 9$, V-test(90°): $p = 0.045$, Figure 2.7a), close to what was expected from the 90° shift of the magnetic field. Similar to zebrafish, medaka did not show group preference of in any of the two magnetic conditions (NW: $n = 13$, mean = 36° , Rayleigh test: $p = 0.49$; NE: $n = 13$, mean = 111° , Rayleigh test: $p = 0.063$, Figure 2.7a).

Next, as was done for the zebrafish, we controlled for putative prolonged activation of cryptochromes. We tested a second cohort of medaka in the same preference assay after being kept in darkness. Also this time a group preference was not observed in any of the magnetic conditions (NW: $n = 11$, mean = $42/222^\circ$, Rayleigh test: $p = 0.66$; NE: $n = 18$, mean = $125/305^\circ$, Rayleigh test: $p = 0.47$, Figure 2.7b). Interestingly, we observed a axial trend in the reorientation of the individual bearings ($n = 8$, mean = $42/222^\circ$, V-test(90°): $p = 0.061$, Figure 2.7b). Taken together these results indicate that also medaka are able to employ the magnetic field information when orienting in darkness. Thus, in conclusion, we found support for a light-independent magnetoreception pathway in both fish species tested.

2. Results

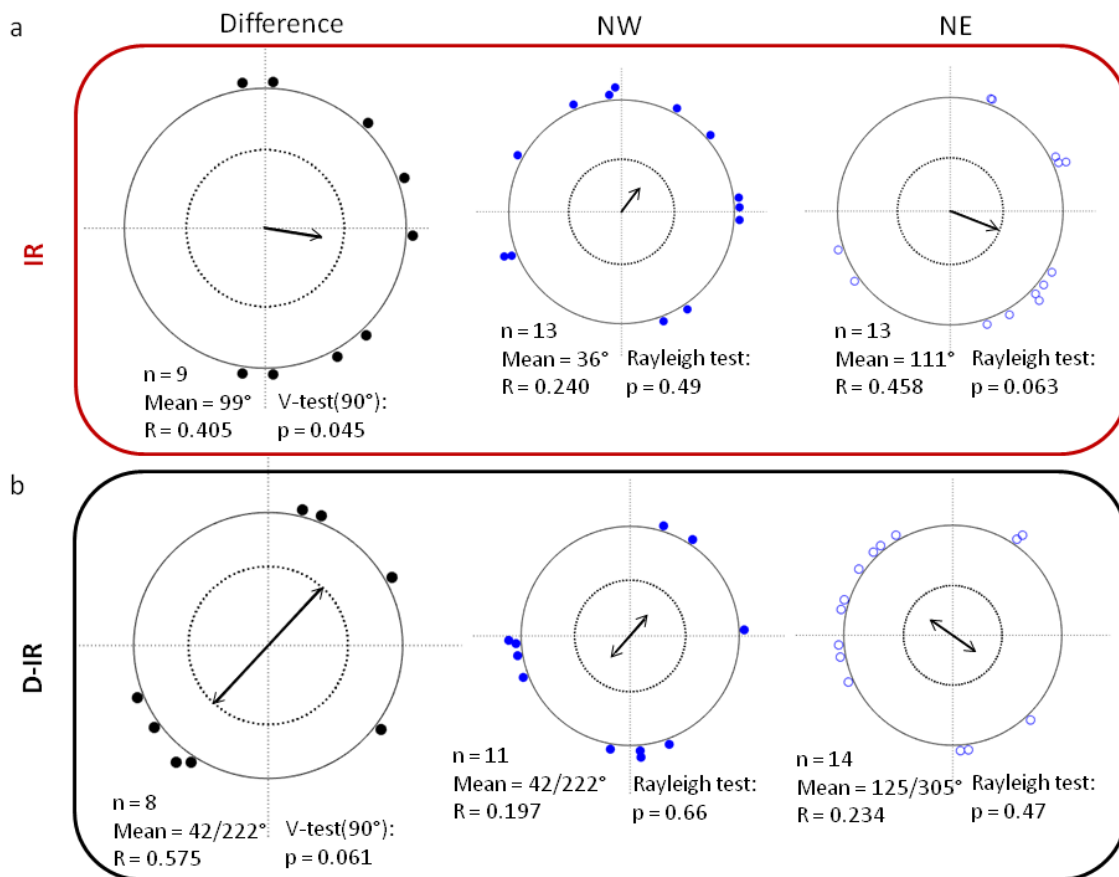


Figure 2.7: Directional preference of medaka tested under IR illumination. a) After being kept in light prior to the experiment medaka showed a significant difference in their bearing (Difference, black dots), however no group preference was observed in the two magnetic conditions (NW, closed dots; NE, open dots). b) Similarly, after being adapted to darkness before the start of the experiment, an individual change in bearing was observed, but no group preference. For all plots each dot represents the bearing (blue) or the angular difference in bearings (black) for a single fish. The central black arrow represents the mean vector and the inner dotted circle represents the significance threshold for the Rayleigh test ($p < 0.05$). The values are given underneath each plot.

2.1.4 Evaluation of magnetotaxis in *C.elegans*

Only recently was magnetosensitivity reported in the invertebrate genetic model organism *C.elegans* (*Caenorhabditis elegans*) Vidal-Gadea et al. (2015). These nematode worms were for instance shown to have a preference for the presence of a magnetic field in darkness. Due to their simple nature, they could be a valuable organism to study the molecular mechanisms of magnetoreception, and potentially also for gaining insights into magnetite production in an organism.

No evidence for magnetotaxis behavior in *C.elegans* in darkness

In order to validate findings by Vidal-Gadea et al. (2015) I used the behavioral assay for magnetotaxis as described in the paper. Specifically, I tested worms of the WT strain N2, which were released at the center of a circular test plate and allowed to move freely. Two target circles were placed equidistantly from the center (magnetic (M) and control (C), Figure 2.8a). Worms that reached the circles within 30 minutes were counted and the magnetotaxis index calculated ($MI = (M-C)/(M+C)$). In addition, I evaluated the relative amount of worms that had reached the two sides. The test plates were covered with aluminum foil to ensure that the test was performed in darkness.

Unfortunately, contrary to what was reported by Vidal-Gadea et al. (2015) I did not observe evidence for magnetotaxis behavior in *C.elegans* of the N2 strain. There was a large variability in the magnetotaxis index, which had a mean of 0.022 ± 0.069 . Although I did observe a small increase, the average number of worms on the magnetic side was 51.1 ± 3.5 %, not significantly different from the control which had 48.9 ± 3.5 % of the worms (mean \pm SEM, t-test: $p = 0.74$) (Figure 2.8).

2. Results

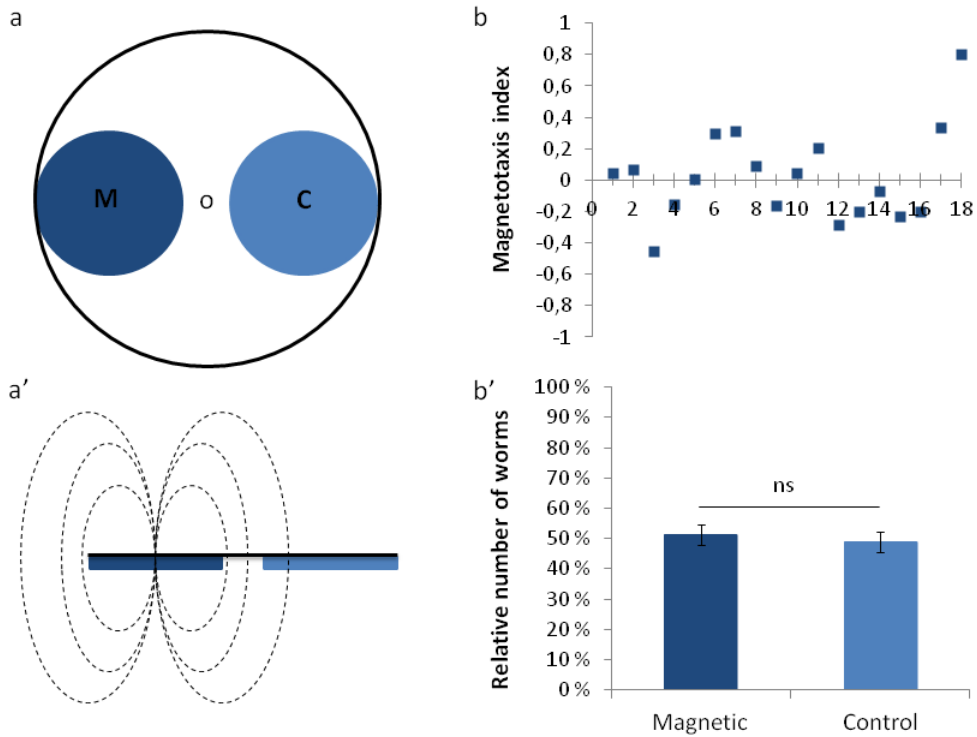


Figure 2.8: *C.elegans* do not perform magnetotaxis behavior in darkness. Magnetotaxis assay seen from above (a) and the side (a'). Worms were released in the center of the plate (o) and the number of worms in each target area (magnetic (M) and control (C)) was counted. b) The magnetotaxis index has a large variability with a mean of 0.022 ± 0.069 . b') The relative number of worms on the control side was 48.9 ± 3.5 %. The magnetic side did not have significantly more worms with a mean of 51.1 ± 3.5 % (t-test: $p = 0.74$).

2.2 Candidate magnetoreceptor cells

It is predicted from the magnetite hypothesis (section 1.2.3) that magnetite is produced in some organisms as part of a sensory system which interacts with the geomagnetic field (Kirschvink et al., 2001). The identification of such putative magnetoreceptor cells could lead to the understanding of the initial step in the neuronal signal transduction. In addition, insights into magnetite production would be of high value for magnetogenetics, which aims at genetically rendering neurons magnetic in order to control their activity via magnetic fields. Thus, I aimed at isolating such candidate magnetoreceptor cells in vertebrate genetic model organisms, for which I had found evidence for light-independent magnetoreception.

2.2.1 Rotation assay for identification of candidate magnetoreceptors

Candidate magnetoreceptor cells have previously been isolated and characterized from the olfactory epithelium of rainbow trout (Eder et al., 2012). This was done using a rotation assay which could differentiate permanently magnetized cells from induced magnetic cells (Figure 2.9a). Thus the first step in my search for magnetic cells in fishes was to establish a similar rotation assay. This was done in close collaboration with Dr. Stephan Eder, who designed and produced the electromagnetic coils.

Two pairs of coils were fitted orthogonally around the objective of an inverted microscope in order to focus their magnetic field on the observed cells (Figure 2.9b,c). A rotating magnetic field was thus generated by a sine wave function with a 90° phase shift between the two coil pairs (Figure 2.9d). In some cases only one coil pair was used in order to employ the field-flip test, where a 180° change instead of a continuous rotation of the cells was achieved. This resulted in a stronger discrimination between cells with permanent and induced magnetization (Eder et al., 2012).

A moderate field strength of 2 mT (peak value) was used in order to generate sufficient torque on the cells. At the same time the field was weak enough to avoid saturated magnetization of other iron rich cells. A low frequency was used to allow cells to follow the rotation of the applied magnetic field. Appropriate settings in

2. Results

the assay was confirmed by the rotation of clearly magnetic objects (Figure 2.10), whereas iron rich cells, such as erythrocytes and macrophages, were never observed to rotate.

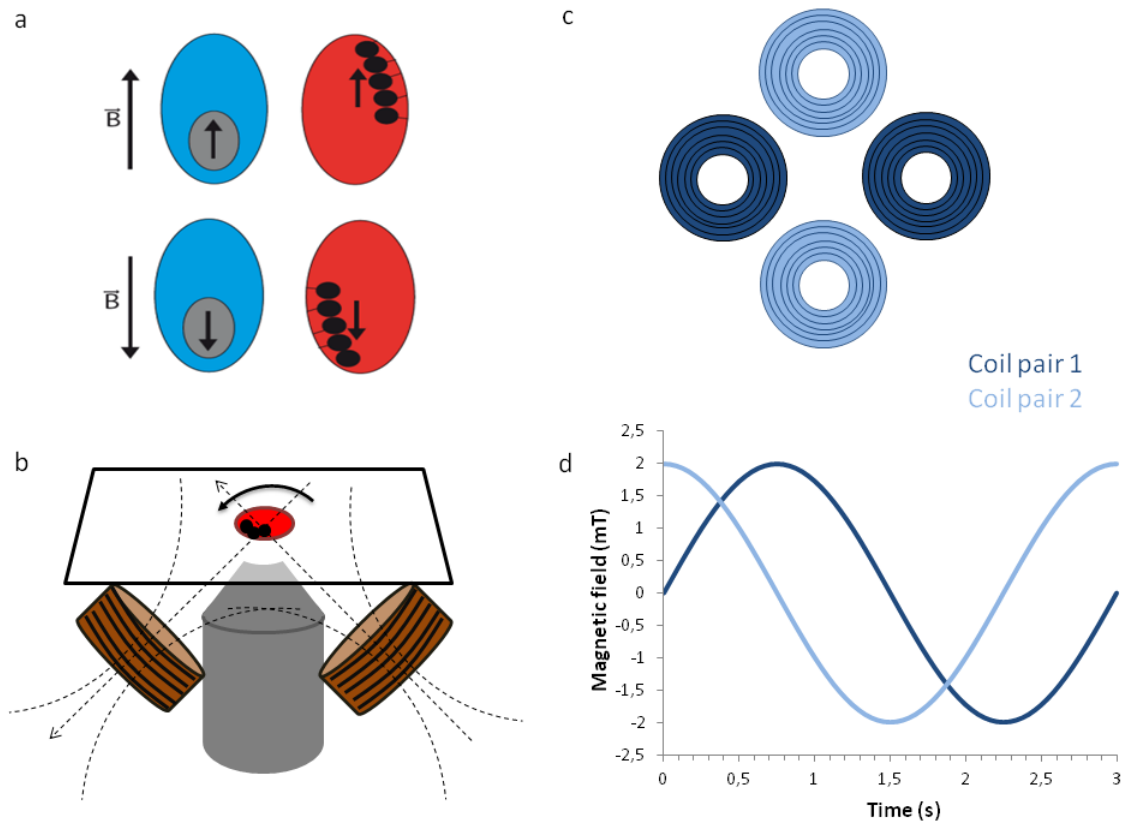


Figure 2.9: Rotation assay for identification of magnetic cells. a) Only cells (red) containing permanently magnetized material attached to the cell (black) would rotate with the magnetic field. Cells (blue) with inducible magnetic material (gray) would only change their internal magnetization. b) Coils were placed around the objective of an inverted microscope in order to focus their magnetic field on the observed cells. Only one coil pair is shown. c) Two pairs of coils, placed orthogonally, were used to rotate the magnetic field. d) The magnetic field generated by the coils follows a sine function, with a 90° phase shift between the two pairs to achieve the rotation. A moderate magnetic field of 2 mT was used at 0.3 Hz.

2.2.2 Candidate magnetoreceptor cells in fishes

Zebrafish have previously been shown to exhibit magnetosensitivity (Shcherbakov et al., 2005; Takebe et al., 2012; Krylov et al., 2016), and are therefore an interesting genetic model organism for investigating the biophysical mechanisms underlying this sense. During my PhD project I showed, together with Dr. Stephan Eder and Dr. Antonella Lauri, that both zebrafish and medaka can use the magnetic field information under IR illumination, even after an extended period in darkness (see section 2.1.3). As these results indicated the potential involvement of magnetite in the sensing process, I searched for candidate magnetoreceptor cells in these fishes.

Other teleost fishes, such as the Atlantic and Pacific salmon, are known to perform long distance migrations across the ocean in order to return to their native river for spawning, years after they first migrated outwards. These fish likely use the GMF information for this challenging navigational task (Putman et al., 2013). Indeed, they have been reported to change their behavior according to the direction of a magnetic field, also in darkness (Quinn et al., 1981). Furthermore, magnetic material, probably SD magnetite has been identified and isolated from tissues of various species of salmon (Kirschvink et al., 1985; Mann et al., 1988; Moore et al., 1990) (Table D.1). Although not a genetic model organism, isolation of cells from these fishes could also contribute to our understanding of magnetoreception.

Thus, in a collaboration with the Norwegian Institute for Nature Research (NINA) I performed a search for candidate magnetoreceptor cells also in wild Atlantic salmon (*Salmo salar*) from the river Imsa. Both young and returning fish (parr and adult, autumn 2013) were investigated, in addition to fish caught upon initial outward migration (smolt, spring 2014).

Cells with magnetic properties in zebrafish

Candidate magnetoreceptor cells have previously been isolated from the olfactory rosettes of trout (Eder et al., 2012), and magnetite have been found in the lateral line and in the head region of salmon (Mann et al., 1988; Moore et al., 1990). Thus I decided to isolate samples from these regions from all the fish species. In addition, for zebrafish and medaka I analyzed the whole fish or the head region. Samples from muscles were taken as control since magnetite has not been reported in these

2. Results

tissues. The tissue samples were gently dissociated to obtain solutions with single cells. After magnetic enrichment of the sample the cells were screened with the rotation assay (Figure 2.9). The laboratory fish were stained with both membrane and nuclear marker before screening in order to confirm the cellular identity of potential magnetic objects.

For zebrafish, in addition to searching for magnetic cells in the AB strain, for which we had demonstrated a behavioral response to magnetic field changes, I also took samples from the Casper and Nacre strains which lack pigments. Despite the fact that the experiment was repeated several times, across fish strains, age, gender and season, I could not reliably find cells with magnetic properties in any region in the zebrafish. The number of cells responding to the rotating magnetic field in each of the regions is summarized in Table 2.1, and two examples are shown in Figure 2.10.

I searched for magnetic cells in the medaka cohort which was shown to respond to the magnetic field change in IR after the extended period in darkness (Figure 2.7), because this finding hints towards the magnetite hypothesis. However, I did not observe cells that followed the magnetic field in the field-flip assay in any of the samples taken from these fish.

Furthermore, I did not observe magnetic cells in any of the samples of the young parr or adult salmon. And although I optimized the dissociation protocol for smolt (see Methods and materials for details), I still did not observe cells which responded to the magnetic field in the olfactory epithelium, ethmoid region or lateral line of these fish.

Extracellular objects with magnetic properties in zebrafish, medaka and salmon

Although magnetic cells proved hard to find, I reliably detected extracellular objects with magnetic properties in both zebrafish and medaka. These objects responded to the rotation and the field-flip test of the applied magnetic field (Figure 2.9). Moreover, the objects appeared black in the transmission microscope, and were strongly reflecting in reflection mode, indicating a crystal structure (Figure 2.10 and D.1). These are all properties consistent with magnetite. The magnetic objects were observed across all tissue samples, although, rarely found in the muscle samples

2.2.2 Candidate magnetoreceptor cells in fishes

Table 2.1: Candidate magnetoreceptor cells found in zebrafish and medaka

Sample	Fish assessed	Magnetic cells
Zebrafish		
Olfactory rosettes	36	1
Brain	8	0
Skin (Lateral Line)	8	0
Muscle	8	0
Head (w/o eyes)	23	1
Body (w/o inner organs)	31	2
Whole fish (w/o inner organs and eyes)	21	0
Medaka		
Olfactory rosettes	8	0
Brain	8	0
Head (w/o eyes)	22	0
Body (w/o inner organs)	14	0

of zebrafish. Similar objects were also observed in all tissue samples that were investigated from medaka.

Interestingly, I also found extracellular objects similar to those observed in the laboratory fish in all three stages of salmon investigated (Figure 2.10 and D.3). The objects were opaque and shown to be permanently magnetized through the field-flip test, as described above (Figure 2.9). The objects were mainly found in the lateral line samples and varied in shape and size, between 1-10 μm . Interestingly, many of the objects in the lateral line of parr were attached to clusters of cells (Figure D.3). However, this was not observed in the older stages. Parr was the only stage of salmon where I found a few of the objects also in the rosettes. Furthermore, magnetic objects were not observed in the dissociated muscle tissue in any of the stages, or in the samples from the ethmoid region. However, the latter could possibly be due to poor dissociation of this tissue.

2. Results

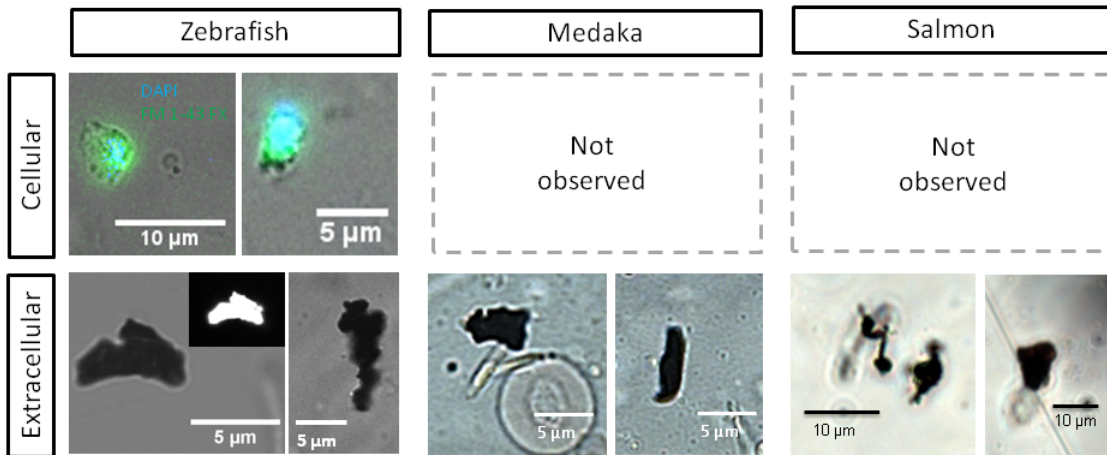


Figure 2.10: Magnetic material observed in fishes. Two magnetic cells isolated from zebrafish, both stained with a nuclear (DAPI, blue) and membrane marker (FM 1-43 FX, green) to confirm their cellular identity. Extracellular objects with magnetic properties were observed across all fish species.

2.3 Microfluidic magnetic sorting of cells

For magnetogenetics, isolation and characterization of magnetic cells is important for subsequent analysis of the cell properties. It is crucial, however, that this step does not induce magnetic contaminations in the samples. To this end, I developed a microfluidic magnetic sorting system to be used both for naturally occurring candidate magnetoreceptor cells as well as bioengineered cells. The performance of the system was tested with macrophages incubated with magnetite nanoparticles, theoretically yielding cells with magnetic moments in the range which has been reported for candidate magnetoreceptor cells (~ 10 fAm², (Eder et al., 2012)). Further, the system was tested for bioengineered cells, in collaboration with Felix Sigmund, a fellow PhD student in the Westmeyer laboratory. Specifically, cells bioengineered to express a surface marker allowing binding of a variety of magnetic particles (Sigmund et al. *in prep*) were successfully sorted. Next, I tested the system for unlabeled magnetotactic bacteria (MTB), which contain chains of biogenic magnetite (Frankel et al., 1979; Uebe & Schüler, 2016). Finally, I validated the microfluidic system for cells dissociated from primary tissue from zebrafish. The results are summarized in Table 2.2.

Table 2.2: Summary of microfluidic magnetic separation result

Chip	Cells	Labeling (nm)	Flow rate (μ l/min)	Efficiency (%)	Reference
2	Macrophages	magnetite, 100	0.5-2	21-90	Myklatun et al. 2017
2	Bioengineered	magnetite, 100	1	52	Sigmund et al. ^a
2	Bioengineered	magnetite, 30	1	23	Sigmund et al. ^a
2	Bioengineered	cobalt, 30	1	18	Sigmund et al. ^a
2	Bioengineered	maghemite, 5	1	16	Sigmund et al. ^a
1	MTB	-	0.1	-	Myklatun et al. 2017
2	Rosettes	-	0.5	-	

^a*in prep.*

2. Results

2.3.1 Microfluidic chip design

For enrichment of cells with magnetic properties I developed a microfluidic magnetic sorting system where there was no contamination risk during the separation process due to no contact between sample and magnetic material. This was achieved by filling a ferrofluid into a channel running in close proximity to the sorting channel (Figure 2.11). In the presence of an external magnetic field, from permanent magnets (NdBFe), the nanoparticles in the ferrofluid aligned, thus extending a rapidly decreasing magnetic field into the nearby channel (Figure 2.11 and 2.12).

The sorting channel had two inlets such that both buffer and the cells containing solution could be injected side by side, with the cells furthest from the ferrofluid (Figure 1.10). However, in the presence of the magnetic field gradient, generated by the permanent magnets and the ferrofluid, cells with sufficient magnetic properties experienced a force orthogonal to the flow direction. This resulted in movement of these cells into the buffer flow, and thus a separation from the non-magnetic cells within the microfluidic chip.

The distance between the ferrofluid and the sample was minimized in order for the cells to be in the steep gradient region as shown in Figure 2.12. The dimensions were in my case limited by the size of the cells as well as the production methods, yielding a channel width twice the height. In order to enable sorting of eukarotic cells the dimensions of the channels were increased compared to the dimensions used for MTB (Figure 2.11, black and gray, respectively). The increased distance to the sample was compensated by a ferrofluid with higher density of magnetic nanoparticles which created a stronger magnetic field gradient 2.12.

2.3.2 Simulations of magnetic field in sorting system

First, I performed simulations of the magnetic field in the channels in order to better predict the performance of the system (Figures 2.11 and 2.12). The magnetic field intensity in the system was estimated with Finite Element Method Magnetics (FEMM) using realistic values for the input parameters, such as the strength of the external NdFeB magnet (40 MGOe) and the distance between the magnet and the channel (1 mm). The magnetic field in the sorting channel is mainly depending on concentration of magnetite nanoparticles in the ferrofluid. Thus, the magnetization

2.3.2 Simulations of magnetic field in sorting system

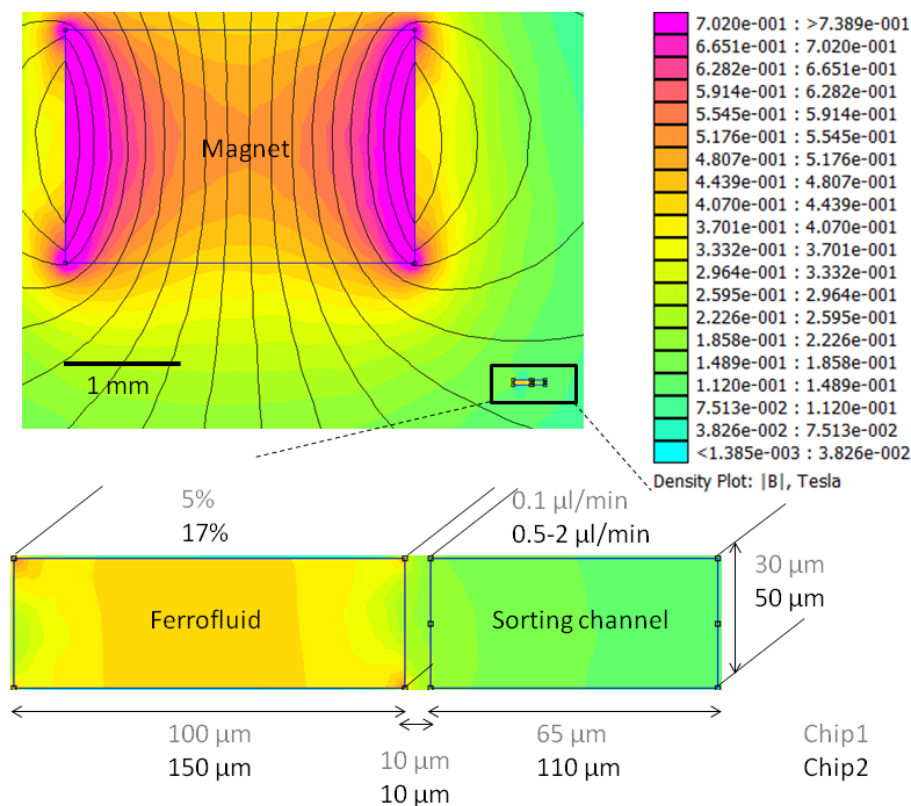


Figure 2.11: Microfluidic magnetic sorting design. The microfluidic channels were placed 1 mm away from the NdFeB magnet with strength 40 MGOe. The size of the channels are indicated for the two chip designs, Chip1 (gray) was used for bacteria while Chip2 (black) was used for larger vertebrate cells. Simulation result shown for Chip2 with a ferrofluid containing 15% magnetite particles. Adapted from Myklatun et al. (2017)

curve of a ferrofluid of different concentrations was calculated from Equation 1.4 and 1.5 (Figure 1.11) and simulations performed for two concentrations. For comparison simulations were performed also for an empty side channel.

The simulations showed that in the presence of a ferrofluid the magnetic field gradient changed across the sorting channel, whereas it remained constant at 65 T/m with only the magnet present (Figure 2.12). The effect of a ferrofluid and its particle concentration was most evident at the wall closest to the ferrofluid. Here a standard ferrofluid with 5% particles could generate a magnetic field gradient of 1050 T/m, 16 times greater than without. In the case for a more dense ferrofluid

2. Results

consisting of 15% particles a gradient of 1750 T/m was achieved, thus amplifying the magnetic gradient 27 times. This gradient was experienced by the cells in the final step of the separation process, ensuring that sorted cells exited with the buffer.

Further away from the wall the magnetic field gradient was reduced. At a distance approximately 50 μm from the wall the gradient was 230 T/m and 480 T/m, for a low and high concentration ferrofluid, respectively (Figure 2.12). This distance corresponds to the center of a sample flow in Chip1, and thus the gradient the bacterial cells experienced when initially introduced in the channel was three times greater than with the magnet only (ferrofluid with 5% particles was used).

At the wall furthest away from the ferrofluid in Chip2 the high concentration ferrofluid (15% particles) allowed for generation of a gradient which was still higher than what could be achieved with the magnet alone (Figure 2.12). In this case the gradient was 210 T/m, again ensuring that cells in the sample flow experience a three-fold increase compared to the case without the presence of a ferrofluid. In the region across the sample flow in Chip2 the magnetic field gradient was more linear and thus the force acting on the cells in the initial phase of the separation process remained constant.

2.3.3 Performance of microfluidic magnetic sorting system

Magnetite loaded macrophages as a model

When macrophages are incubated with magnetic nanoparticles these are phagocytosed by the cells and internalized (Figure 2.13a). The macrophages thus serve as a good model for the candidate magnetoreceptor cells, which are postulated to contain magnetite nanoparticles. Synthetic particles with a hydrodynamic diameter of 100 nm were used in the experiments, since these have a magnetite core of 30 nm, which is similar to crystals observed in animals (Shaw et al., 2015) and magnetotactic bacteria (Uebe & Schüller, 2016). The accumulation of particles should yield a high magnetic moment of the cells, within the range reported for candidate magnetoreceptor cells in fish ($\sim 10 \text{ fAm}^2$) (Eder et al., 2012).

The magnetized macrophages were used to evaluate the performance of Chip2 which had dimensions in order to enable sorting of larger vertebrate cells (Figure 2.11). Monitoring of the separation process was done at the observation point

2.3.3 Performance of microfluidic magnetic sorting system

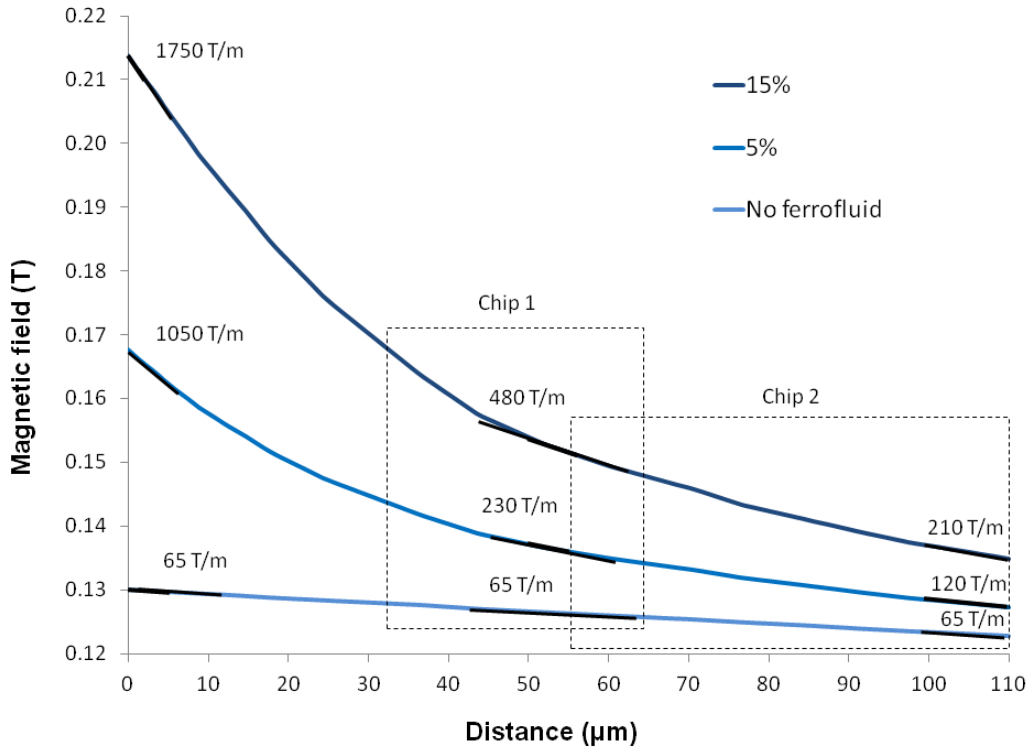


Figure 2.12: Magnetic field simulations with FEMM for different concentrations of magnetite nanoparticles in the ferrofluid. The resulting magnetic field across the sorting channel, given a 40 MGOe neodymium magnet placed 1 mm away from the ferrofluid. Values for the magnetic field gradient are indicated at different points in the channel. The difference in gradient was most evident at the wall closest to the ferrofluid. The two dashed boxes indicate the initial position of cells in Chip 1 and Chip 2. Adapted from Myklatun et al. (2017)

halfway through the chip. The number of cells in the sorting channel was quantified for different sample flow rates, using a program custom written by Dr. Michele Capetta. The cells that were observed in the buffer flow (upper half of the channel) in the presence of the external magnet was considered as successfully sorted, and thus the sorting efficiency was defined as the relative number of cells in the buffer flow.

First, in order to ensure that laminar flow was established prior to starting the separation process, the flow of cells in the absence of the external magnet was observed. For the lowest sample flow rate of $0.5 \mu\text{l}/\text{min}$ only $1 \pm 1 \%$ of the cells were observed in the buffer flow, thus verifying a low rate of false positives in the

2. Results

system. When the permanent magnets were placed close to the ferrofluid the relative amount of cells in the buffer flow halfway through the channel was increased to $90 \pm 1 \%$, showing that a majority of these cells could be sorted in the system (Figure 2.13b).

As expected due to shorter interaction time of the cells with the magnetic field gradient, the sorting efficiency was reduced for higher flow rates. At sample flow rate $1 \mu\text{l}/\text{min}$ the relative number of sorted cells halfway through the chip was $69 \pm 6 \%$, while at $2 \mu\text{l}/\text{min}$ $21 \pm 4 \%$ of the cells were sorted (Figure 2.13c). At these flow rates the amount of cells in the buffer flow in the absence of the external magnet was $2 \pm 1 \%$.

In order to also experimentally characterize the effect of the ferrofluid on the sorting efficiency I assessed macrophages in a device with an empty side channel. In this case a sorting efficiency of $6 \pm 1 \%$ was observed for a flow rate of $1 \mu\text{l}/\text{min}$, in the presence of the external magnet. Thus a 10-fold decrease in sorting efficiency was observed compared to separation in presence of the ferrofluid. Furthermore, when comparing the position of the cells in the channel, the shift in mean position in the presence of a magnet was 2.9 times greater if the ferrofluid was present in the side channel (Figure 2.13d), indicating three-fold amplification of the magnetic force.

2.3.3 Performance of microfluidic magnetic sorting system

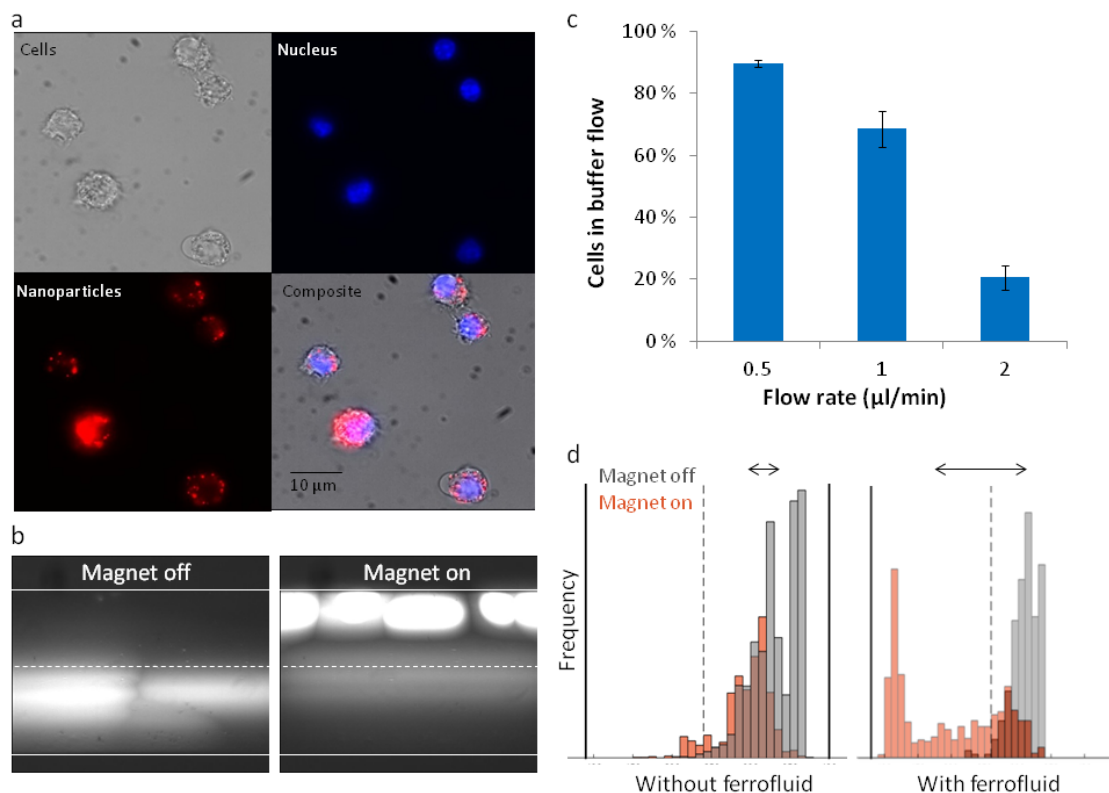


Figure 2.13: Microfluidic magnetic sorting of macrophages. a) The cells were loaded with magnetic particles (red) and labeled with a fluorescent nuclear stain (blue). b) Maximum intensity projection images of the cells moving in the sorting channel without (left) and in the presence of the external magnet (right) at a sample flow rate of $0.5 \mu\text{l}/\text{min}$. The width of the channel was $110 \mu\text{m}$ c) The relative number of cells in the buffer flow in the presence of the external magnet for three different sample flow rates as indicated in the figure. Graphs represent mean with SEM over trials. d) Distribution of position of cells in the channel in presence (orange) and absence (gray) of the external magnet. Without the ferrofluid present in the side channel (left) the shift in mean position (arrows) was 2.9 times smaller than in the presence of a ferrofluid (right). The walls and midline of the channel is marked with solid and dotted lines, respectively. Adapted from Myklatun et al. (2017).

2. Results

Bioengineered cells expressing surface markers

Towards magnetogenetics there are also semigenetic approaches being developed. These include genetic control of surface markers and labeling with magnetic particles. In collaboration with Felix Sigmund, a fellow PhD student, the microfluidic magnetic sorting system was tested for cells expressing an avidin marker on the surface (Sigmund et al. *in prep*). This marker allowed the cells to bind to biotinylated particles of different sizes and magnetic materials of the core (see Materials and methods for details, Table 5.7). The cells were labeled and sorted with a sample flow rate of $1 \mu\text{l}/\text{min}$ in Chip2.

First, cells labeled with magnetite particles were tested. The particles were the same as the ones used in the macrophage experiments described above (100 nm, Figure 2.13). In absence of the external magnets a laminar flow was observed with $1 \pm 1\%$ of the cells in the buffer flow. When the magnets are added $52 \pm 10\%$ of the cells were moved out of the sample flow at the observation point halfway through the sorting channel, thus representing a significant increase (t-test, one tail: $p = 0.001$) (Figure 2.14a).

Other particles tested proved to yield less efficient sorting, however an increase of the number of cell in the buffer flow was always observed in the presence of the external magnets. With smaller magnetite particles (30 nm, Figure 2.14b) the relative number of cells in the buffer flow was increased from $9 \pm 4\%$ to $23 \pm 8\%$ when the magnet was added (t-test, one tail: $p = 0.07$). Similarly, 30 nm cobalt particles resulted in the same trend with an increase in the amount of cells that were moved out of the sample flow; $4 \pm 4\%$ and $18 \pm 8\%$ in absence and presence of external magnets, respectively (t-test, one tail: $p = 0.09$, Figure 2.14c). Finally, when 5 nm maghemite particles were bound to the cell surface a significant increase of sorted cells, from $4 \pm 2\%$ to $16 \pm 3\%$, was observed when the external magnets were placed (t-test, one tail: $p = 0.01$, Figure 2.14d).

2.3.3 Performance of microfluidic magnetic sorting system

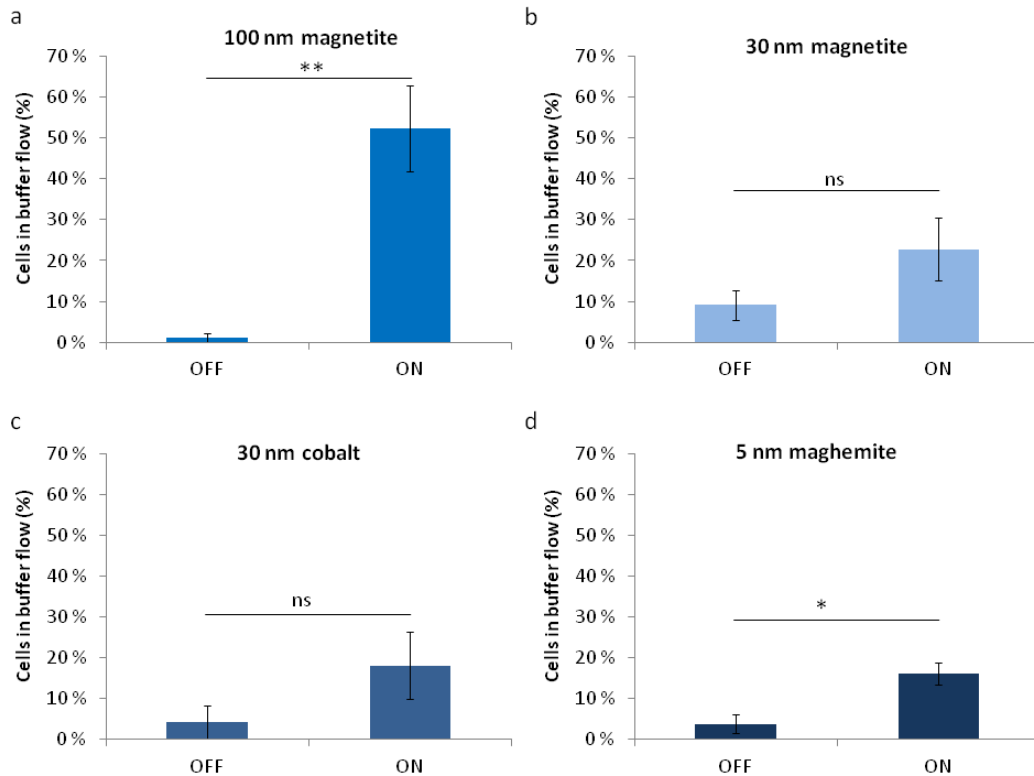


Figure 2.14: Microfluidic magnetic sorting of bioengineered cells expressing a surface marker. Different magnetic particles were bound to the cells: 100 nm magnetite (a), 30 nm magnetite (b), 30 nm cobalt (c) and 5 nm maghemite (d). Graphs represent mean with SEM over trials and the result of a one tailed t-test comparing the relative number of cells in the buffer flow in the absence (OFF) and presence (ON) of the external magnets (* $p < 0.05$, ** $p < 0.01$). Sample flow rate was $1 \mu\text{l}/\text{min}$ for all trials.

Magnetotactic bacteria

In order to evaluate the performance of the sorting system for naturally occurring magnetic cells, I used MTB of the wildtype strain *Magnetospirillum gryphiswaldense* (MSR-1) (Schleifer et al., 1991). These bacteria contain one chain of magnetite particles per cell and have an estimated magnetic moment in the order of 0.1 fAm^2 (Schüler et al., 1995; Ērglis et al., 2007; Le Sage et al., 2013) (Figure 2.15a). For these experiment I used Chip1 with reduced dimensions. The side channel was filled with a commercial ferrofluid with an assumed magnetite concentration of $\sim 5\%$.

The flow of fluorescently labeled bacteria was observed halfway through the

2. Results

microfluidic sorting channel (Figure 2.15b). To ensure that laminar flow was established in the system the flow was observed first in the absence of the external permanent magnets, before these were placed and the shift of the sample flow was observed (one trial). Trials were discarded if any disturbance in the system perturbing the laminar flow was observed. Moreover, to control for variation in the position of the external magnets, these were replaced between each trial.

Due to the small dimensions of the sorting channel, and to allow sufficient interaction time of the cells with the magnetic field gradient, a sample flow rate of $0.1 \mu\text{l}/\text{min}$ was used. It was evident from the videos that some bacteria were flowing in the buffer flow and along the wall closest to the ferrofluid in the presence of the external magnet (Figure 2.15b). This indicates an efficient sorting of the fraction of bacteria with highest magnetic moments.

Furthermore, similar to the analysis performed by Lin et al. Lin et al. (2007) a shift in the flow of bacteria was observed in the presence of the external magnet for three trials taken together. As shown from the histograms in Figure 2.15c, the mean position of the bacterial flow was $29.7 \pm 0.2 \mu\text{m}$ from the wall furthest from the ferrofluid in the absence of the magnet (OFF, blue). When the magnet was placed on the device the mean position of the sample flow was $41.8 \pm 0.2 \mu\text{m}$, thus crossing the midline of the sorting channel (Figure 2.15c, ON, red). Thus a significant shift of $12.1 \mu\text{m}$ towards the buffer was observed in the presence of the external magnet compared to the laminar flow case without the magnet (t-test: $p < 0.001$).

2.3.3 Performance of microfluidic magnetic sorting system

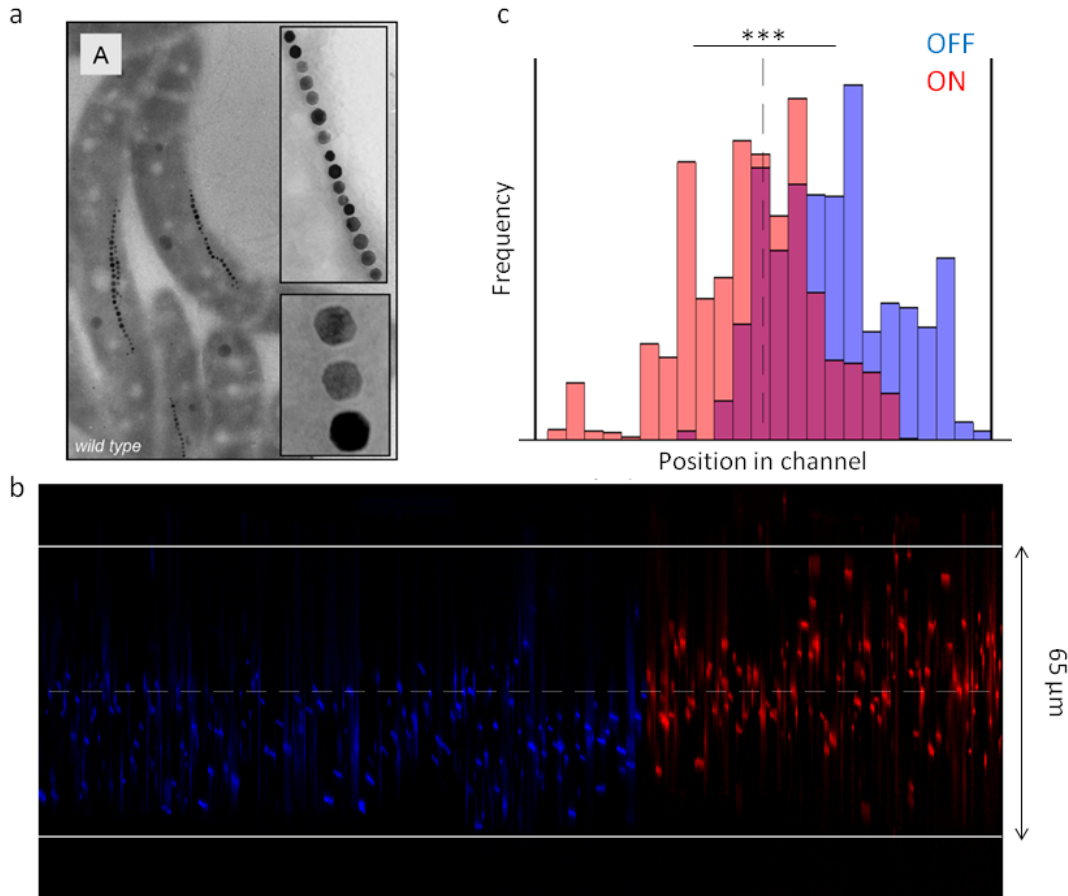


Figure 2.15: Microfluidic magnetic sorting of magnetotactic bacteria in Chip1. a) *Magnetospirillum gryphiswaldense* contain a chain of magnetite crystals, from Faivre & Schüler (2008). b) Fluorescent signal from bacteria halfway through the microfluidic channel in absence (blue) and presence (red) of the external magnet. c) The mean position of sample flow was significantly shifted by $12.1 \mu\text{m}$ towards the ferrofluid in the presence of the magnet (ON, red) compared to without the magnet (OFF, blue) (t-test: $p < 0.001$). Data pooled from three trials, with multiple placements of the external magnet. Adapted from Myklatun et al. (2017)

2. Results

Cells from zebrafish olfactory rosette

Finally, since the sorting device was developed for the search of candidate magnetoreceptor cells I validated the microfluidic system for cells dissociated from primary tissue. Specifically, I observed the behavior of cells from the olfactory epithelium (rosettes) of zebrafish. Laminar flow conditions were observed throughout the experiment. As expected, based on the lack of observed magnetic cells in the rotation assay (Figure 2.10), I also did not observe an increase of cells in the buffer flow in the presence of the magnet (Figure 2.16).

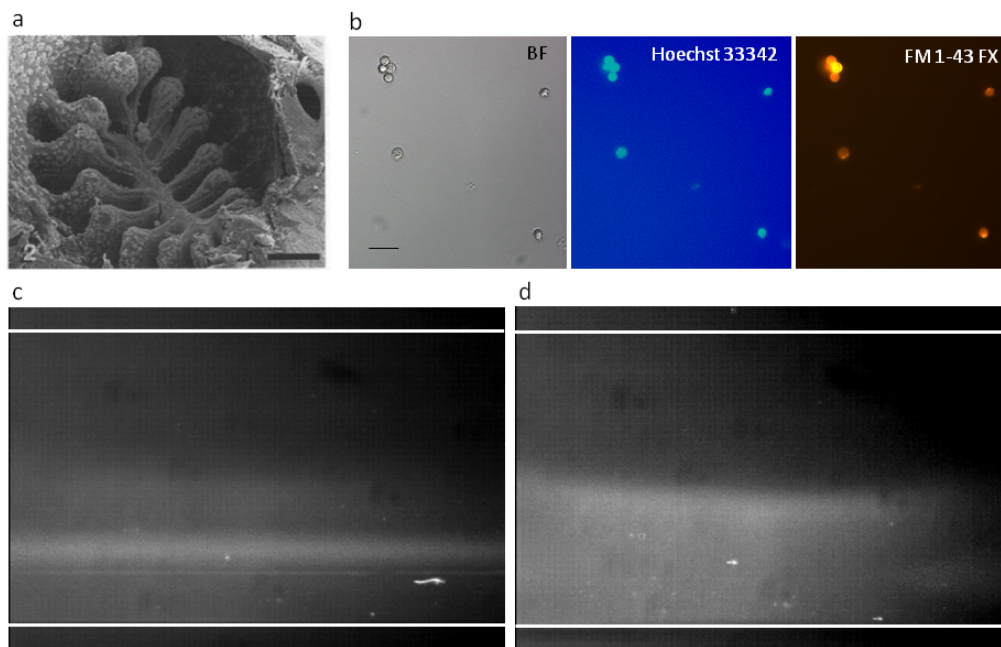


Figure 2.16: Microfluidic magnetic sorting of olfactory rosettes from zebrafish. a) Structure of a rosette from Hansen & Eckart (1998), scale bar $100 \mu\text{m}$. b) Dissociated cells from the olfactory epithelium labeled with membrane and nuclear markers, scale bar $10 \mu\text{m}$. c and d) Maximum intensity projection of the cells flowing through the microfluidic chip in absence (c) and presence (d) of external magnets. The brighter area represents the fluorescent signal from the cell nuclei.

Chapter 3

Discussion

3.1 Magnetoreception in genetic model organisms

3.1.1 Magnetoreception, the natural inspiration for magnetogenetics

The geomagnetic field (GMF) varies systematically across the surface of the Earth and thus offers a potential frame of reference during long and short distance migrations as well as for general orientation (Figure 1.2). Several animals have been reported to use different parameters of the Earth's magnetic field, such as direction or inclination, in order to determine their position and course (Wiltschko & Wiltschko, 2005). For instance, lobsters use this sense to return home (Boles & Lohmann, 2003), migratory birds to find their bearing to their breeding and wintering grounds (Wiltschko & Wiltschko, 1996) and mole rats show a preferred geomagnetic orientation when they build their nest (Němec et al., 2001).

Such a sense must involve a process that turns the magnetic field information into neuronal signals, however, the very nature of these processes remains unclear. If one could gain a better mechanistic understanding of these processes, one would not only solve one of the remaining mysteries in nature, but also gain valuable information for the novel field of magnetogenetics, which aims to genetically target neurons such that they become responsive to magnetic fields.

3. Discussion

Genetic model organisms for magnetoreception studies

The lack of understanding of the magnetoreceptive mechanisms is mainly due to the fact that behavioral evidence has emerged from relatively large sized animal models that are not optically or genetically addressable. Despite some information is gained from smaller insects, these are typically not transparent (Figure 3.1). Although recent studies in the transparent nematode *C.elegans* have begun to offer insights into invertebrate magnetoreception (Vidal-Gadea et al., 2015; Bainbridge et al., 2016), their behavioral responses are not yet well characterized.

This is also the case for vertebrate genetic model organisms, such as the teleost fishes zebrafish (*Danio rerio*) and medaka (*Oryzias latipes*). Their small size, transparent juvenile stages and their amenability to genetic manipulation, allows for non-invasive investigation of neural correlates. Furthermore, the fishes are accessible for whole-brain activity recording. Thus, these fishes are becoming vertebrate models of choice in developmental, cell biology and neuroscience.

Recent reports have demonstrated that zebrafish respond to directional changes of magnetic fields (Shcherbakov et al., 2005; Takebe et al., 2012; Osipova et al., 2016; Krylov et al., 2016), thus we focused our work on this model. We further compared it to the other laboratory fish, medaka, for which magnetoreception had not yet been studied. Although medaka is similar to zebrafish in terms of culturing and available manipulation techniques (Wittbrodt et al., 2002), the fishes are complementary model organisms. In addition to its smaller genome (Kasahara et al., 2007), less genetic redundancy and amenability to genetic inbreeding (Hyodo-Taguchi & Egami, 1985), medaka migrates between fresh and brackish waters in the wild, a behavior for which magnetoreception capabilities would be beneficial.

Robust responses to magnetic field changes is the crucial first step towards understanding magnetoreception, which underlying biophysical mechanisms might one day form the basis for magnetogenetics (Meister, 2016). Thus, as sensitivity to magnetic field was not well characterized in the vertebrate model organisms, especially in medaka, I aimed, together with Dr. Antonella Lauri and Dr. Stephan Eder, to establish a robust and reproducible behavioral assay for magnetoreception.

3.1.2 Behavioral assessment of magnetoreception

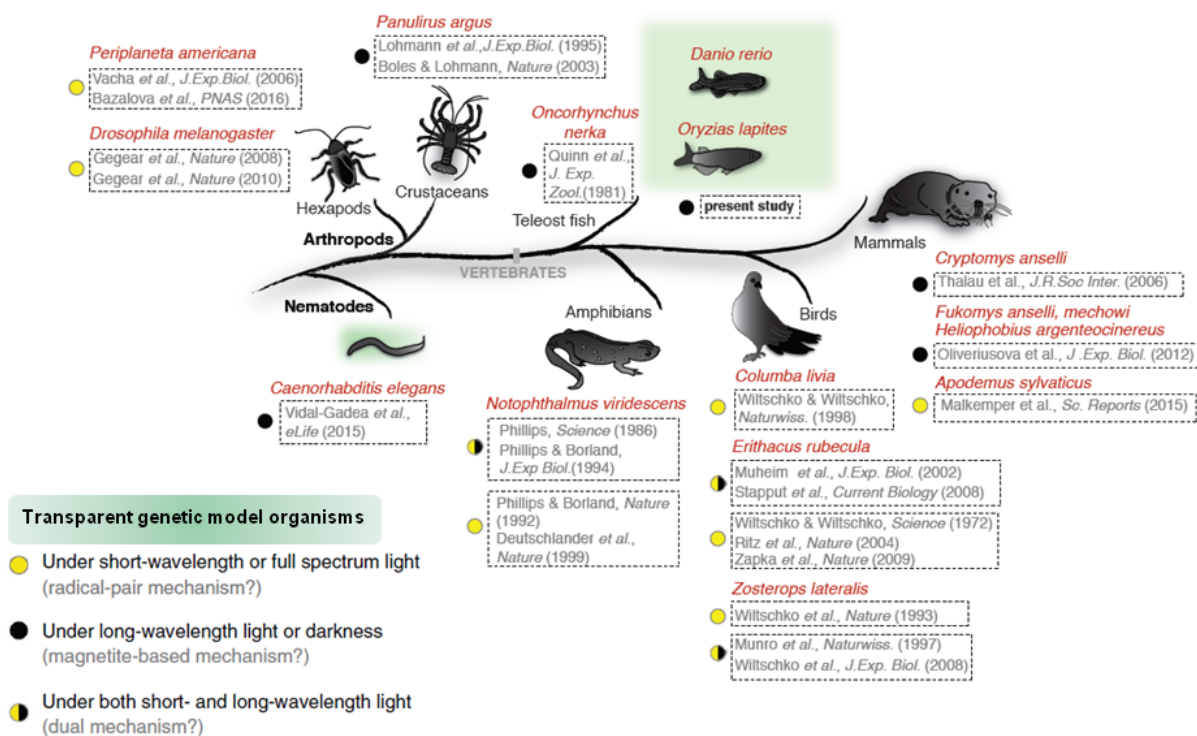


Figure 3.1: Overview of animals tested for magnetoreception, highlighting some key studies. Brain imaging in order to investigate neural correlates of magnetoreception is only possible in a few of the tested animals (green background). The circles indicate if the studies show evidence for a light-dependent mechanism (yellow) or a mechanism independent of short wavelength light (black). Some animals show evidence for both mechanisms (yellow/black). Adapted from Myklatun, Lauri et al. (2018), illustration by Dr. Antonella Lauri.

3.1.2 Behavioral assessment of magnetoreception

Most behavioral assays for assessment of sensitivity to the parameters of the geomagnetic field (GMF) rely on a preference towards certain directions. This can be manifested through alignment of body axis in the GMF, so-called magnetic alignment (MA), which is shown in a large range of animals (Begall et al., 2013; Malkemper et al., 2016). However, more commonly, animals show a preference in their bearing

3. Discussion

(BE), *i.e.* in their direction of movement. A well known example is the seasonal migratory behavior of birds (Wiltschko & Wiltschko, 1996) or fishes (Putman et al., 2013), or the homing of *e.g.* lobsters (Boles & Lohmann, 2003). Other animals have shown a spatial preference (SP) within a closed arena dependent on the direction of the magnetic field, for instance in the position where they choose to build their nest (Němec et al., 2001; Malkemper et al., 2015).

With such internal motivation it is relatively easy to design an experiment in order to test if the animals use the information from the GMF in their directional choice. It can then be further tested which parameters of the magnetic field animals are sensitive to. This was for instance done by Wiltschko and Wiltschko when they demonstrated the inclination compass in European robins in 1972 by inverting the vertical component of the GMF (Wiltschko & Wiltschko, 1972).

Other studies focus more on responses to unnatural magnetic field stimuli such as presence of a magnetic field stronger than that of the Earth (Gegear et al., 2008), or a continuous change of the magnetic field direction. For instance, cockroaches showed increased restlessness (Bazalova et al., 2016) and subterranean rodents exhibited a stress response (Burger et al., 2010) in the presence of a low frequency oscillating magnetic field. Thus, the perturbed magnetic field is likely causing confusing sensory input in these animals leading to the altered behavior. However, such studies need strict control conditions as the behavior might be altered for reasons other than a magnetic sense.

Intra-subjective approach for spontaneous directional preference

It has previously been shown that groups of zebrafish escape from the center of an arena with a bimodal directional preference which was dependent on the axis of the GMF (Takebe et al., 2012). Interestingly, the preference was only evident when groups originating from a single parent couple were analyzed separately. This could be due to the similar genetic background in such groups, or potentially due to their shared environment during maturation.

However, zebrafish are known to exhibit high inter-individual differences even within one genetic cohort (Guryev et al., 2006; Rey et al., 2013). Thus, together with Dr. Stephan Eder, I further improved the release assay by adopting an intra-subjective approach for testing. Specifically, we tested each fish twice, with the

3.1.2 Behavioral assessment of magnetoreception

GMF shifted towards North-East (NE) and North-West (NW). This allowed us to compare the individual fish's bearing after release in the two magnetic conditions. By calculating the angular difference between these bearings we could directly test whether the reorientations were 90° , which would be expected from the 90° shift in direction of the applied magnetic field. This approach was independent of a group preference and would thus reduce the variability in the result.

Indeed, although the fish originated from one genetic cohort we did not observe a common group preference of the zebrafish that were tested in light (Figure 2.3). However, as expected if the individual fish have a directional preference in their initial bearing, we observed a significant axial distribution of the angular differences compatible with the change in magnetic field direction (Figure 2.3). The axial distribution indicated that the fish did not differentiate the direction of the 90° shift and was consistent with the previously reported bimodal preference in zebrafish (Takebe et al., 2012; Osipova et al., 2016; Krylov et al., 2016).

This experimental procedure where the angular differences were calculated in order to control for the individual preference of the fish has some resemblance to the analysis presented by Lohmann et al. (1995). In their study on lobsters the maximal deviation from a baseline direction of individual animals was analyzed after the direction of the magnetic field was changed. Thus, their result, similar to what is described here, did not assume a directional preference common to all the animals. Furthermore, comparison to an expected mean was for instance also performed in order to test if salamanders exhibited homing in the appropriate direction, also when the vertical component of the GMF was inverted (Phillips, 1986) (see also discussion below).

Control of potential electric noise effects

There are several challenges when designing a magnetic field sensitivity assay, because magnetic fields are always coupled with electric fields. After all, artificial magnetic fields are produced with coil systems, and current flow in turn is caused by an electric field. For this reason, care must be taken such that coils are not too close to the test objects and that magnetic fields are not changed too rapidly, which in turn induce electric currents. Furthermore, when applying different magnetic field conditions in order to test behavioral responses to these, it is important to

3. Discussion

keep the electric current the same in all conditions such that only the magnetic field is changed (Kirschvink, 1992; Kirschvink et al., 2010). Such a design also ensures that heating due to ohmic dissipation is comparable in all testing conditions.

Unlike other studies on zebrafish where groups were tested in the natural GMF or in a field where the direction is shifted 90° (Osipova et al., 2016; Krylov et al., 2016), we added an extra control for the presence of current. We achieved this by shifting the horizontal component of the GMF 45° towards East or West, still allowing the fish to experience the 90° shift between the two tests. This way we controlled for the presence of current, as it was equal (but opposite direction) in the two magnetic conditions. Thus we can be more confident that the differences observed in behavior can be attributed to the magnetic field change and is not due to effects resulting from the presence of electric noise or ohmic heating (Figure 2.2).

An alternative assessment paradigm

Although the sudden release of the fish into a bigger arena might serve as a motivation to move outwards, it is not clear why zebrafish would have a directional preference in the magnetic field. Takebe et al. (2012) suggested that it could be useful that groups of fish have a different directional preference during predator escape, such that the fish would spontaneously diverge and thus increase chances of survival. However, a lack of inner motivation for spontaneously selecting a given bearing might result in large variabilities in the observed behavior.

These challenges could be overcome through conditioned experiments where fish are trained to prefer a certain magnetic direction through either positive or negative reinforcement. Such experiments have been performed, *e.g.* in the genetic model organisms *Drosophila* (Gegear et al., 2008) and zebrafish (Shcherbakov et al., 2005). However, it is often more desirable to study the native response to magnetic field changes in order to understand the influence of the GMF on behavior in nature. For instance, although not well characterized yet, it was recently shown that the intensity and direction of a magnetic field influences the rheotactic behavior of zebrafish (Cresci et al., 2017).

Further, zebrafish are known to choose a preferred area when exploring a novel environment, which is referred to as homebase selection (Stewart et al., 2010). The homebase, usually selected over a period of 30 minutes, is defined by the frequency

3.1.2 Behavioral assessment of magnetoreception

of visits, the time spent and distance traveled within the selected area being higher compared to the rest of the arena (Stewart et al., 2010, 2011). Several environmental cues, such as visual and odor cues, are likely to play a role in the choice of a homebase. However, it is not yet known if an egocentric cue such as the direction of the GMF might also influence the exploration of a fish in a new environment (Salas et al., 2003).

In order to potentially gain some first insights into this I investigated the behavior of our zebrafish in the first minute after release from the center of the arena. Specifically, the circular arena was divided in 12 segments and the one where the fish spent most of its time was taken as the preferred segment. Since the area selection is shown to be different between individuals (Stewart et al., 2010), I again adopted the intra-subjective approach and analyzed the change in segment between the two magnetic conditions for each fish (Appendix C).

Zebrafish of the AB strain did not show a significant change in their position in the first minute after release, neither in light nor under IR illumination (Figure C.1). However, this was not unexpected from the short observation time and the thigmotactic behavior they exhibit in darkness (Figure 2.4). Conversely, the group that was kept in darkness for one hour prior to testing did show a significant reorientation of position, consistent with the magnetic field direction (Figure C.1). This observation thus strengthens the conclusion of a light-independent mechanism of magnetoreception in these fishes. The fact that only this group yielded a significant reorientation might simply be due to the higher number of fish tested in this condition (see Table 5.1).

It is not known if medaka perform a similar homebase selection as reported for zebrafish (Stewart et al., 2010). However, the looping behavior in darkness would likely result in an area of the arena being preferred over others (Figure 2.5). Thus, I also investigated the spatial preference in the CAB strain of medaka. Due to the much slower movement from the center of arena, compared to zebrafish, the second minute of exploration was used for this analysis (Figure A.2). Both groups that were tested in IR, after being acclimated in light or darkness, showed a significant change in their spatial preference (Figure C.2). Interestingly, this time, both groups of medaka showed an axial response in their reorientation (Figure 2.7, Myklatun, Lauri et al. (2018)).

3. Discussion

This provides an interesting first evidence that homebase selection could be a common trait to teleost fishes and that the choice of area might be influenced by the direction of the GMF. Further studies would be necessary to investigate this behavior in more detail in order to determine if the choice is a real homebase, because we based the selection on only one of the parameters normally used in defining a homebase (time spent in segment). In addition we only observed the fish for a short period of time. However, zebrafish might establish a homebase within a few minutes (Stewart et al., 2011) and exhibit stable exploration patterns over time (Stewart et al., 2012). Nevertheless, we did observe a significant change in the preferred position of individual zebrafish and medaka compatible with a response to a the 90° directional shift of the GMF.

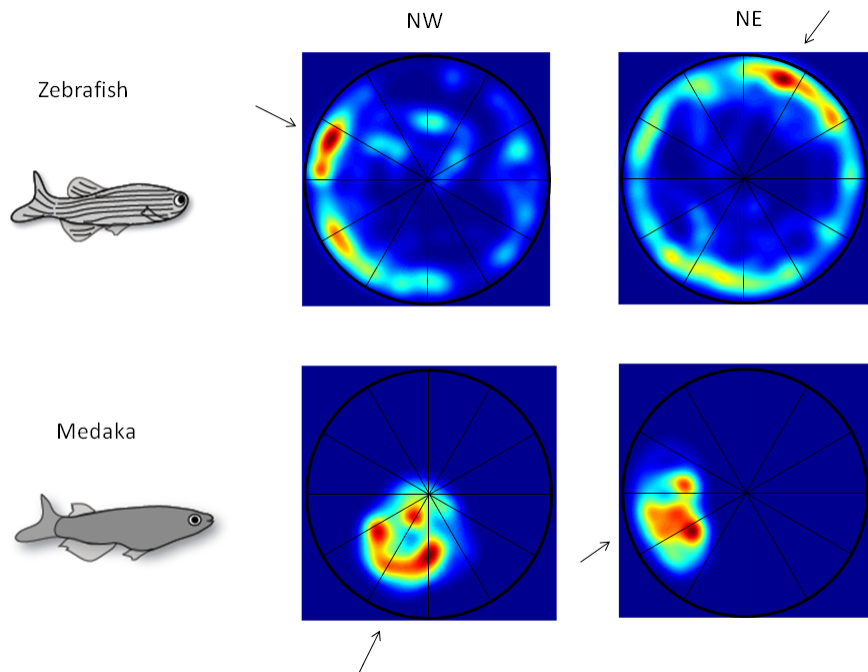


Figure 3.2: Examples of spatial preference in the teleost fishes zebrafish and medaka, represented by a density map of position during one minute of exploration. The preferred segment of the arena is indicated with an arrow and is changed when the GMF is shifted towards North-West (NW) or North-East (NE). Fish illustrations by Dr. Antonella Lauri.

3.1.3 Mechanisms underlying magnetoreception

Despite the growing body of evidence for magnetoreception across the animal kingdom (Figure 3.1), the mechanisms underlying magnetoreception are still largely unclear. There are currently two main hypotheses. The radical pair (RP) hypothesis postulates that the GMF influences chemical processes in the cryptochromes after photon absorption (Hore & Mouritsen, 2016) (see section 1.2.2). In contrast, signal transduction according to the magnetite hypothesis relies on mechanical interaction of the GMF with magnetic particles (Kirschvink et al., 2001) (see section 1.2.3).

Behavioral assessments and diagnostic tests

The manipulation tools available for genetic model organisms are also useful for investigating the molecular mechanisms of magnetoreception. However, other diagnostic tools must be used for animals where generation of genetic mutants that lack one or more genes is more challenging, or if one wants to test for the involvement of magnetite particles, where no set of candidate genes exist. These diagnostic tools are usually experimental conditions expected to interfere with the putative biophysical reception mechanisms. Hence, effects on the directional behavior under these conditions could be assessed. Table 3.1 summarizes these diagnostic tools.

First, insights into the underlying mechanisms of magnetoreception could already be gained from studying the nature of the magnetic compass. For instance, a RP-based mechanism is consistent with an inclination compass, while a polarity compass generally is associated with a magnetite-based mechanism (however see Winklhofer & Kirschvink (2010)). The presence of an inclination compass can be tested by inverting the vertical component of the GMF (Figure 1.2). Several animals have shown to change their heading under this condition, indicating the use of an inclination compass (Wiltschko & Wiltschko, 1972; Phillips, 1986; Wiltschko & Wiltschko, 1996; Light et al., 1993). Other animals are insensitive to such inversions and thus possess a polarity compass (Quinn et al., 1981; Lohmann et al., 1995; Marhold et al., 1997; Wang et al., 2007), and likely a magnetoreceptor mechanism involving magnetite.

Further insights could be gained by testing the light-dependency of animal's ability to use their magnetic sense. Specifically, RPs are known to be formed in

3. Discussion

cryptochromes after photon absorption, thus predicting that light of certain wavelengths is necessary if these are involved in magnetoreception. Long wavelength light or darkness have been shown disrupt the magnetic response in some animals, including for instance birds (Wiltschko et al., 1993) and salamanders (Phillips & Borland, 1992b). Furthermore, both fruit flies and cockroaches lacking cryptochrome genes showed the same behavioral response as the insects did in absence of short wavelength light (Gegear et al., 2008; Bazalova et al., 2016), possibly indicating a link between the two conditions. Other animals navigate normally in darkness (Quinn et al., 1981; Light et al., 1993; Lohmann & Lohmann, 1993; Marhold et al., 1997), which is not consistent with the RP hypothesis. Examples of animals tested for magnetoreception and whether the study is performed in light or darkness is shown in Figure 3.1.

Similar to the specific wavelengths necessary for some animals to detect the parameters of the GMF, birds seem to be able to use their compass only within a narrow range of magnetic field intensities (Wiltschko, 1978; Wiltschko et al., 2007c). However, this functional window could be expanded after an adaptation period in the altered intensity (Winklhofer et al., 2013). The narrow functional range may be taken as a hint towards a RP mechanism because the yield of the putative chemical reaction has been shown to be dependent on the magnetic field intensity (Ritz et al., 2000). Although, the response of magnetite should not be dependent on the strength of the magnetic field, similar to a compass needle, there is likely a threshold to be overcome also for this mechanism.

Testing of animals under radio frequency magnetic fields has long been an accepted diagnostic test for involvement of a RP-based magnetoreceptor. Magnetite particles are not expected to be influenced by oscillating magnetic fields as the interaction time is too short to allow the particles to realign (Ritz et al., 2004). However, even very weak magnetic fields oscillating in the lower MHz frequency range are assumed to resonate with the precession of electron spins in the RPs, affecting the singlet-triplet interconversion and thereby interfere with the sensing mechanism (Ritz et al., 2004). Disorientation has been observed in birds at the Larmor frequency (Thalau et al., 2005; Wiltschko et al., 2015), as well as during oscillations with broad-band frequencies (Malkemper et al., 2015; Schwarze et al., 2016b). The latter is expected to be more effective, since there are still open ques-

3.1.3 Mechanisms underlying magnetoreception

tions concerning the effect of magnetic fields oscillating at the Larmor frequency Nießner & Winklhofer (2017).

Behavioral assessment of animals treated with a short magnetic pulse is often used to test for involvement of magnetite particles. This is based on remagnetization experiments performed on MTB, which turned north-seeking bacteria to south-seeking after application of a magnetic pulse (Kalmijn & Blakemore, 1978). The pulse is predicted to interfere with the structure of the magnetite-based magnetoreceptor, by either remagnetization of SD chains or disruption of SPM particle clusters (Davila et al., 2005). Altered behavioral responses have been observed after pulse treatment (Wiltschko et al., 1994; Beason et al., 1995; Irwin & Lohmann, 2005; Ernst & Lohmann, 2016), indicating that magnetite structures are involved in the sensing mechanism in these animals. As a diagnostic tool for the presence of magnetite in the magnetoreceptors, it could be interesting to follow up our experiments with assessment of fish treated with a magnetic pulse. However, as the magnetoreceptors in vertebrates are not identified yet, it might be difficult to predict the outcome of such treatment. Specifically, if only the directional preference is altered, but not abolished, as observed in lobsters (Ernst & Lohmann, 2016), our intra-subjective approach might not provide the required readout.

Table 3.1: Diagnostic tools for mechanisms of magnetoreception

Diagnostic tool	Magnetite hypothesis	Radical pair hypothesis
Inclination compass	X	V
Polarity compass	V	X
Light-independent	V	X
Narrow functional window	X	V
Effect of oscillating field	X	V
Effect of magnetic pulse	V	X

Radical pairs, magnetite or both?

It is important to state that the two putative mechanisms, involving magnetite particles or radical pairs, are not mutually exclusive. They could both coexist to provide complementary information in one animal or even work together as one system. For instance, a single domain magnetite particle, free to rotate, could affect

3. Discussion

other processes in the cell, and thereby act as a magnetic sensor. The movement of the particle might strengthen or reduce the stray field in one area, depending on the dipole orientation of the magnet, and lead to magnetically induced chemical changes, *e.g.* in a radical pair system (Winklhofer & Kirschvink, 2010). Other combinations of cryptochromes with magnetic material have recently been suggested (Qin et al., 2016), however this has been considered unlikely due to insufficient magnetic moments of the protein complex (Meister, 2016; Winklhofer & Mouritsen, 2016).

Interestingly, some animals show evidence for two separate magnetoreceptor systems. In general it is suggested that a radical pair mechanism is used to determine directional information through inclination (compass) whereas a magnetite-based system can provide positional information through polarity or intensity (map). This combination was for instance demonstrated by Phillips in 1986 when salamanders were tested with an inverted vertical component of the GMF. The animals that were exhibiting an induced simple compass response changed their bearing by 180° , while salamanders navigating towards their home did not, indicating a true navigation behavior in the latter case and the involvement of two magnetoreceptor systems (Phillips, 1986). Similarly, experienced birds which likely had formed a map of their migratory route were affected by a remagnetization pulse, while juvenile birds relying on only their instinct to follow a certain compass direction were not (Munro et al., 1997).

Furthermore, Beason & Semm (1996) showed that birds exhibited an altered directional response after the putative magnetite receptors were knocked out by a magnetic pulse. However, when blocking signals from the ophthalmic nerve, previously shown to respond to magnetic stimuli (Beason & Semm, 1987; Semm & Beason, 1990), the birds regained their seasonally appropriate direction, potentially indicating a second magnetoreceptor system taking over (Beason & Semm, 1996). Other evidence for two coexisting magnetoreceptor systems include the altered, but directional response in some animals under long-wavelength light (Phillips & Borland, 1992a; Wiltschko et al., 2007b)

3.1.3 Mechanisms underlying magnetoreception

Light-independent magnetoreception indicates magnetite

Although evidence exist for involvement of both RP- and magnetite-based mechanisms in some animals, we were interested in testing for potential presence of magnetite in the laboratory strains of zebrafish and medaka. Thus, we applied one of the diagnostic tools described above by testing their directional preference in absence of visible light. Magnetic orientation in darkness is predicted by the magnetite hypothesis as signal transduction in this case is based on mechanical interaction of the GMF with magnetic particles (see section 1.2.3).

In order to assess the fish in darkness we used an IR illumination source (1060 nm) which allowed us to observe their behavior using an IR sensitive camera. This wavelength is known to not be perceived by several fish species, including zebrafish (Shcherbakov et al., 2013). The altered swimming behavior in both zebrafish and medaka (Figures 2.4 and 2.5) is likely confirming that the fish also in our experiments perceived the IR illumination as darkness (see also discussion below). Furthermore, cryptochromes are only known to be activated by light of much shorter wavelengths (<565 nm) (Wiltschko & Wiltschko, 2014). Because a low number of photons of these wavelengths would be enough for a magnetoreceptor system, we went to great extent to make the rest of the room dark, and specifically the arena where the fish were tested, by covering all additional light sources, such as those on the power supplies. Although a recent report claims that the crucial step of the magnetic sensing occurs in darkness (Wiltschko et al., 2016), activated cryptochromes have not been observed in birds after a longer period in darkness (< 60 minutes) (Nießner et al., 2014; Wiltschko et al., 2014), and thus we also tested our fish in this condition.

Previous studies on zebrafish assessing magnetoreception, which were all performed in light, reported an axial preference of the fish (Takebe et al., 2012; Osipova et al., 2016; Krylov et al., 2016). This is consistent with the fact that our fish did not distinguish in which direction the GMF was shifted, yielding an axial distribution of the reorientation angles (2.3). We observed that when we tested the spontaneous preference of a group of zebrafish under IR illumination they exhibited the same axial response as observed in light (Figure 2.6). Furthermore, we observed a significant reorientation of zebrafish in the absence of visible light, even after preadaptation to complete darkness. Although the zebrafish showed a polar response in this case, potentially due to the extended period in darkness (see discussion below), the results

3. Discussion

indicate a light-independent mechanism.

There are no previous reports on magnetoreception in medaka, and thus we did not know what to expect in terms of modality of the distributions or if they perceive the magnetic field at all. We observed a polar response under IR illumination and an axial response after preadaptation in darkness. Thus the question remains whether medaka possess a polarity compass and whether the axial response was a result of the testing conditions, as might have been the case for zebrafish. Further studies will be necessary to determine the nature of the magnetic sense of medaka. Nevertheless, we did observe a significant reorientation of medaka with the shift of the GMF in darkness.

Thus, taken together, we provide the first evidence for light-independent magnetoreception in both zebrafish and medaka. The magnetite hypothesis is therefore the most likely candidate in these teleost fishes. Interestingly however, I did not observe the candidate magnetoreceptor cells which has been reported in other fishes (Eder et al., 2012). However, this might be due to limitations in the methodology as discussed below.

Other effects of testing in darkness

The absence of visible light in our behavioral tests were meant to serve two purposes. First, and most importantly, as magnetoreception involving a RP system is predicted to be light-dependent (Hore & Mouritsen, 2016), orientation in darkness could indicate a magnetite-based magnetoreceptor system. Thus, by testing the fishes in darkness we aimed to distinguish the two hypotheses. Second, we reasoned that the absence of visual cues should enhance the use of other egocentric cues, such as the magnetic field direction if the fish were sensitive to this. In fact in zebrafish we did observe more thigmotactic swimming behavior in darkness (Figure 2.4), likely indicating increased involvement of the lateral line system during exploration of the arena. Thigmotaxis in zebrafish could also be a stress response due to the sudden change of lighting conditions (Kalueff et al., 2013).

Medaka on the other hand, showed a peculiar behavior when tested in darkness as they swam in small circles (Figure 2.5). Interestingly, the only study to my knowledge reporting such behavior in medaka is a recent report from NASA. They observed a looping behavior when the fish were tested in a microgravity environment

3.1.3 Mechanisms underlying magnetoreception

in space (Chatani et al., 2015). Thus, this behavior might be evident when some navigational cues are missing from the environment, such as gravity or light, and could be a different strategy for navigation in these cases. However, as the fish in the NASA study were kept at the international space station (ISS) the fish were orbiting the Earth and consequently also experiencing the continuous change of its magnetic field. This could, likely in addition to the microgravity environment or the absence of light, also lead to a stress response of the fish (see section 3.1.5 and Myklatun, Lauri et al. (2018)).

It is interesting to note that looping behavior has been observed also in rodents in darkness. Similar to what we observed in medaka, the loops performed by the rodents were often drifting and is thus likely a strategy for exploration in darkness (Zadicario et al., 2005). Furthermore, it seems that the looping is preceding the establishment of a homebase in these animals as they are attempting to accumulate spatial information in the absence of visual cues (Avni et al., 2006).

The medaka fish, after exploring the arena swimming in small circles, went on to touch the wall with their head. The looping behavior led to the spontaneous preference assessed at the 6 cm radius not yielding a meaningful result (Figure B.3). However, when assessing the position of the first contact with the wall through increasing the crossing radius, also medaka showed a significant reorientation (Figure 2.7). Analysis of the zebrafish behavior at this increased radius did not change the result for the fish tested under IR illumination (Figure B.2), likely due to their rather linear swimming trajectory towards the wall immediately after release from the center (Figure A.1). The group of zebrafish tested under WL illumination, on the other hand, did not significantly reorient at the larger radius (Figure B.1) because they did not touch the wall immediately upon release (Figure A.1).

As it has been suggested that the cryptochromes can stay activated for an extended period of time after onset of darkness (Nießner et al., 2014; Wiltschko et al., 2014), we also kept one group each of zebrafish and medaka in darkness prior to testing. However, this might have had other side effects than just switching off a magnetoreceptor system. Although our intention was to interfere with the cryptochromes, these proteins also regulate other processes in the body. For instance, some cryptochromes are known to be involved in the circadian rhythm (Chaves et al., 2011). Thus, the difference in distributions observed, both for zebrafish and

3. Discussion

medaka, after being preadapted in darkness might be a consequence of the extended period of time without light. Furthermore, it could potentially also be due to an altered perception of the magnetic field information caused by interference with the cryptochromes. Altered behavioral responses, however still significantly consistent with a response to the magnetic field direction, have been observed in a number of animals at longer wavelengths (Phillips & Borland, 1992a; Phillips & Sayeed, 1993; Muheim et al., 2002).

Magnetosensitivity of *C.elegans* in darkness

Magnetosensitivity was recently shown in darkness in *C.elegans*, an invertebrate genetic model organism (Vidal-Gadea et al., 2015). In an burrowing assay it was demonstrated that the worms follow the GMF field lines at a certain angle, depending on the origin of the species. They went on to show that the worms would move up or down depending on their feeding state. Further, the authors presented a simple magnetotaxis assay for screening of magnetic sensitivity in different strains or mutants, where the preference for the presence of a magnetic field was demonstrated (Vidal-Gadea et al., 2015). However, it is not clear why this preference would exist and how it relates to the directional preference in the burrowing assay. Furthermore, I have not been able to replicate these results in the WT strain N2 (Figure 2.8). Although there was a large variability between the trials, the average number of worms close to the magnet was not significantly different from the control site (2.8).

C.elegans are known to be sensitive to a number of stimuli, such as temperature or chemical gradients (Mori, 1999; Chung et al., 2006), making it crucial to control for variation in these conditions. Despite the fact that the authors measured the temperature in the setup they did not use double wrapped coils, which would have allowed for better control of unspecific effects (Kirschvink, 1992; Kirschvink et al., 2010). Double wrapped Helmholtz coils has wires in both directions within each coil allowing the current to flow parallel or anti-parallel. In the first case a magnetic field is generated at their center. However, when the current runs anti-parallel within the coils (sham mode) the magnetic field from each wire is canceled. Thus, double wrapped coils generate the associated electric noise, heat and vibrations without the presence of a net magnetic field (Kirschvink, 1992).

Interestingly, when another laboratory performed a similar study on *C.elegans*

3.1.4 Candidate magnetoreceptor cells

using double wrapped coils, no magnetosensitivity was observed (Landler et al., 2018). Moreover, the AFD neurons, which intact function seemed to be necessary for magnetotactic behavior and were shown to be activated upon magnetic stimulation in the original study, are also known to be temperature sensitive (Mori & Ohshima, 1995; Kimura et al., 2004). Hence, the question of magnetosensitivity in *C.elegans* and the involvement of AFD neurons remains, and further studies are necessary in order to determine whether this model organism is useful for magnetoreception studies.

3.1.4 Candidate magnetoreceptor cells

Detection of the magnetoreceptor

The magnetite hypothesis predicts the presence of biogenic magnetite clusters associated with neurons, as these would interact with the GMF. Over the years many studies have reported presence of magnetic material in a variety of animals exhibiting magnetoreception. However, the search for magnetoreceptor cells is still suffering from insufficient methodologies as most techniques either rely on direct observation of a small candidate structure, thus limiting the search area, or on indirect observation of the magnetic signature of magnetite (Shaw et al., 2015).

Further, there are three main challenges one has to overcome when searching for the magnetite-based magnetoreceptor (Shaw et al., 2015). First, the anatomical location of the cells is unknown, and given that magnetic fields can travel unperturbed through biological tissues, the cells could be anywhere. Second, the cells are expected to be rare; signals corresponding to the order of $\sim 10^8$ SD magnetite particles have been reported in fishes (Kirschvink, 1989). Moreover, if the cells are too close together they could influence each other and might thus be spread over a large anatomical area. Third, the elemental composition of magnetite is not unique since iron is abundant and necessary in many biological processes, thus increasing the risk of contaminations or false positives in simple iron detection assays. The latter has for instance brought the magnetoreceptors reported in the beak of pigeons into question (Fleissner et al., 2003; Treiber et al., 2012).

3. Discussion

Rotation assay for magnetic cells

The rotation assay developed by Eder et al. (2012) was the first technique that identified single candidate cells based on their magnetization and allowing for subsequent characterization with reflection or electron microscopy and elemental analysis. This overcame the location and rarity problem as samples from the whole animal could be assessed. Moreover, screening for only permanently magnetized cells increased the likelihood of detecting magnetite as opposed to other iron structures. The rotation could further be used to measure the magnetic moment of single cells (Eder et al., 2012).

The assay was recently criticized for also identifying cells contaminated during preparation due to the inconsistent and large variety of cells isolated (Edelman et al., 2015). However, when I used the rotation assay to search for candidate magnetoreceptor cells in fishes I, on the contrary, experienced finding only very few cells responding to the magnetic field (Table 2.1). It remains unclear whether these were real magnetoreceptor cells or contaminations, although the large variation in shape and location speaks for the latter.

Thus, although there is evidence of a light-independent magnetoreception in both zebrafish and medaka, I was not successful in isolating candidate magnetoreceptor cells from these fishes. Moreover, magnetic cells were also not observed in salmon. However, the rotation assay presents one limitation, which might also explain the lack of identified magnetoreceptor cells; detection relies on the torque on the cells (Eder et al., 2012). Thus only cells containing SD magnetite attached to the cells would move with the magnetic field (Figure 2.9a). More critically, if the cells were to contain SPM magnetite crystals these would only under certain circumstances experience the torque, *i.e.* when the magnetization is anisotropic, for instance in a chain formation (Winklhofer & Kirschvink, 2010; Eder et al., 2012). However, such SPM magnetite crystals would only follow the rotating field, but would not be able to move in a field changing by 180° (Eder et al., 2012), which was employed in the field-flip assay during some of my searches.

Thus, as some of the theoretical considerations around the magnetite hypothesis involves interaction of the GMF with SPM particles (section 1.2.3, (Davila et al., 2003)), these putative magnetoreceptors would not necessarily be detected in the rotation or field-flip assay. Despite the fact that only SD magnetite has been

3.1.4 Candidate magnetoreceptor cells

reported in fishes (Table D.1), it is possible that the discrepancy between magnetic orientation in darkness and the lack of magnetic cells is due to the presence of a SPM-based sensor in the teleost fishes.

Identity of extracellular objects

In the search for the magnetite-based magnetoreceptors I observed only a very small number of magnetic cells (Table 2.1). However, I could reliably detect extracellular objects responding to the changing magnetic field. These extracellular magnetic objects had properties consistent with magnetite, such as the opaque and reflective appearance. It is thus a possibility that these were a part of a magnetoreceptor, for instance in an extracellular receptor system. Alternatively, magnetic clusters could have formed from magnetoreceptor cells that were disrupted during the dissociation process. However, this would be unlikely since the dissociation process left >90% of the cells vital. Thus, if the magnetic material arose from disrupted magnetoreceptors a larger fraction of cells with magnetic properties would have been expected.

Interestingly, I found similar extracellular magnetic objects both in the samples from laboratory fishes and in the wild salmon, raising the question whether these structures have the same origin. While the salmon were caught from a wild environment, zebrafish and medaka were raised in a controlled environment where they were fed only with live artemia because the dry feed had strong magnetic signature (Tetra flakes, ST3, Figure E.1). Furthermore, the preparation of the tissue samples were the same, using only non-magnetic tools. However, contaminations are still easily introduced in the preparation process. It is for instance shown that magnetite contamination can be entrained from many standard plastic equipment (Kobayashi et al., 1995).

Further studies would thus be necessary to determine if the extracellular objects are in fact part of a magnetoreceptor. They could for instance be the same particles that was detected in salmon three decades ago (Kirschvink et al., 1985; Mann et al., 1988; Walker et al., 1988; Moore et al., 1990). Alternatively they are just a result of contamination, either from sample preparation or environment during the lifetime of the fish. Although this is a likely option, one would have to exclude that these extracellular structures have been part of a magnetic sensory system.

3. Discussion

3.1.5 Towards neural correlates of magnetoreception

Like the molecular mechanisms, also the neural correlates of magnetoreception remains unknown. This is again mainly due to lack of characterized magnetosensitivity in optically transparent animals allowing for *in vivo* monitoring of brain activity. Although *C.elegans* have recently been suggested as a model organism for such studies (Vidal-Gadea et al., 2015; Bainbridge et al., 2016), scientists have so far been relying on time consuming staining techniques on brain slices, or on electrophysiological recordings in selected brain areas. This has yielded some interesting findings. For instance, by using the immediate early gene *c-fos* as a marker for neuronal activity, the navigation circuit in mole rats was shown to be affected by a low frequency oscillating magnetic field (Burger et al., 2010). Similarly, areas known to be involved in spatial orientation was found active in pigeons, and further, the lagena organs were suggested for primary sensory input (Wu & Dickman, 2011). Electrophysiological recordings have implicated the involvement of the trigeminal nerve in responding to magnetic stimuli in trout (Walker et al., 1997) and in birds (Beason & Semm, 1987).

Sensitivity to magnetic fields has now been validated in zebrafish and for the first time been reported in medaka. As vertebrate genetic model organisms these teleosts should be the model of choice for investigation of neural correlates of magnetoreception, due to the many genetic tools available. For instance, zebrafish lines expressing calcium responsive proteins in the nervous system have been used to monitor brain activity (Akerboom et al., 2012). For such studies juvenile fish are of great advantage because they are still transparent and thus optically addressable. Further, with their relatively small size and the availability of various pigmentation mutants, analysis of the whole brain is technically feasible (Ahrens et al., 2012; Randlett et al., 2015).

Juvenile medaka as a model for magnetoreception

If younger fish respond to changes in the GMF with a robust behavioral response, they could be valuable in the search for neural correlates of magnetoreception. Thus, together with Dr. Antonella Lauri, we set up a simple magnetic stimulation paradigm that would assess magnetosensitivity in juvenile fish. In order to

3.1.5 Towards neural correlates of magnetoreception

maximize the likelihood of detecting a behavioral and neural responses dependent on the magnetic field, we perturbed the intensity and direction of the GMF continuously. In essence, we applied a magnetic field of GMF strength which was oscillating at 1 Hz. These experiments were performed using double wrapped Helmholtz coils in order to control for unspecific effects from electric noise, heat and vibrations (Kirschvink, 1992). Such coils offers a control similar to the $\pm 45^\circ$ field change we presented to the adult fish.

We found that juvenile medaka showed hyperactivity during exploratory behavior under influence the oscillating magnetic field, compared to when experiencing the sham mode of the double wrapped coils. Specifically, they significantly increased their swimming velocity after onset of the magnetic field stimulus, indicating that these fish sensed the magnetic field perturbation (Figure F.1, Myklatun, Lauri et al. (2018)). These results are similar to the restlessness observed in cockroaches (Bazalova et al., 2016), or the stress response observed in mole rats (Burger et al., 2010) when exposed to slowly oscillating magnetic fields. Interestingly, this behavior was not observed in juvenile zebrafish, leaving the question open whether they cannot yet sense the magnetic field at the younger stages or if in these fishes the sensory confusion does not lead to a difference in behavior (Figure F.1, Myklatun, Lauri et al. (2018)).

Continuous stimulation with magnetic field changes should keep stimulating the primary magnetic sensors, making it compatible with whole-brain mapping techniques. There are in general two approaches that can be employed when analyzing brain activity in these small fishes. One can either look at the brain from fish swimming freely, by analyzing *e.g.* p-ERK levels on fixed specimens (Randlett et al., 2015), or from partially restrained fish using *in vivo* calcium imaging (Ahrens et al., 2012). In order to potentially gain some first insights Dr. Antonella Lauri and I stimulated juvenile medaka with the same oscillating magnetic fields for which the behavioral response was observed ($\sim 40 \mu\text{T}$). The brain activity during the stimulus was analyzed by Dr. Antonella Lauri through a brain mapping technique based on immunohistochemical detection of a phosphorylated ERK which is present in activated neurons (Randlett et al., 2015).

Interestingly, we observed increased activity in the lateral hindbrain region, expressed as the mean fluorescence of the normalized pERK signals (Myklatun, Lauri

3. Discussion

et al., 2018). The hindbrain plays a role in motor control (Kinkhabwala et al., 2011), and might receive input from the lateral line system (Alexandre & Ghysen, 1999), which has been implicated in magnetoreception through the presence of magnetite particles in salmon (Moore et al., 1990).

Increased activity in the habenula was previously reported in the context of magnetic stimulation in rats and birds (Semm, 1983), and has been implicated in electromagnetic field detection in lamprey (Hikosaka, 2010). It has also been suggested that the olfactory epithelium is a site for candidate magnetoreceptor cells in fish (Walker et al., 1997; Eder et al., 2012). However, we did not observe a significant difference in activity in these regions. Although further investigation of other candidate regions would be necessary, as well as more in-depth studies using live imaging techniques, this demonstrates the usefulness of the medaka fish model in studies aiming to identify the neural correlates of magnetoreception.

3.2 Microfluidic magnetic sorting

Reliable magnetic sorting techniques are essential for subsequent biophysical or chemical analysis of both naturally occurring cells, such as the putative candidate magnetoreceptors, or cells bioengineered for magnetic manipulation. For these downstream analyses it is crucial to avoid contamination with metallic materials during the enrichment step, in order for magnetic characteristics to be correctly attributed to the cell. It is further desirable to have visual control of the sorting process as well as tunable separation parameters such that a large range of cells can be sorted. This could be realized for instance in microfluidic systems with a magnetic separation principle (Pamme, 2006; Hejazian et al., 2015) (Figure 1.10).

3.2.1 Microfluidic chip design

Reducing contamination risks

Table 3.2 summarizes the performance of different continuous flow magnetic separation systems, including macroscopic systems such as the commercial Miltenyi columns (Miltenyi et al., 1990). Although this system has been well established in laboratories, there is a high risk of contamination and unspecific entrapment of cells during the sorting process as the sample travels through a mesh of superparamagnetic particles. Further, it has been shown that unwanted iron-rich cells are trapped due to the high magnetic fields in these columns (Franken et al., 2015). Thus, I focused on developing a microfluidic system for increased control of both sorting process and contamination risk.

Obtaining similar magnetic field gradients (> 1000 T/m) in a microfluidic system is challenging. For instance, Sun et al. (2016) recently demonstrated that gradients up to 4000 T/m could be achieved close to ($5 \mu\text{m}$ distance) a structure of magnetic particles when embedding these inside the microfluidic channel (Sun et al., 2016). However, these high gradients are peak values at the edges of the structures and thus does not extend throughout the channel. The gradient was estimated to be around 50 T/m in most of the channel, and is thus comparable to what I observed in the presence of a magnet alone (Figure 2.12). And although the multitarget cell sorter developed by Adams et al. (2008) achieved high magnetic gradients in the order of $10\,000$ T/m close to the nickel strips, the contamination risk is still high in such a

3. Discussion

system because the strips are integrated inside the sorting channel. Furthermore, the large magnet pulling the cells to the bottom of the chip (~ 200 T/m) produces a background magnetic field of 0.5 T (Adams et al., 2008), thus reaching a high level of magnetization also for iron rich samples potentially enriching unwanted cells.

In order to avoid contact between the sample and magnetic material I decided for a design where a magnetic structure for enhancing the magnetic field was embedded in close proximity to the sorting channel. Specifically, it has previously been shown that the presence of nickel particles in a side channel enhanced the magnetic field gradient, and that the magnetic force on the cells was 3.3 times greater than with a magnet alone (Lin et al., 2007). I thus based my design on this concept, however, since nickel is a toxic substance I replaced these microparticles with the ferrofluid containing magnetite nanoparticles, a solution which is also known to retain phase stability (Scherer & Figueiredo Neto, 2005).

Optimizing the particle based microfluidic approach

The particle based approach for microfluidic magnetic sorting was recently further explored by Zhou and Wang (2016). They demonstrated through magnetic simulations and experimental validation with magnetic particles that there are three main factors that need optimization in such a system (Zhou & Wang, 2016): 1) The distance between the sample and the magnetic side channel, 2) interaction time of sample with the magnetic field gradient and 3) the particle concentration influencing how much the magnetic field gradient is enhanced.

Thus, in order to further optimize the system presented by Lin et al. (Lin et al., 2007) I reduced the distance between the sample and the magnetic particle, by making the gap between the two channels $10 \mu\text{m}$ instead of $25 \mu\text{m}$. This distance is

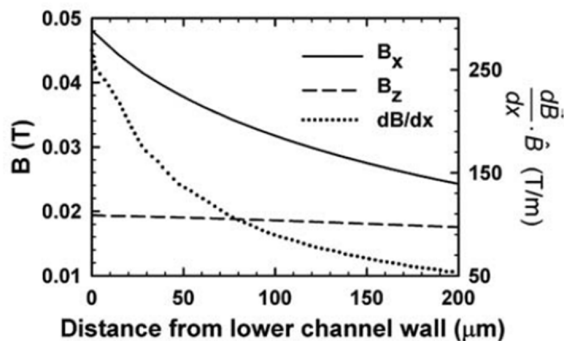


Figure 3.3: The magnetic field gradient decreases rapidly as the distance between to the sorting channel increases. From (Xia et al., 2006).

3.2.1 Microfluidic chip design

an important factor and should be as small as possible due to the rapidly decreasing magnetic field gradient with distance (Xia et al., 2006) (Figure 3.3). Moreover, the width of the sorting channel was reduced as much as possible, limited by the size of the cells and the production methods (width would be minimum twice the channel height). It has been demonstrated that reducing the channel dimensions, and thus the distance between sample and the magnetic particles, had a stronger effect on the sorting efficiency than the longer residence time provided by larger channels given a constant flow rate (Zhou & Wang, 2016).

However, increasing the residence time in the microfluidic channel will prolong the interaction time of the magnetic field gradient with the sample, consequently increasing the likelihood of a cell being successfully sorted. The interaction time can for instance be efficiently be controlled through the flow rate, and is further influenced by the shape of the side channel. Zhou and Wang (2016) compared rounded structures to triangular shapes of a side channel which was filled with iron powder in order to enhance the magnetic field gradient. It was clear from both the theoretical and experimental trajectories of magnetic particles that although the force achieved by the structures were similar (~ 70 pN), the half circle was extending the magnetic force along the flow direction, resulting prolonged interaction time (Zhou & Wang, 2016). Similarly, Xia et al. (2006) expanded the microneedle to a comb structure in order to have multiple interaction points along the sorting channel (Xia et al., 2006). Conversely, I used a straight channel running in close proximity to the sorting channel along its whole length in order to maximize the interaction time.

Finally, as expected from theory, the particle concentration influences how much the magnetic field gradient is enhanced and thus the force acting on the sample. This is also in agreement with my simulation results, which are further discussed below. Thus, as the system dimensions were increased in order to sort larger vertebrate cells I compensated the increased distance by using a ferrofluid of higher particle concentration.

Magnetic simulations

To better characterize the magnetic field gradient and thus the force in the microfluidic system I performed magnetic simulations with accurate values for the

3. Discussion

distances between the different elements in the system. More challenging, however, is obtaining realistic values for the ferrofluid magnetization. I used the saturation magnetization of bulk magnetite (480 kA/m) in order to estimate the magnetic moment of single particles, resulting in $2.5 \cdot 10^{-19} \text{ Am}^2$, and used this value in Equation 1.4 for the theoretical magnetization curves in Figure 1.11.

However, the magnetic moment of a magnetite nanoparticle varies with its size in a non-linear way. In addition, the magnetic moment also depends on how it was synthesized and the local structure. It has been shown, for a given route of synthesis that the magnetization of a particle has a size dependence with a peak for 10 nm particles exhibiting $2.6 \mu\text{B}/\text{fu}$ (Thapa et al., 2004), corresponding to $62.7 \cdot 10^{-3} \text{ Am}^2/\text{g}$. Similar values has also been reported by others ($60.1 \cdot 10^{-3} \text{ Am}^2/\text{g}$, (Goya et al., 2003)). As ferrofluids typically consist of particles in this range, the magnetic moment per particle can be estimated to $1.7 \cdot 10^{-19} \text{ Am}^2$, given the magnetite density of $5.2 \text{ g}/\text{cm}^3$.

Thus, the magnetic field gradient might have been overestimated in this study since the saturation magnetization for magnetite was used in the calculation of the ferrofluid magnetization curve. However the reported saturation magnetization of the ferrofluid (99 mT) is in good agreement with the magnetization curves obtained with the applied model (Figure 1.11).

3.2.2 Performance of sorting system

Large variability in cell magnetization

Using microfluidics with its precise sample control and tunable parameters is ideal for isolation of naturally occurring magnetic cells which have a large span of magnetic moments. For instance, magnetic separation of red blood cells based on their intrinsic magnetic susceptibility ($5.35 \text{ Bohr magnetons per heme group}$, corresponding to $5 \cdot 10^{-23} \text{ Am}^2$) was first demonstrated in 1975 (Melville et al., 1975), and sorting of red blood cells has in later years been refined through microfluidic techniques (Han & Frazier, 2004, 2006). Malaria infected blood cells which contain the paramagnetic crystal hemozoin exhibit a higher magnetic moment, with a magnetic susceptibility of up to $320 \cdot 10^{-6}$ per crystal (Coronado et al., 2014) corresponding to $2.5 \cdot 10^{-16} \text{ Am}^2$ for a crystal size of $1 \mu\text{m}$ in a magnetic field of 1 T. Microfluidic iso-

3.2.2 Performance of sorting system

lation of infected blood cells for diagnostic purposes has been suggested (Zborowski & Chalmers, 2011; Nam et al., 2013).

The macrophages successfully sorted in this study were incubated with magnetite nanoparticles, theoretically yielding a high magnetic moments. These cells could represent a good model for putative candidate magnetoreceptor cells, for which magnetic moments are measured up to 100 fAm² per cell (Eder et al., 2012). On the other hand, MTB exhibit much lower magnetic moments, in the order of 0.1 fAm² (Schüler et al., 1995; Ērglis et al., 2007; Le Sage et al., 2013), which is close to the theoretical limit for overcoming the thermal fluctuations ($k_B T$) when interacting with the weak geomagnetic field ($\sim 50\mu\text{T}$).

When reducing the dimensions of the microfluidic channels and consequently the flow rate in the system I could induce a significant shift in the mean position of a flow of MTB within the channel. With the external magnet I observed a 12 μm displacement of the flow compared to when the magnet was absent. This corresponds to about 20% of the channel width already halfway through it. This shift was enough for the mean position of the flow to cross the midline, and thus efficiently sort the sample. Furthermore, it was evident from the videos that the fraction of bacteria with highest magnetic moments was efficiently sorted as these were observed along the wall. Taken together I demonstrated that the microfluidic system can be used for a large range of cells, both in terms of size and magnetic moments.

Robust data analysis

In order to achieve improved visualization of the cells I used a fluorescent imaging as bright field microscopy did not yield sufficient contrast. The acquisition frame rate was thus limited by the photon counts and in order to obtain a good fluorescent signal of the cells I used a relatively long exposure time. This resulted in the cells appearing elongated with different lengths and intensities depending on the speed of the single cells. These varied as the velocity profile in a microfluidic channel of radius R is a function of distance from the wall, r ($\sim 1 - (r^2/R^2)$). In most of the frames the cells produced a continuous signal across the whole field of view. Although, sorted cell close to the wall were clearly flowing with a lower velocity and thus did not cover the whole frame, this did not present problems for the automated

3. Discussion

analysis.

In fact, reducing each frame to a vertical line through a mean intensity projection along the x-axis allowed for easy assessment of the width and intensity of each object passing in the channel. This in turn improved the accuracy of the quantification analysis of cells. Specifically, narrow signals with high intensity, which would be included by simple thresholding algorithms, are caused by cell debris or free magnetic particles in the solution. Moreover, the signal from cells outside the focal plane appears weaker, but can be identified by the width of the signal.

In addition, the number of cells in a sample could differ. For instance, during the experiments with macrophages the flow rate was $1 \mu\text{l}/\text{min}$, while the camera frame rate was 20 fps. In these conditions the average fraction of frames showing a cell was about 0.08, and assuming a Poisson distribution with mean 0.08 for the number of cells in one single frame, the probability of imaging more than one cell per frame was <0.003 . Thus, under these conditions the assumption that each frame would contain maximum one cell would introduce negligible errors in the estimated sorting efficiency. However, the MTB sample contained a much higher density of cells, increasing the likelihood of detecting more than one cell per frame. This could be efficiently adjusted for by defining an intensity threshold, thus allowing detection of several cells in each frame. This way the histograms could still be generated and thus the sample profile in the flow compared.

Further improvements of system design

The microfluidic magnetic sorting system was shown to efficiently sort naturally occurring magnetic cells such as magnetotactic bacteria, as well as bioengineered cells and macrophages with magnetic particles. The increased dimensions in Chip2 did improve the handling of larger cell types, such as HEK cells. Moreover, the simulations showed that the increased distance was well compensated for by the high density of magnetic nanoparticles in the ferrofluid. Thus, for more efficient sorting of the bacteria or for sorting of mutants with lower magnetic moments the high density ferrofluid could be used in the Chip1 system. According to my simulations this would result in a 100% increase of the magnetic field gradient (Figure 2.12) and thus double the force acting on the magnetic cells.

It could be considered whether other materials would improve the magnetic prop-

3.2.2 Performance of sorting system

erties of the ferrofluid. Nickel, which has been used in a previous implementations of a particle-based sorting system (Lin et al., 2007), has a saturation magnetization (488 kA/m) similar to that of magnetite (480 kA/m). Metallic iron on the other hand, has a saturation magnetization which is about three times higher (1711 kA/m). However, the phase stability of a ferrofluid depends on a balance between the attractive and repulsive forces. To avoid particle agglomerations the maximum diameter of the cores therefore scales with the magnetization as $\sim M^{-2/3}$ (Scherer & Figueiredo Neto, 2005). Hence, if metallic iron were to be used as material in a ferrofluid smaller cores would be necessary, resulting in similar particle magnetic moments as compared to what could be achieved with magnetite.

It was recently shown that the magnetic field gradient could be improved by changing the shape of the side channel, forming half circles or triangles along it (Zhou & Wang, 2016). Other shapes could also be explored. However, keeping the distance of 10 μm would be important as the gradient decrease rapidly with distance (Xia et al., 2006) Figure 3.3).

Another level of control could be added through hydrodynamic focusing of the sample flow. Such focused flow is achieved in a design with an extra inlet and outlet (Figure 3.4a). In this case the sample is injected at the center inlet while a buffer flow on both sides will ensure a narrow distribution of cell position in the channel in absence of the external magnets. Furthermore, this would also move the cells closer the ferrofluid in the initial phase of the sorting process. Hence, the cells would be in an area with higher magnetic field gradient, further increasing the sorting efficiency for a given flow rate.

The design for two outlets demonstrated by Adams et al. (2008) for differently magnetized samples could perhaps be realized also with the ferrofluid approach (Figure 3.4b). The separation of the two magnetic samples is based on the angle of the nickel strips relative to the flow direction of the sample because deflection is achieved only if $F_m > F_d(\sin\theta)$ (Adams et al., 2008). Thus, one can imagine to replace the two strips of nickel with ferrofluid filled channels. The ferrofluids could further contain different densities of magnetite particles in order to achieve varying magnetic gradients and separation of samples with different magnetic moments (Figure 2.12).

Although microfluidic systems offer reliable, tunable and contamination free separation of magnetic cell populations, one of the main limitations of microfluidic

3. Discussion

systems is the low throughput of the sample due to the small dimensions of the channels. Thus, the challenge is to find a balance between close proximity of to the magnetic structures creating the gradient field and maximizing the dimensions of the system. However, if one would be able to increase the magnetic force acting on the cells, as discussed above, this would allow for higher flow rates in the system in order to improve the throughput of sample.

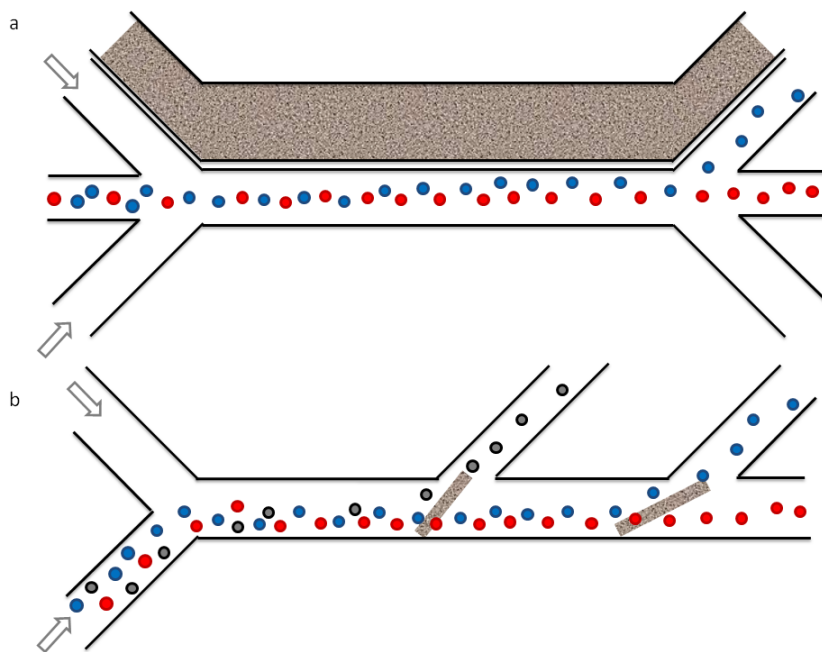


Figure 3.4: Alternative designs for microfluidic magnetic sorting. a) Three inlets/outlets would allow for more precise sample control as well as moving the sample in the region of stronger magnetic field gradient generated by the ferrofluid. b) Adapted design from Adams et al. (2008) for separation of differently magnetized samples by changing angle and density in underlying ferrofluid channels.

3.2.3 Future applications of microfluidic magnetic sorting

Bioengineered cells have low magnetic moments

Bioengineered cells for magnetogenetics often relies on the paramagnetic properties of the iron storage protein ferritin (Kim et al., 2012; Stanley et al., 2012, 2015; Wheeler et al., 2016; Liu et al., 2016). However, ferritin contains less uncompensated ferric iron spins and has a magnetization in the order of $0.1 \text{ Am}^2/\text{kg}$ in a 1 T

3.2.3 Future applications of microfluidic magnetic sorting

field (Makhlouf et al., 1997). Hence, ferritin has much weaker magnetic moments compared to the ferrimagnetic material magnetite ($92 \text{ Am}^2/\text{kg}$). If bioengineered cells are to be useful for magnetogenetics they need to exhibit stronger magnetic moments than ferritin (Meister, 2016). Hence, the microfluidic magnetic sorting system could potentially be valuable in a directed evolution approach for rendering cells magnetic (Liu et al., 2016). In this case contamination-free enrichment of the cells with high magnetic moments is of great importance.

My results demonstrate that a large range of samples, in terms of both size and magnetic moments, could be efficiently sorted in the microfluidic system with small adjustments to the design. However, further optimization steps, such as the ones discussed above, might be necessary in order to efficiently sort ferritin containing cells.

Characterization of magnetic cell properties

The microfluidic system could further be used to estimate the magnetic moment of a sample. This could be achieved by balancing the magnetic force ($m \cdot \nabla B$) and the drag force ($3\pi\eta rv$) on a particle in laminar flow following Stokes' law and calculating the crossing velocity (v). For a cell to be efficiently sorted it should cover a distance equal to half the width of the sorting channel (w) within the time it spends in the system. This residence time and thereby the time the magnetic force is allowed to act on the cell, is determined by the flow rate of the sample as well as the cross section of the channel ($t = l/hwf$). Thus the minimum magnetic moment of the sorted cells can be estimated by

$$m = \frac{3\pi r \eta f}{lh \nabla B}, \quad (3.1)$$

where m is the magnetic moment and r is the radius of the cell, η is the viscosity of the buffer, f is the total flow rate, l and h is the length and height of the sorting channel, respectively, and ∇B is the magnetic field intensity gradient.

Figure 3.5 shows an example of how the threshold of successfully sorted cells changes with flow rate for different magnetic field gradients. Thus, by adjusting the flow rate during sorting the magnetic moment of a sample can be estimated. For instance, the magnetite containing macrophages have a radius of ca. $5 \mu\text{m}$ and were

3. Discussion

efficiently sorted with a total flow rate of $5.7 \mu\text{l}/\text{min}$. Assuming a magnetic gradient of $300 \text{ T}/\text{m}$ the sorted cells have an estimated magnetic moment larger than about 15 fAm^2 , corresponding to a realistic number of ca. 2000 magnetite nanoparticles per cell.

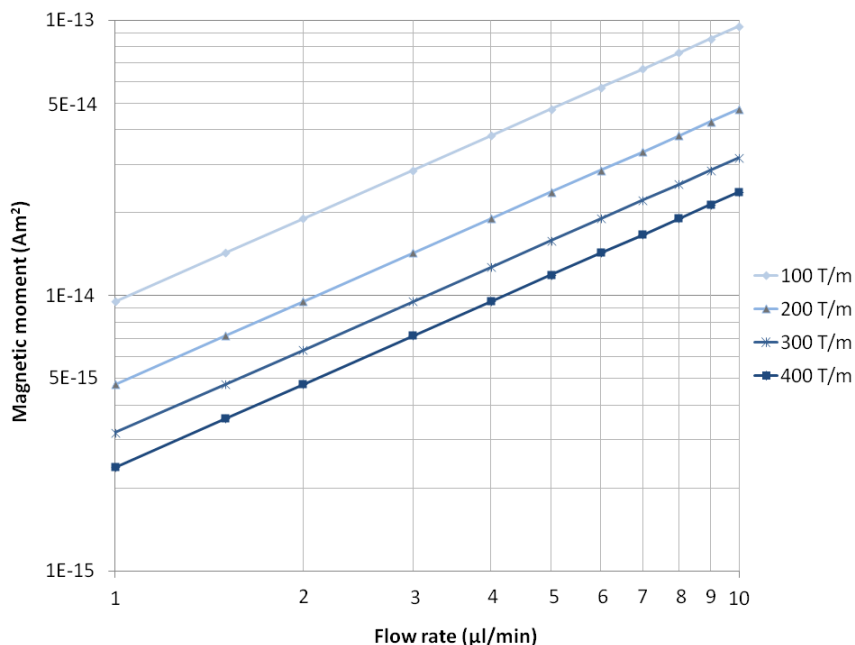


Figure 3.5: The relationship between total flow rates (sum of buffer and sample) and the threshold for sorted magnetic moments can be used to estimate the magnetic moment of a sample. The graph shows values assuming a cell of $10 \mu\text{m}$ diameter, for different magnetic field gradients. Adapted from Myklatun et al. (2017)

Direct comparison of samples

The microfluidic system, could be valuable during optimization processes of bio-engineering approaches, not just for directed evolution, but also for characterization of samples, as describe above. Moreover, the video analysis could be used to directly compare different samples. For instance, one could evaluate two populations of differently magnetized cells by using different fluorescent markers. If introduced simultaneously into the channel selective imaging the cells would allow them to be analyzed separately and direct comparison the two populations could be made through the software. This is similar to how the cell behavior was characterized in the absence and presence of external magnets (blue and red, respectively, in Figure

3.2.3 Future applications of microfluidic magnetic sorting

2.13).

Furthermore, the tunable parameters allowing to determine thresholds for magnetic moments could prove useful for separation of highly magnetized cells from heterogeneous populations. This would be difficult to achieve in commercial column-based sorting systems, in which also the background field is high such that undesired iron-rich cells could be fully saturated leading to enrichment of these (Franken et al., 2015). In contrast, my system presents a relatively low background magnetic field (150 mT) generated by the particles, thus reducing this problem.

The system I developed produce high magnetic field gradients without the risk of introducing contaminations, allowing for safe separation of cells which are to be subjected to downstream biophysical or chemical analysis. Moreover, the tunable parameters and visual control makes the system ideal both for directed evolution approaches and assessment of sample magnetization. Taken together, the microfluidic magnetic sorting system is likely to become useful in a number of steps towards magnetogenetics.

3. Discussion

Table 3.2: Continuous flow magnetic separation techniques

Method	Sample	Flow rate ($\mu\text{l}/\text{min}$)	Gradient (T/m)	Reference
Electromagnet ^a	Magnetic particles	~ 0.2	< 40	Siegel et al. 2006
Electromagnet ^{a,d}	Magnetic particles	$2.7 \cdot 10^{-3}$	< 250	Lin et al. 2007
Ferrromagnetic structure ^c	Whole blood	4500	< 8000	Melville et al. 1975
Ferrromagnetic structure ^c	Labeled cells	160-1600	1000	Miltenyi et al. 1990
Ferrromagnetic structure ^a	Labeled bacteria	0.5	50-250	Xia et al. 2006
Ferrromagnetic structure ^{a,c}	Labeled bacteria	83	$\sim 10\ 000$	Adams et al. 2008
Magnetic particles ^a	Labeled cells	0.2	$< 2000^b$	Lin et al. 2007
Magnetic particles ^a	Magnetic particles	1-4	$< 1000^b$	Zhou & Wang 2016
Magnetic particles ^{a,c}	Labeled cells	~ 23 -115	50-4000	Sun et al. 2016
Magnetic particles ^a	Labeled cells	0.5-2	< 1750	Myklatun et al. 2017
Quadrupole array	Labeled cells	100-750	174	Sun et al. 1998

^a microfluidic system

^b estimated from figure

^c contamination risk

^d active flow

Chapter 4

Conclusions

In my PhD work I developed tools for research aimed at understanding the interaction of magnetic fields with magnetically sensitive neurons in organisms. The work was motivated by the novel scientific field of magnetogenetics, whose goal is to control neuronal processes, with genetic precision, via application of magnetic fields. In the biomimetic approach the aim is to learn how nature implemented a magnetic sense to then use aspects of it for other biological systems. Thus, the first crucial step is a more comprehensive understanding of the molecular mechanisms and the genes involved in magnetoreception. There are currently two hypotheses for how animals can sense the Earth's magnetic field; through mechanical interaction with biogenic magnetite particles or through influencing a chemical reaction involving radical pairs.

In a collaborative effort with geophysicists and neurobiologists, I successfully established a behavioral assay to quantify the reorientation of individual fish. Specifically, their change in bearing or spatial preference was compared to the directional shift of an applied magnetic field of geomagnetic field intensity. The tests were performed in darkness in order to directly test the magnetite hypothesis against the light-dependent radical pair hypothesis.

Using this assay, I identified two vertebrate genetic model organisms, zebrafish and medaka, that responded according to the directional change of the magnetic field. The reorientation was evident also under infrared illumination, even after keeping the fish in darkness over an extended period prior to the assessment. Thus, I was able to obtain behavioral evidence for a light-independent magnetoreception

4. Conclusions

for these two fishes. Conversely, I could not find evidence for magnetosensitivity in the invertebrate model organism *C.elegans*, despite positive reports in literature.

The behavioral evidence for light-independent magnetoreception was not in line with the radical pair hypothesis, however it would be consistent with a magnetite-based mechanism. Thus, to test the prediction of the magnetite hypothesis I investigated whether magnetic biomineralizations were present in the fishes. To this aim I used a rotating magnetic field in order to screen dissociated primary tissue for cells with magnetic properties. I did not find evidence for magnetite-based magnetoreceptor cells, neither in wild salmon nor in the laboratory fishes zebrafish and medaka. Although extracellular magnetic material was present in all samples it remains unclear whether these were part of a magnetoreceptor system. Furthermore, it is possible that the rotation assay employed failed in detecting cells containing superparamagnetic magnetite, since these would only under certain conditions experience a torque. Thus the identity of the putative receptor cells remains undiscovered, and future development of new techniques for their assessment is necessary.

Finally, I successfully developed a microfluidic magnetic sorting system. The system allowed for contamination free enrichment of magnetic cells, essential for their downstream biophysical and chemical analysis. Despite the lack of magnetoreceptor cells, I demonstrated the performance of the system by efficiently sorting both magnetically labeled eukaryotic cells and naturally occurring magnetotactic bacteria. These cells have a low magnetic volume, operating at the theoretical limit for magnetic interaction energies to overcome thermal fluctuations. They are thus realistically representing the magnetic properties necessary for future magnetogenetic applications.

In conclusion, I predict that the microfluidic system will be useful in future searches for magnetic cells, such as the magnetoreceptors and other magnetic cells produced in bioengineering approaches towards magnetogenetics. Furthermore, I identified light-independent magnetoreception in two genetic model organisms. These are both optically and genetically addressable, which opens the possibilities of interrogation of candidate key genes as well as the neural correlates of magnetoreception. Thus, my work on magnetosensitive genetic model organisms together with the microfluidic sorting system provides a foundation for future research towards magnetogenetics.

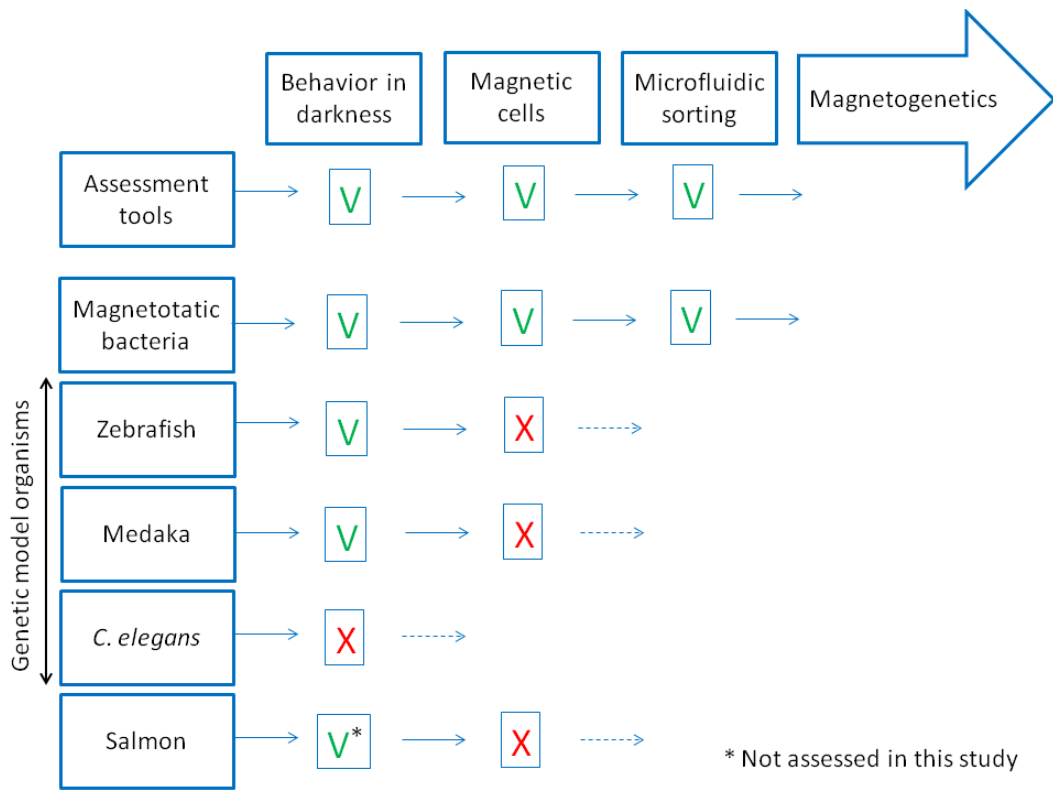


Figure 4.1: Summary of project outcome

4. Conclusions

Chapter 5

Materials and methods

5.1 Magnetoreception in genetic model organisms

5.1.1 Behavioral experiments in zebrafish and medaka

Set up for spontaneous directional preference

The behavioral experiments in zebrafish and medaka took place in two different locations; at the Institute of Zoology at University of Hohenheim, in collaboration with Dr. Denis Shcherbakov, and at the Geophysical observatory of Ludwig-Maximilian Universität (LMU) in Furth, in collaboration with Dr. Stephan Eder. The experimental set up was identical in the two locations, with the exception of the Helmholtz coils that were used in order to manipulate the geomagnetic field (GMF). In Hohenheim the coils were wooden with a diameter of 2 m, while in collaboration with LMU we used metal coils with a diameter of 1.2 m. The principle for shifting the GMF is the same for both locations, however numerical example is provided for the setup in Furth (Figure 2.2).

The GMF in the room used for experiments were measured to be $50.6 \mu\text{T}$ in total intensity with an inclination angle of $62,8^\circ$. The two pairs of Helmholtz coils were used to shift the horizontal component of the geomagnetic field ($23.3 \mu\text{T}$) by 45° towards either North-East (NE) or North-West (NW). The directional shift of the GMF was achieved by applying a current in the coils in the East-West orientation, corresponding to an applied magnetic field of $16.5 \mu\text{T}$. The intensity was adjusted by applying field of $6.8 \mu\text{T}$ in the South direction (Figure 2.2). The direction, 45° shift

5. Materials and methods

compared to GMF, was controlled with a compass, while the intensity was measured using a magnetometer in order to compare the resulting magnetic field to the GMF. This is a configuration which has equal amount of current flowing in both magnetic conditions and thus adds an extra control for the presence of current and potential electric noise effects.

At the center of the coils we placed a wooden table. The test arena (glass petri dish, Ø 17 cm H 3 cm) was placed inside a card board box (Black hardboard TB4, Thorlabs, Germany) on top of an infrared (IR) illumination table, made of an array of LEDs (1060 nm, ELD-1060-525, Jenoptik, Germany) with a diffuser on top. The current layout of the LED array, was designed such that the magnetic fields caused by the LED current compensated for. At the center of the test arena there was a transparent plastic cylinder (Ø 6 cm), which could be removed by a custom non-magnetic and automatic lifting mechanism. Both the IR table and the lifting mechanism was custom made by Dr. Stephan Eder.

For the experiments in light a white light (WL) ring illumination (Leica) was centered above the test area. The behavior of the fish was monitored with a camera (Sony DCR-HC23E), mounted above the arena and run in nightshot mode at 25 frames per second (FPS), with the infrared source on the camera covered. The infrared illumination from below was on during all the experiments to ensure that the image quality was the same for all trials. The set up was covered with a black curtain (Blackout fabric BK5, Thorlabs) to not let any light enter, in addition all other light sources in the room were covered with black tape (Black masking tape T743-2.0, Thorlabs) to ensure that there would be no visual cues for orientation.

Experimental procedure

Prior to the start of the experiment fish were acclimated individually for one hour, either in light or in darkness. The magnetic field condition was set and a fish was brought into the arena and placed within the inner cylinder, always with the same water depth of 2 cm. 20 seconds after the experiment was started an automatic mechanism lifted the cylinder and released the fish. The fish were observed for one (zebrafish) or two (medaka) minutes after release.

During the experiments with LMU the experimenters stayed in the room as all conditions and recordings were controlled manually. While in Hohenheim we left the

5.1.1 Behavioral experiments in zebrafish and medaka

room before start of the experiment and controlled the recording from a separate room, using DASyLab (Data Acquisition System Laboratory, National Instruments)

After the experiment the fish was brought back to the individual container, and the petri dish was washed before the next fish was placed. After a waiting period of ca. 45 minutes, the fish was tested again with changed magnetic field conditions. The starting condition was randomized such that half of the individuals started in NE and the other half in NW. Handling of the fish was done in red light for the fish that were kept in darkness prior to testing. The light in the room was switched off during the all experiments.

Animals used in the experiments

Adult zebrafish (AB) and medaka (CAB strain) were used in the experiments. A summary of all animals used in the spontaneous directional preference assay is presented in table 5.1. All groups of zebrafish originated from a single parent couple, thus exhibiting similar genetic background. Medaka were collected from several individuals belonging to the same genetic cohort.

The eggs were collected and kept in an incubator at 28°C for the first four days, for zebrafish and 7-10 days for medaka. Then the larvae were raised in the facility under normal conditions until testing. The fish were kept in a 14 h light / 10 h dark cycle both in the incubator and in the fish facility, where they were fed with artemia twice per day. Medaka in addition received dry feed once per day.

All animal experiments were approved by the government of Upper Bavaria and were carried out in accordance with the approved guidelines.

Data analysis

Tracking of the nose and the center of mass of the fish was performed with a program custom written in MATLAB (MathWorks, USA) by Dr. Michele Cappetta. In order to assess the bearing (BE) of individual fish the program analyzed the coordinates to find the point where the nose of the fish was first crossing the virtual 6 or 8.5 cm radius line. The first to analyze the immediate bearing upon release, and the latter in order to assess the point where the fish first touch the wall with its head. The bearing was then defined as the angle from the center of the arena to the crossing point, relative to geomagnetic North. The reorientation, defined as the difference

5. Materials and methods

Table 5.1: Fish used in experiments

Strain	# Fish	Age (months)	Gender (f/m)	Acclimation	Test illumination
Zebrafish					
AB*	16	6	7/9	WL	WL
AB*	16	6	6/10	WL	IR
AB	24	12	8/16	dark	IR
Medaka					
CAB	24	4	8/20	WL	IR
CAB	20	8	5/15	dark	IR

*Hohenheim

in bearing between the two magnetic conditions ($BE_{NE} - BE_{NW}$), was calculated for each individual fish. Fish that did not cross the line within two minutes after release were excluded from the analysis. Manual corrections were added in the few cases (5 of 247) where the software could not assign a bearing.

For assessing the spatial preference (SP) of individual fish the arena was divided in twelve segments and the preferred area was defined as the segment in which the centroid coordinate of the fish was most frequently during one minute after release. Manual corrections were added in the few cases where the tracking software could not correctly track the fish for the entire observation time (6 of 199). Due to the slower movement out of the center of the arena, SP in medaka was assessed during the second minute after release. Fish that were not observed for two minutes (due to problems during recording), and two cases where the release mechanism failed, were excluded from the analysis. The difference in preferred segment (reorientation) between the two magnetic conditions was converted to an angle (in steps of 45°) for each fish.

Statistical analysis for the distributions of angular differences were done with Oriana 4 (Kovach Computing Services). For both BE and SP the distribution of differences (either polar or axial) were compared to the expected mean of 90° with the V-test, which tests for uniformity of circular data with the alternative hypothesis of a non-uniform distribution with a specified mean (Batschelet, 1981).

The circular plots for BE were generated in MATLAB by plotting one dot for

5.1.2 Magnetic preference behavior in *c.elegans*

each fish. For SP the angular differences were binned and in this case the center value of the bin was plotted.

In order to analyze the thigmotactic behavior of zebrafish, the fish tested in WL and IR after acclimation in light were analyzed using Ethovision software (Ethovision XT, Noldus, Netherlands). Thigmotaxis was defined as presence in a zone of the arena at 2.5 cm from the wall. Significant difference in time spent in zone for the two lighting conditions was tested with a 2 two tailed t-test.

Medaka swimming behavior in darkness

To assess the swimming strategy of sexually mature medaka in IR compared to WL fish were tested in both lighting conditions. 11 fish of mixed gender of the CAB strain, aged 6 months were observed individually for two minutes in a circular arena (15 cm diameter). Half of the fish were tested first in darkness, and then in light, while the remaining fish were tested first in light then in darkness. The arena was illuminated from below with a ring of LEDs (1060 nm) in addition to a WL illumination table. The IR source was always on, while the illumination table was switched on for the WL trials. A piece of white paper was placed underneath the arena in order to create a homogeneous background. Fish were imaged at 20 FPS from above with an NIR sensitive camera (Ximea MQ013RG-E2, Germany). The whole setup was placed within a black box made of carton not transparent to light (Black hardboard TB4, Thorlabs, USA) in order to observe the fish in darkness. The natural swimming behavior in the two lighting conditions were assessed with Ethovision software (Ethovision XT, Noldus, Netherlands). Continuous circling behavior was assessed through the rotation parameter in the software, were 720° rotations of the fish heading was counted (using 0° threshold, not accepting any backwards movement, minimum distance traveled 1 cm). Statistical significance between the two lighting conditions was tested with a paired, two tailed, t-test.

5.1.2 Magnetic preference behavior in *c.elegans*

Magnetoperception has recently been shown in the genetic model organism *C. elegans* (Vidal-Gadea et al. 2015), and the magnetotaxis assay described in this paper was tested in our laboratory. Adult wildtype N2 (var. Bristol) *C. elegans* were cul-

5. Materials and methods

tivated for 10 hours on NGM agar plates coated with *E. coli* OP50. Thereafter the adults were removed and the remaining embryos were shipped from our collaborator (Dr. Spanier, Technical University Munich) on agar plates with *E. coli* OP50 after synchronization.

The worms were stored at 20°C to reach the young adult stage and tests were performed on day four with young adult *C. elegans* hermaphrodites. Worms and empty agar plates were left unsealed on the bench in order to avoid temperature or CO₂ gradients. The test plates with agar were placed on top of a circular magnet (NdFeB N42, S-35-05-N, Supermagnete) and a plastic piece of the same size, which were both covered by paper with the two circles drawn in order to avoid visual differences. The magnet and the plastic circles were both 3,5 cm and placed equidistantly from the center of the plate, oriented in the east-west direction of the room. In the centers of the two circles 2 μ l of 1 M NaN₃ was placed to avoid worms reaching this area from moving further. Worms were washed off the plate with 2 ml S-basal buffer, and 5 μ l of worms (ca. 50 worms) were transferred to the center of the testing plates. They were released by removing the surrounding buffer with paper tissue. The plates were covered with aluminum foil and left approximately 30 min.

Worms that had reached the two target circles were counted and the magnetic index ($MI = (M-C)/(M+C)$) was calculated in addition to the relative amount of worms on each side. Statistical significance was tested with two tailed t-test.

5.2 Candidate magnetoreceptor cells

5.2.1 Candidate magnetoreceptor cells in laboratory fish

Dissociation

The zebrafish (AB, Nacre or Casper) and medaka (Cab) were euthanized with an overdose of MS222. Samples were prepared in a clean environment using ceramic scalpels and titanium forceps in order to avoid magnetic contamination. Tissue samples were extracted in Ringers buffer with calcium. In the case of head or whole body samples the eyes and inner organs were removed due to risk of contamination.

Dissociation was done with activated papain (0.25 mg/ml papain mixed with 1.25

5.2.1 Candidate magnetoreceptor cells in laboratory fish

mg/ml L-cystein) in Ringers buffer without calcium. Alternatively samples were dissociated with collagenase type 2 (2 mg/ml) in PBS. Samples were incubated with the enzymes for 10 min at room temperature. Then the olfactory rosettes and brain were gently triturated for 5 min, while samples from lateral line (skin), muscles, head or whole body were mechanically dissociated with the Miltenyi gentle MACS dissociator. Chemical dissociation through papain was stopped by addition of Ringer with calcium 1:1. If density of cells in the sample was low, cells were spun down for four minutes at 10.000 rpm and the supernatant removed. If necessary, for later observation, cells were fixed in Ringer w/Ca²⁺ containing 4% PFA.

In order to evaluate the cells after dissociation one zebrafish of the AB strain and two medaka of the Cab strain was assessed. The rosettes, brain and the rest of the head region (without eyes) were dissociated as described above, however no fluorescent markers used. Trypan blue was added 1:1 to a small sample and 10 μ l was counted to assess the viability of the cells. The average count for one fish is summarized in Table 5.2.

Table 5.2: Dissociation of laboratory fish

Sample	Enzyme	Cell number	Vital cells
Zebrafish			
Rosettes	papain	$2.8 \cdot 10^4$	97%
Brain	papain	$1.1 \cdot 10^5$	95%
Head	collagenase	$8.5 \cdot 10^5$	99%
Medaka			
Rosettes	papain	$1.0 \cdot 10^4$	>90%
Brain	papain	$5.5 \cdot 10^5$	>90%
Head	collagenase	$1.0 \cdot 10^6$	>90%

Search for magnetic cells

After dissociation the samples were labeled with fluorescent markers for nucleus (Hoechst 33342) and membrane (FM 1-43 FX) for validation of cellular identity. They were then filtered through a cell strainer (100 μ m) before magnetic enrichment in order to increase the fraction of magnetic cells. This was achieved by running the sample through a flow chip (μ -slide, ibidi, Germany). A strong mag-

5. Materials and methods

netic gradient was applied from underneath through an iron needle attached to a permanent magnet in order to keep magnetic material in the chip. In the case of dense samples these were washed with addition of buffer while in the presence of the magnet. Dissociated tissue samples were next observed on an inverted microscope (Axiovert 200 M, Zeiss, Germany), in the flow chip in which the sample was sorted, in order to avoid drying of the sample. I used a 20x or 63x magnification objective in bright field.

Identification of magnetic objects was performed with a field-flip test or the rotation assay as described by Eder et al. (2012) (Figure 2.9). For the field-flip test a single pair of Helmholtz coils were used to create an oscillating magnetic field with intensity of approximately 2 mT and frequency 0.1-0.3 Hz, whereas two coil pairs were used to obtain the rotation. In both cases custom coils were designed and built by Dr. Stephan Eder to fit around the detection objective of the microscope. The two coil pairs were tilted to create a focused magnetic field (2 mT, 0.3 Hz) in the field of view of the objective (Figure 2.9). Two sinusoidal signals, 90° phase shifted, were used to create the rotating magnetic field. This was done with a function generator (ETC M631 Arbitrary Waveform Generator, CGC Instruments, Germany) controlled by a computer. Turning objects were observed with fluorescence and reflection (50 % mirror) in order to further characterize their nature.

5.2.2 Candidate magnetoreceptor cells in salmon

In collaboration with Ims Aquatic Research Station, part of Norwegian Institute for Nature Research (NINA), studies on wild salmon were performed. Wild salmon are known to perform long distance migration, probably using the geomagnetic field information for navigation. Experiments were performed at the aquatic research station located close to the river Imsa and the capture site of the fish.

Returning adult salmon (November 2013)

Adult fish, 2-4 years, were caught during the autumn upon return to the river Imsa and kept in tanks 2-4 months, until testing. The olfactory rosettes, the lateral line area and the underlying muscle was collected from three adult salmon (male, 502-621 mm, 864-1777 g) using ceramic scalpel and titanium forceps and washed

5.2.2 Candidate magnetoreceptor cells in salmon

in sterile HBSS (55037C, Sigma-Aldrich, Germany). The samples were cut in small pieces and dissociated approximately one hour after collection. In order to find the best dissociation condition for salmon, dissociation was done with collagenase type 1 (C0130, Sigma-Aldrich, Germany) and type 2 (C6885, Sigma-Aldrich, Germany) at different ratios and concentrations, ranging from 0.5-2 mg/ml, in HBSS and incubated for ca. two hours (summarized in Table 5.3).

The lateral line samples from different dissociation conditions were mixed and filtered through a cell strainer with 100 μm mesh size, sorted through the Miltenyi LS magnetic columns (Miltenyi) and finally run through a flow chip (μ -Slide, ibid, Germany) with a gradient needle, as described for zebrafish samples. Only a small fraction of the total sample volume was sorted due to the inefficient dissociation for all conditions. The rosette sample was sorted through a flow chip with a gradient needle. The samples were the observed under the microscope (Leica) with the field-flip assay, as described above (2 mT, 0.3 Hz).

Table 5.3: Dissociation conditions for adult salmon

Sample	#	Collagenase Type 1	Collagenase Type 2
Rosettes	3	1 mg/ml	1 mg/ml
Muscles	2	1 mg/ml	-
Lateral line	1	0.5 mg/ml	0.5 mg/ml
Lateral line	1	2 mg/ml	-
Lateral line	1	2 mg/ml	1 mg/ml

Juvenile salmon (November 2013)

Juvenile salmon (parr, ca. 1.5 years) were caught in the fish trap across the river on a daily basis. The olfactory rosettes, the lateral line area and the underlying muscle were collected from three parr (139-152 mm, 28-33 g), using ceramic scalpel and titanium forceps, and washed in sterile HBSS. The samples were cut in small pieces and dissociated approximately one hour after collection. Dissociation was done with 2 mg/ml collagenase type 1 in HBSS and incubated for ca. two hours. The lateral line sample (n = 3) and the muscle sample (n = 4) were then filtered through a cell strainer with 100 μm mesh size, sorted through the Miltenyi LS magnetic columns

5. Materials and methods

and finally run through an ibidi chip with a gradient needle. The rosette sample ($n = 2$) was sorted through an ibidi chip with a gradient needle. The samples were then observed under the microscope with the field-flip test as described above (2 mT, 0.3 Hz).

The rest of the samples from parr and adult salmon were kept in 4 % PFA in HBSS for future studies.

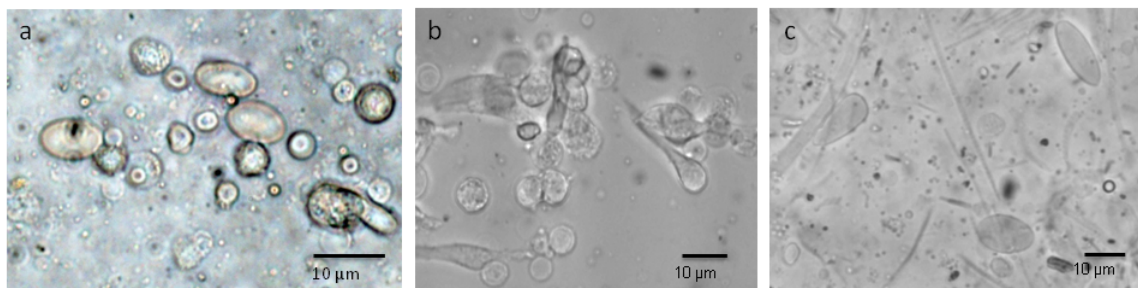


Figure 5.1: Dissociated cells from salmon. a) Cells from the rosette of parr appear to be in a hypotonic solution. b) After optimized dissociation protocol the bottle shaped neurons of the rosette from smolt clearly visible. c) Dissociated tissue from lateral line of smolt

Smolt on the way out (May 2014)

Due to interesting findings in parr and adult salmon, further experiments were performed in collaboration with Ims Aquatic Research Station in May 2014. Smolt on the way out were caught daily in the fish trap across the river. Rosettes, muscle and lateral line samples were collected from 10 smolt (144-168 mm, 24-39 g) using ceramic scalpel, titanium forceps and sterile filtered ($0.22 \mu\text{m}$ syringe filter) water from the river. Samples from three fish were dissociated for observation of magnetic cells, while the remaining samples were stored in PFA, Glutaraldehyde or a mix of the two for future studies. In order to improve viability of the cells after dissociation a number of different conditions were tested (summarized in Table 5.4). The viability of the cells was tested with Trypan blue staining and observation of the shape of neurons and erythrocytes.

The dissociated sample was sorted through the LS magnetic columns (Miltenyi) and through a flow chip (μ -slide, ibidi, Germany) with a gradient needle underneath, and then observed with the field-flip assay (2 mT, 0.3 Hz) through the microscope.

5.2.3 Solutions and chemicals

Table 5.4: Tissue dissociation conditions for salmon

Buffer	Enzyme	Conc. (mg/ml)	Dissociation	Cell viability
Olfactory rosettes				
Ringer	papain/L-cystein	0.25/1.25	Good	High
River*	papain/L-cystein	0.25/1.25	Good	Medium
Lateral Line				
HBSS	Collagenase Type 1	2	OK	Medium
River	Collagenase Type 1	2	Good	High
River	papain/L-cystein	0.25/1.25	Bad	-
Ringer w/Ca ²⁺	Collagenase Type 1	2	OK	Medium
Ringer wo/Ca ²⁺	papain/L-cystein	0.25/1.25	Bad	-
PBS w/Ca ²⁺	Collagenase Type 1	2	Good	High

5.2.3 Solutions and chemicals

Table 5.5: Chemicals used for dissociation

Product	Catalog number	Supplier
HBSS w/Ca ²⁺	55037C	Sigma-Aldrich
PBS w/Ca ²⁺	D1283	Sigma-Aldrich
PBS wo/Ca ²⁺	D1408	Sigma-Aldrich
Collagenase type 1	C0130	Sigma-Aldrich
Collagenase type 2	C6885	Sigma-Aldrich
Papain	P4762	Sigma-Aldrich
L-cystein	C-1276	Sigma-Aldrich
PFA 16%	28906	Thermo Fisher Scientific
2.5% Glutaraldehyde*	15960	Science Services Munich
Hoechst 33342	H3570	Thermo Fisher Scientific
FM 1-43 FX	F35355	Thermo Fisher Scientific

*in sodium cacodylate buffer

5. Materials and methods

Table 5.6: Dissociation buffers

Ringer's solutions for zebrafish	
116 mM	NaCl
2.9 mM	KCl
1.8 mM	CaCl ₂ *
5 mM	HEPES
pH 7.2	
Ringer's solution for salmon wo/Ca ²⁺	
134 mM	NaCl
5 mM	KCl
5.5 mM	Glucose
10 mM	HEPES
1 mM	EGTA
pH 7.2-7.4	
Ringer's solution for salmon w/Ca ²⁺	
130 mM	NaCl
5 mM	KCl
3 mM	CaCl ₂
1 mM	MgCl ₂
5.5 mM	Glucose
10 mM	HEPES
pH 7.2-7.4	

*only with Ca²⁺

5.3 Microfluidic magnetic sorting

5.3.1 Microfluidic magnetic sorting chip

For sorting of magnetic cells I designed microfluidic sorting chips which were produced by Micronit (Netherlands). There were two parallel channels, one for creating the magnetic field and one for sorting the sample. The magnetic channel had one inlet, one outlet and was 100 μm wide in Chip1 and 150 μm in Chip2. The sorting channel had two inlets and outlets, to allow separation of the sample, and was 65 μm and 110 μm wide in Chip1 and Chip2, respectively. Channels in Chip1 were 30 μm high and in Chip2 the height of both channels were 50 μm . The distance between the ferrofluid and sorting channel was 10 m in both cases (see Figure 2.11).

The magnetic channel was created by filling it with ferrofluid containing 10 nm magnetite particles. In Chip1 a commercial ferrofluid was used (FER-01, Supermagnete, Germany), while in Chip2 a ferrofluid with a higher particle concentration of 17.7% Vol was used (EM900, Ferrotec, Japan). A ferrofluid does not create a magnetic field unless it is in the presence of an external magnetic field. This was added by bringing an array of three neodymium magnets (QM-08x03x02-N, Magnet Shop, Germany) in close proximity to the ferrofluid channel.

Simulations of magnetic field in microfluidic channel

To predict the magnetic field and gradients produced in the microfluidic channels, and thereby the sorting efficiency, magnetic simulations were performed with Finite Element Method Magnetics (FEMM). The actual sizes of the external magnet, microfluidic channels and distances were used in the simulation of a cross section of the device. The microfluidic channels (for ferrofluid and sample) were separated by 10 m and placed 1 mm away from a NdFeB permanent magnet (MGOe 40), generating a magnetizing field H perpendicular to the flow direction in the channels (Figure 1.10). A non-linear relationship, based on the Langevin function with the correction for interparticle correlations, was assumed for the magnetization curve of the ferrofluid (Equations 1.4 and 1.5). The magnetic moment of a single nanoparticle was assumed to have the saturation magnetization of magnetite (480 kA/m). Simulations were run for particles concentrations 5% Vol and 15% Vol as well as the case without the presence of a ferrofluid.

5. Materials and methods

5.3.2 Sorting of magnetic cells

Magnetized macrophages

Cells of the murine macrophage cell line Ana-1 were grown in RPMI 1640 medium containing 10% FBS and 1% PS, incubated at 37C with 5% CO₂. The macrophages were grown to confluence on 10 cm petri dishes and were incubated with 10 μ l magnetite nanoparticles (nano-screenMAG/R Biotin 100 nm, Chemicell) for 6 hours. The cells were washed twice in PBS to remove excess particles not taken up by the cells. Macrophages were then removed from the plate using Accutase, spun down at 0.4 relative centrifugal force (RCF) for 3 min and resuspended in 3 ml PBS. Cells were labeled with a fluorescent nuclear stain (Hoechst 33342, Thermo Fisher Scientific) for visualization and filtered through a cell strainer with mesh size 70 μ m to avoid large clusters of cells that would clog the microfluidic channels. The sample was diluted to ca $1 \cdot 10^6$ cells/ml in PBS containing 20% glycerol to avoid cells settling in the syringe.

The microfluidic chip is placed in a holder (Micronit, Netherlands) and the channels were connected with plastic tubing to syringes. The center of the sorting channel was observed on an inverted microscope (Axiovert 200M, Zeiss, Germany) with a 40x objective and imaged with a fluorescence camera (Ximea MQ003MG-CM) at 20 fps. The cells were filled in a 1 ml syringe (Injekt, Braun, Germany) and injected using a syringe pump (Elite 11, Harvard Apparatus, USA), while the buffer (PBS) was injected using a 2 ml syringe, resulting in a constant 1:4.7 ratio of the sample to buffer flow rate. The buffer syringes is larger in order to have a higher velocity of the buffer in the channel as this will make the flow broader and prevent diffusion of cells to the magnetic side. The buffer is pushed in on the side closest to the magnetic channel filled with ferrofluid, while the sample is pushed in from the opposite side. The sample flow rate was adjusted in the range 0.5-2 μ l/min.

Establishment of laminar flow was confirmed by the two separate flows and videos were recorded for the baseline. Trials where laminar flow was not established was discarded. The permanent magnets were placed on top of the microfluidic chip, approximately 1 mm away from the ferrofluid channel and videos were recorded. The performance of the system was tested on multiple placements of the external permanent magnet.

5.3.2 Sorting of magnetic cells

For the assessment of the sorting efficiency in the absence of ferrofluid macrophages were prepared and tested following the same protocol. A sample flow rate of 1 $\mu\text{l}/\text{min}$ was used in this case.

Bioengineered cells

Together with Felix Sigmund, HEK 293 cells expressing a surface marker with avidin (Sigmund et al. *in prep.*) were incubated over night with an excess of biotin labeled nanoparticles, as summarized in Table 5.7. Excess particles were washed off with PBS before cells were labeled with a nuclear fluorescent stain (Hoechst 33324, Sigma-Aldrich, Germany) for visualization. The cells were diluted in PBS containing 20% glycerol and filtered through a cell strainer with 40 μm mesh size prior to sorting in order to avoid clogging of the microfluidic channels. Sorting of cells were performed in Chip2, with the same settings as used for macrophages. The flow rate was kept at 1 $\mu\text{l}/\text{min}$.

Table 5.7: Magnetic nanoparticles

Core material	Size	Product name	Supplier
Magnetite	100 nm	nano-screenMAG-Biotin (4501)	Chemicell
Magnetite	30 nm	Iron oxide nanoparticles with Biotin (SHB-30)	Ocean Nanotech
Maghemite	5 nm	Iron oxide(II,III), magnetic nanoparticles solution (747416)	Sigma-Aldrich
Cobalt	30 nm	TurboBeads PEG-Biotin (4006)	TurboBeads

Magnetotactic bacteria

Wild type bacteria of the strain *Magnetospirillum gryphiswaldense* (MSR-1) were kindly provided by Prof. Drik Schüler. The bacteria were immobilized in 35% ethanol before being diluted in PBS containing 10% glycerol and fluorescently labeled with DAPI (2-(4-Amidinophenyl)-6-indolecarbamide, Sigma-Aldrich). For this experiment a Chip1 with reduced dimensions was used. Cells were injected through plastic tubing from a 0.5 ml syringe at 0.1 $\mu\text{l}/\text{min}$ while the buffer (PBS) was injected at the second inlet by a 1 ml syringe, using a syringe pump (Elite 11, Harvard Apparatus, USA). The flow of cells was observed halfway through the

5. Materials and methods

sorting channel on an inverted microscope (Axiovert 200M, Zeiss, Germany) and imaged with a fluorescence camera (Flea3, Point Grey, Canada) at 60 fps.

In order to ensure laminar flow in the system prior to sorting the flow was observed also in the absence of the external magnets, which was placed multiple times. Trials where laminar flow was not observed without the magnets were discarded. Due to the much smaller size the large amount of cells in the flow, the mean position of the cell flow in the channel was compared with and without the magnet.

Cells from zebrafish olfactory rosette

The olfactory rosettes of zebrafish (AB strain) were dissociated and fixed as described above. The sample was filtered through a cell strainer with mesh size 40 μm and labeled with Hoechst 33342 for visualization. The cells were diluted in buffer containing 20% glycerol and filled in a 1 ml syringe. Ringer with calcium as the buffer was filled in a 2 ml syringe. The sample was sorted in Chip2 with 17% nanoparticles in the ferrofluid. The flow rate was kept at 0.5 $\mu\text{l}/\text{min}$, and the behavior of the cells with and without the external magnets present was observed on the inverted Zeiss microscope. Videos were recorded with a fluorescent camera (Ximea MQ013RG-E2, Germany) at 20 fps with 50 ms exposure time.

5.3.3 Data analysis

Analysis of recorded videos for quantification of the sorting efficiency of the cells, both MTB and cells with magnetic particles as well as zebrafish cells, was done using a custom code in MATLAB (Mathworks, USA) written by Dr. Michele Cappetta.

To obtain a good fluorescent signal of the cells a long exposure time was used during video acquisition, resulting in the cells being represented as elongated horizontal strips. These varied in length and intensity depending on the speed of the single cells. In order to quantify the sorting efficiency of the system, we measured the vertical shifts caused by the force acting on the cells due to the external magnetic field. This was done by first computing the mean over the horizontal dimension (x-axis) of each single frame in order to obtain an intensity profile that is a function only of the vertical position (y-axis). This way each single frame was converted into a vertical sequence of pixels, and a video was converted in an image where each

single column is representing the vertical intensity profile of the single frames.

Next, the median projection along the x-axis of this image was computed and subtracted from each single column in order to correct for any background inhomogeneities, leaving the frames that were not containing a cell columns with a flat vertical profile with low counts. The maximal intensity and the full width half maximum (FWHM) of the single columns in the corrected image were the computed in order to automatically detect the frames containing a cell. The position of the cells in the channel was then determined as the position of the peak intensity along the y-axis for each of the selected frames. The two experimental conditions, with and without the external magnets, could thus be compared by the histograms which represented the distribution of cell positions in the sorting channel. Final quantification was done by counting the the relative number of cells passing on each side of the channel before and after placing the external magnets.

For the experiments with MTB there was a much higher density of cells in the sample flow, thus increasing the likelihood of detecting more than one cell per frame. Thus the program was adapted such that instead of detecting one position of the maximum intensity a filter was applied which leave pixels with intensities above a certain threshold. All pixels above the threshold are then defined as part of a cell and counted. This way we could analyze the mean position of the flow of bacteria, and distributions could then be compared as before in order to determine the shift induced by the presence of the magnetic field gradient.

5. Materials and methods

Appendix A

Initial behavior of zebrafish and medaka upon release from the center of a circular arena

A. Initial behavior of zebrafish and medaka upon release from the center of a circular arena

Initial trajectories of zebrafish

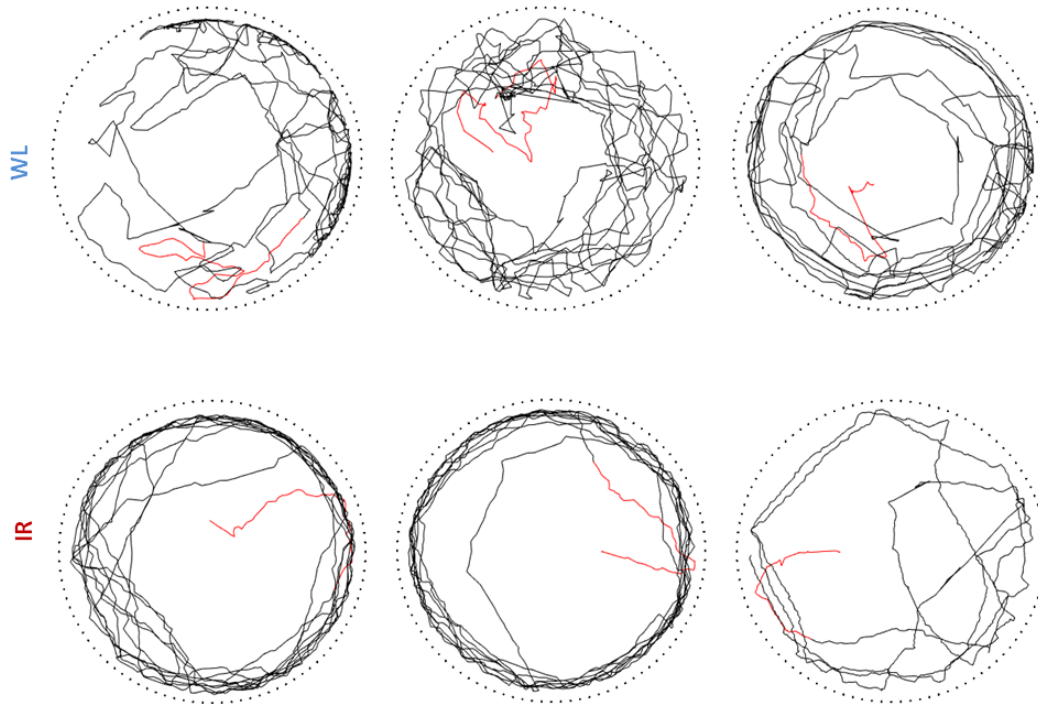


Figure A.1: Trajectories of zebrafish during one minute in light (WL) or under IR illumination (IR). The three first seconds after release from the center of the arena are marked in red, showcasing the linear initial trajectories in darkness compared to in light. The border of the arena is marked with a dotted black line.

Latency to first cross of virtual circle

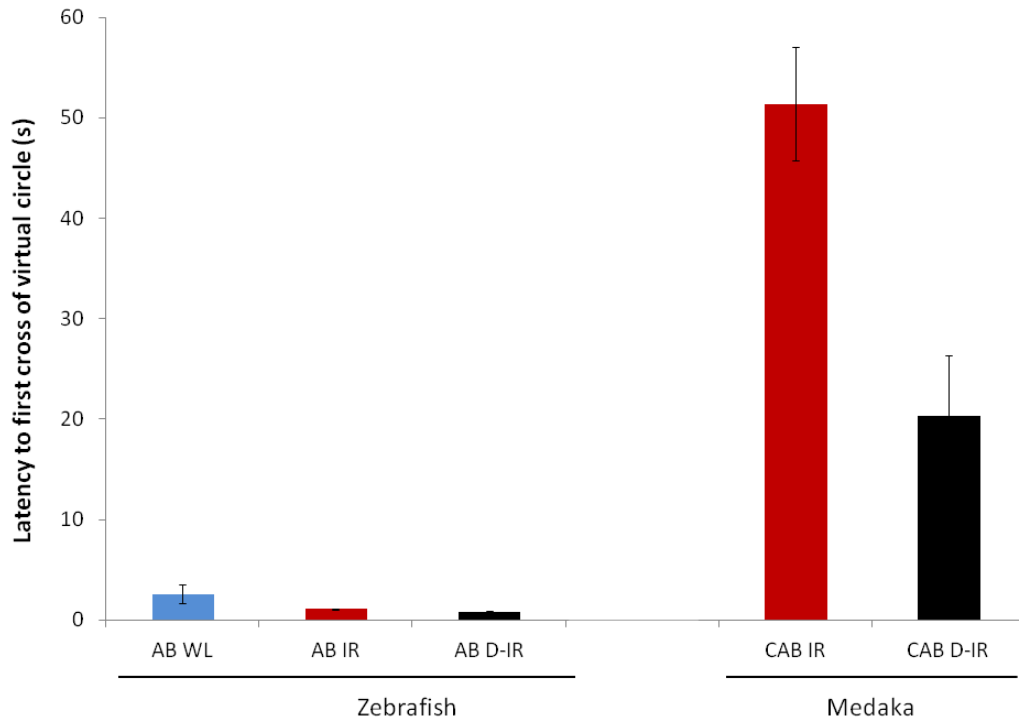


Figure A.2: Latency to first cross of virtual circle of 6 cm radius. Medaka spend significantly more time at the center of the arena upon release compared to zebrafish. Bars represents mean time until first cross in seconds, while error bars indicate SEM

A. Initial behavior of zebrafish and medaka upon release from the center of a circular arena

Appendix B

Spontaneous preference at different crossing radii

B. Spontaneous preference at different crossing radii

Zebrafish crossing 8.5 cm in light

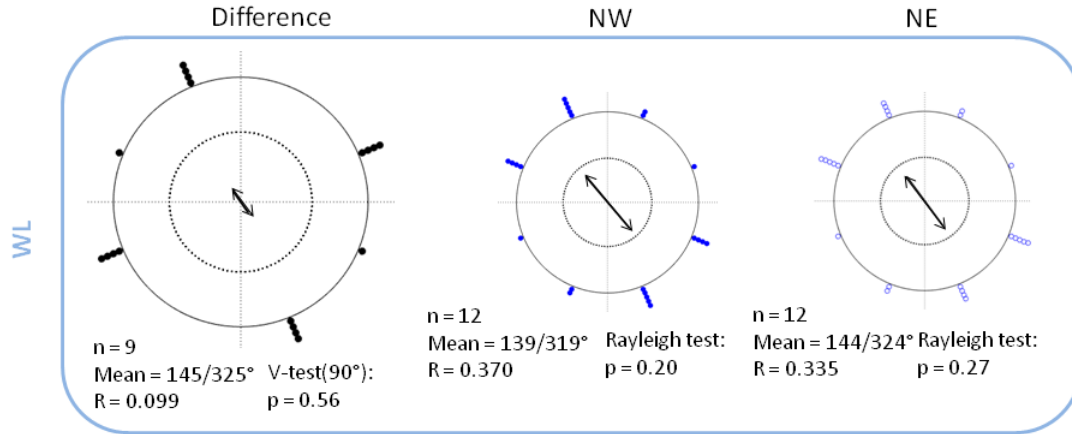


Figure B.1: Directional preference of zebrafish tested under WL illumination. Zebrafish did not show a significant difference in their bearing assessed at the initial wall touch, analyzed by crossing the 8.5 cm radius circle (Difference, black dots). A group preference was also not observed in the two magnetic conditions (NW, closed dots; NE, open dots). For all plots each dot represents the bearing (blue) or the angular difference in bearings (black) for a single fish, as well as its mirror point in the case of axial symmetry. The central black arrow represents the mean vector and the inner dotted circle represents the significance threshold for the Rayleigh test ($p < 0.05$). The values are given underneath each plot.

Zebrafish crossing 8.5 cm in darkness

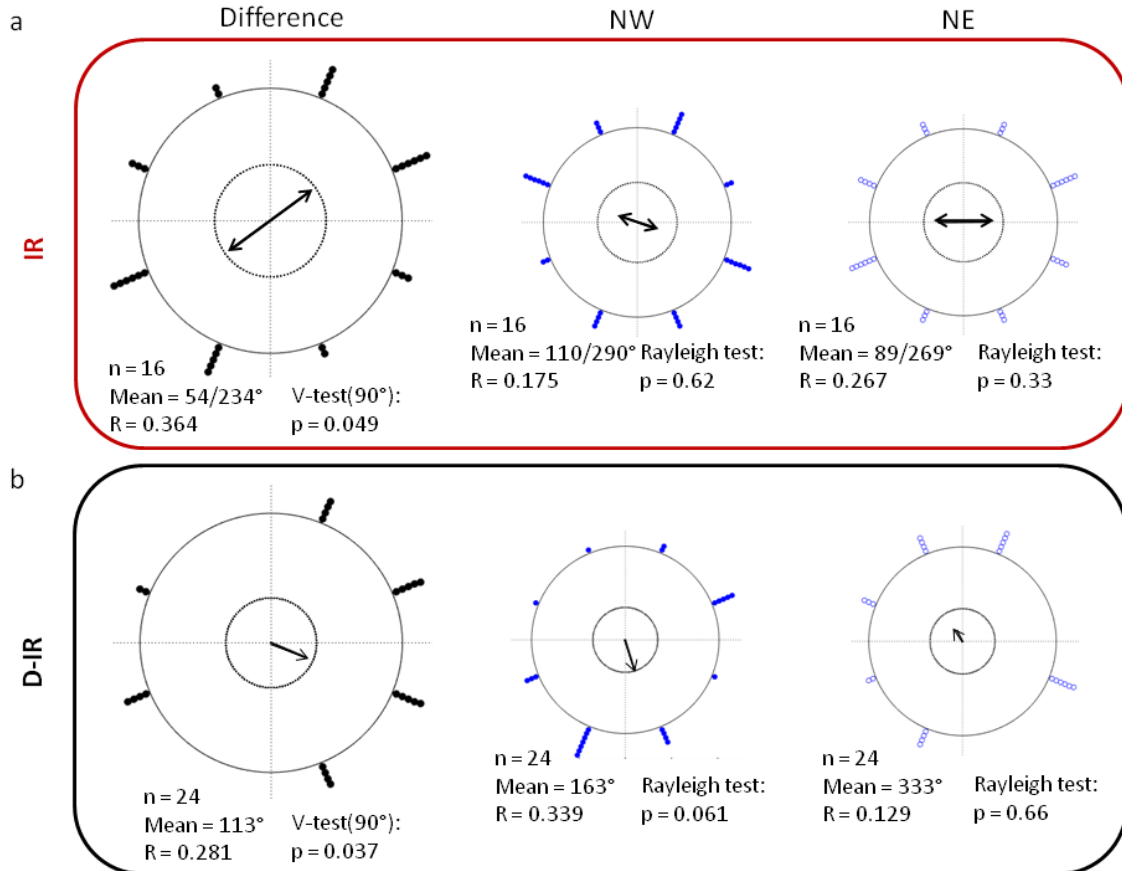


Figure B.2: Directional preference of zebrafish tested under IR illumination assessed at the initial wall touch. a) After being kept in light prior to the experiment (IR) zebrafish showed a difference in their bearing with a significant axial distribution (Difference, black dots). A group preference was not observed in the NE condition (NE, open dots), or in NW (NW, closed dots). b) After preexposure to darkness before the start of the experiment (D-IR), the fish show a significant difference in their bearing (Difference, black dots), however no group preference was observed. For all plots each dot represents the bearing (blue) or the angular difference in bearings (black) for a single fish, as well as its mirror point in the case of axial symmetry. The central black arrow represents the mean vector and the inner dotted circle represents the significance threshold for the Rayleigh test ($p < 0.05$). The values are given underneath each plot.

B. Spontaneous preference at different crossing radii

Medaka crossing 6 cm in darkness

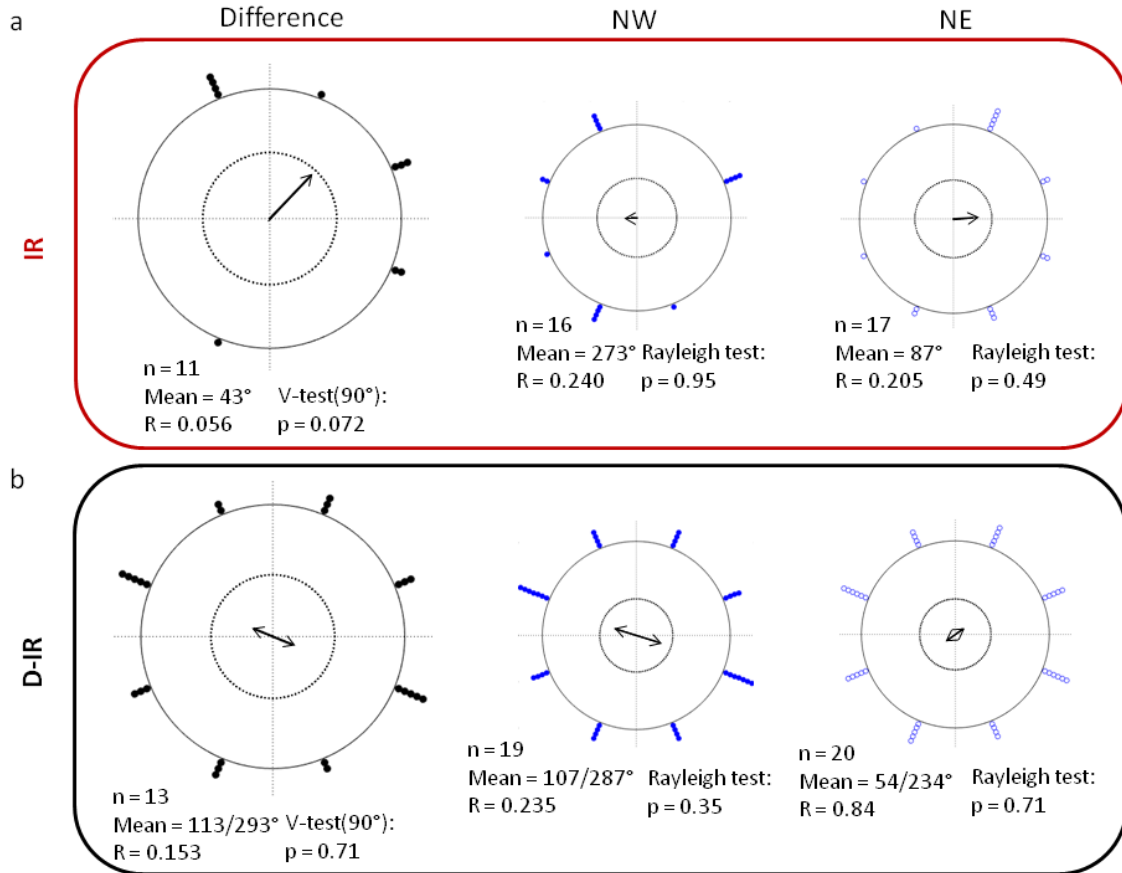


Figure B.3: Directional preference of medaka tested under IR illumination assessed at 6 cm crossing radius. a) After being kept in light prior to the experiment medaka did not show a significant difference in their bearing (Difference, black dots), or group preference in the two magnetic conditions (NW, closed dots; NE, open dots). b) Similarly, after preexposure to darkness before the start of the experiment, neither individual change in bearing nor a group preference was observed. For all plots each dot represents the bearing (blue) or the angular difference in bearings (black) for a single fish, as well as its mirror point in the case of axial symmetry. The central black arrow represents the mean vector and the inner dotted circle represents the significance threshold for the Rayleigh test ($p < 0.05$). The values are given underneath each plot.

Appendix C

Spatial preference in zebrafish and medaka

C. Spatial preference in zebrafish and medaka

Spatial preference in zebrafish (AB)

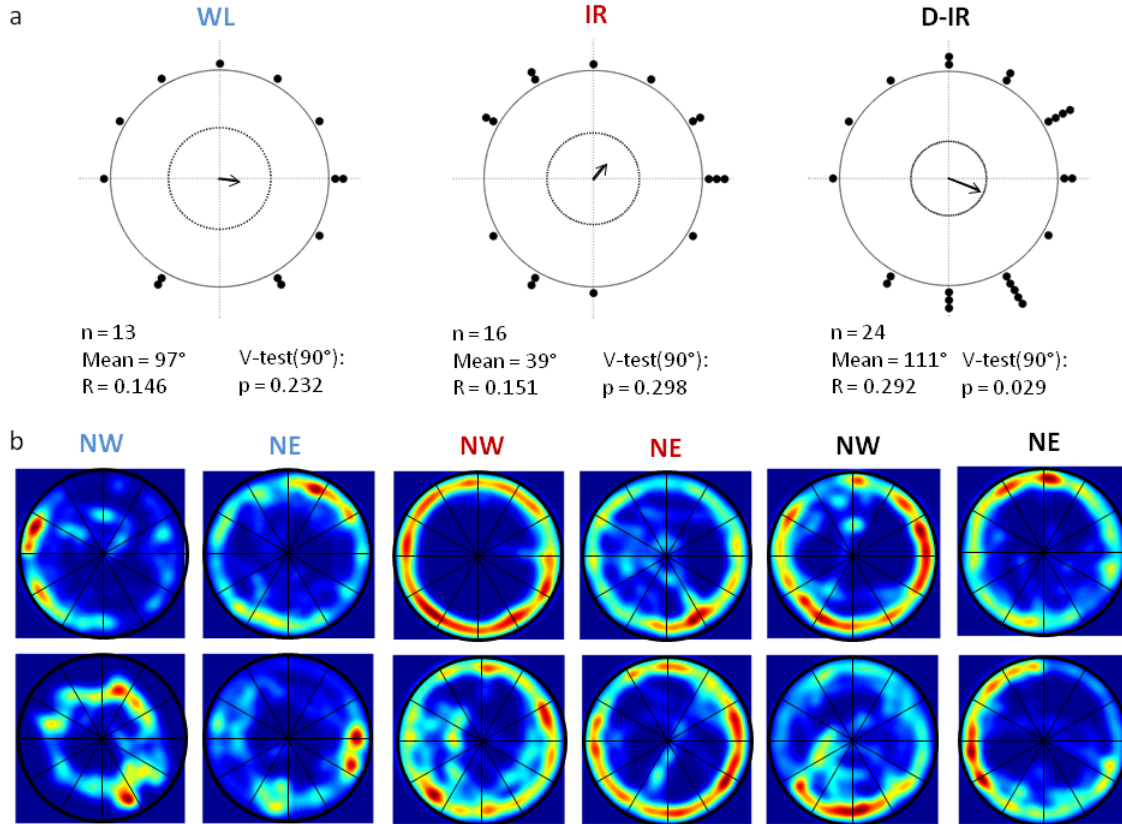


Figure C.1: Reorientation of spatial preference of the three zebrafish groups tested; in light (WL), under IR illumination after preadaptation in light (IR) or in darkness (D-IR). a) Distribution of segment changes. b) Representative heat maps from two fish for each lighting condition showing the position of the fish in the first minute after release from the center with the magnetic field shifted towards NE or NW. The segments show the division of the arena in order to determine the preferred position. For the circular plot each dot represents the angular difference in segment preference (black) for a single fish. The central black arrow represents the mean vector and the inner dotted circle represents the significance threshold for the Rayleigh test ($p < 0.05$). The values are given under the plot.

Spatial preference in medaka (CAB)

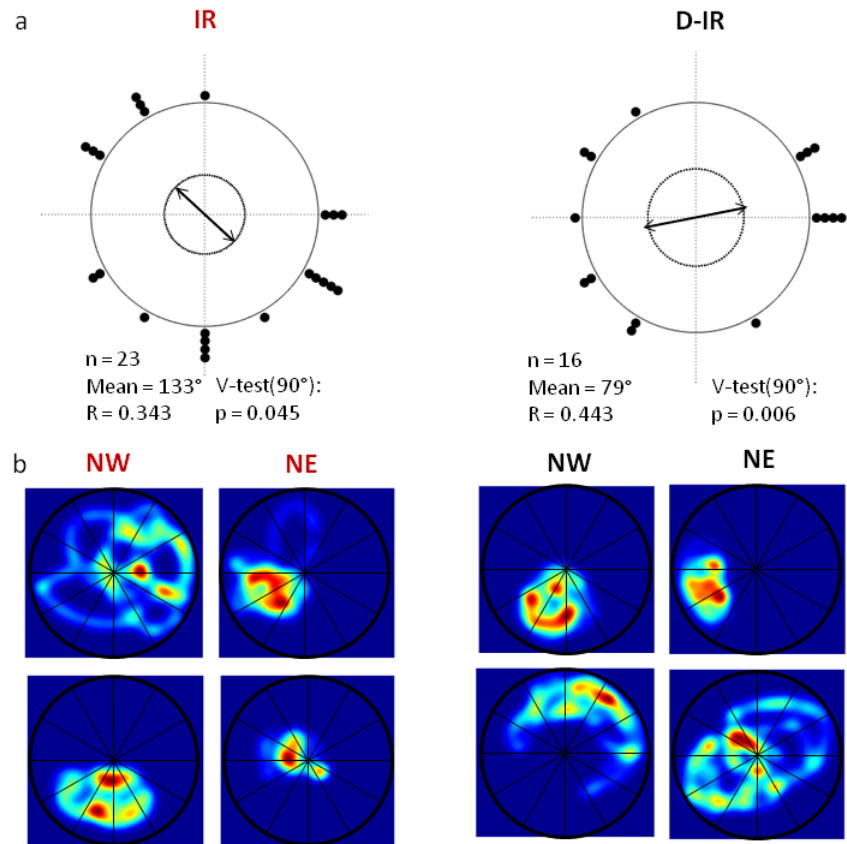


Figure C.2: Reorientation of spatial preference of the two medaka groups tested; under IR illumination after preadaptation in light (IR) or in darkness (D-IR). a) Distribution of segment changes. b) Representative heat maps from two fish for each lighting condition showing the position of the fish in the first minute after release from the center with the magnetic field shifted towards NE or NW. The segments show the division of the arena in order to determine the preferred position. For the circular plot each dot represents the angular difference in segment preference (black) for a single fish. The central black arrow represents the mean vector and the inner dotted circle represents the significance threshold for the Rayleigh test ($p < 0.05$). The values are given under the plot. Adapted from Myklatun, Lauri et al. (2018)

C. Spatial preference in zebrafish and medaka

Appendix D

Magnetic material in fishes

D. Magnetic material in fishes

Extracellular magnetic material in zebrafish

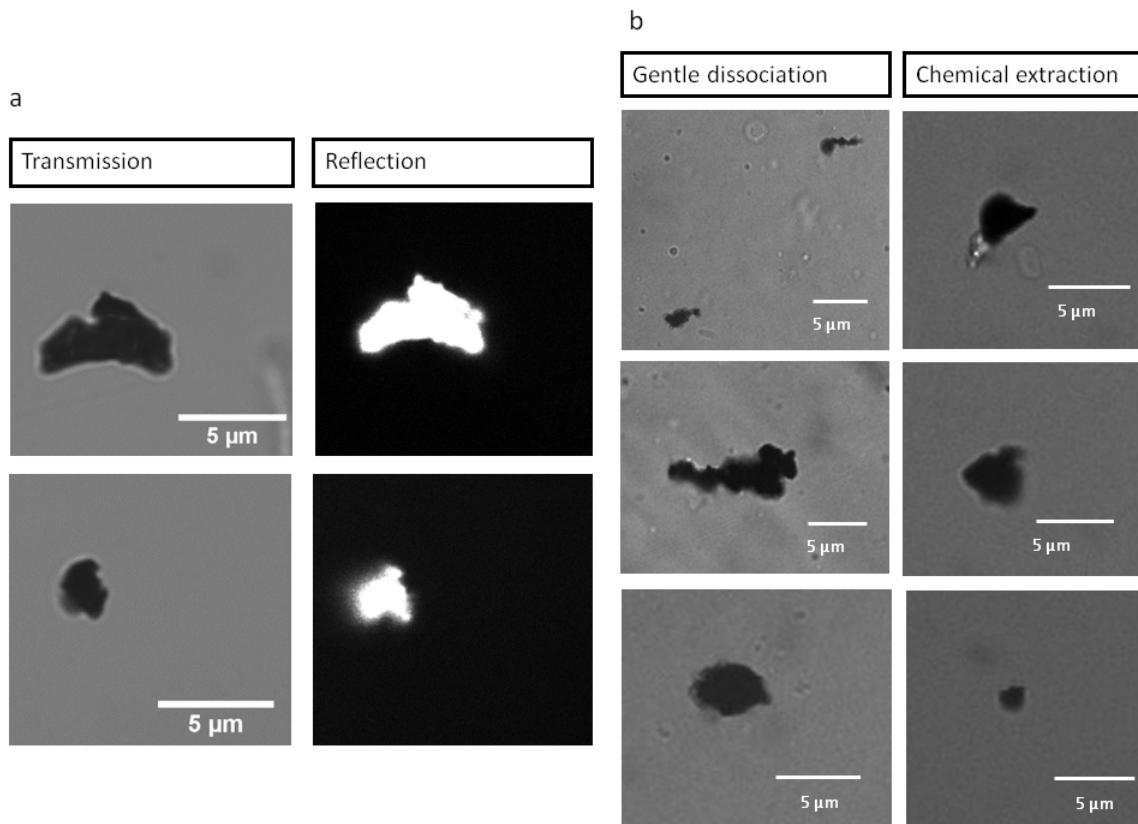


Figure D.1: Extracellular magnetic objects isolated from zebrafish. a) The objects appear black under transmitted light, but bright in the reflected mode. b) Magnetic objects identified during gentle dissociation could also be found after the chemical extraction used for EM.

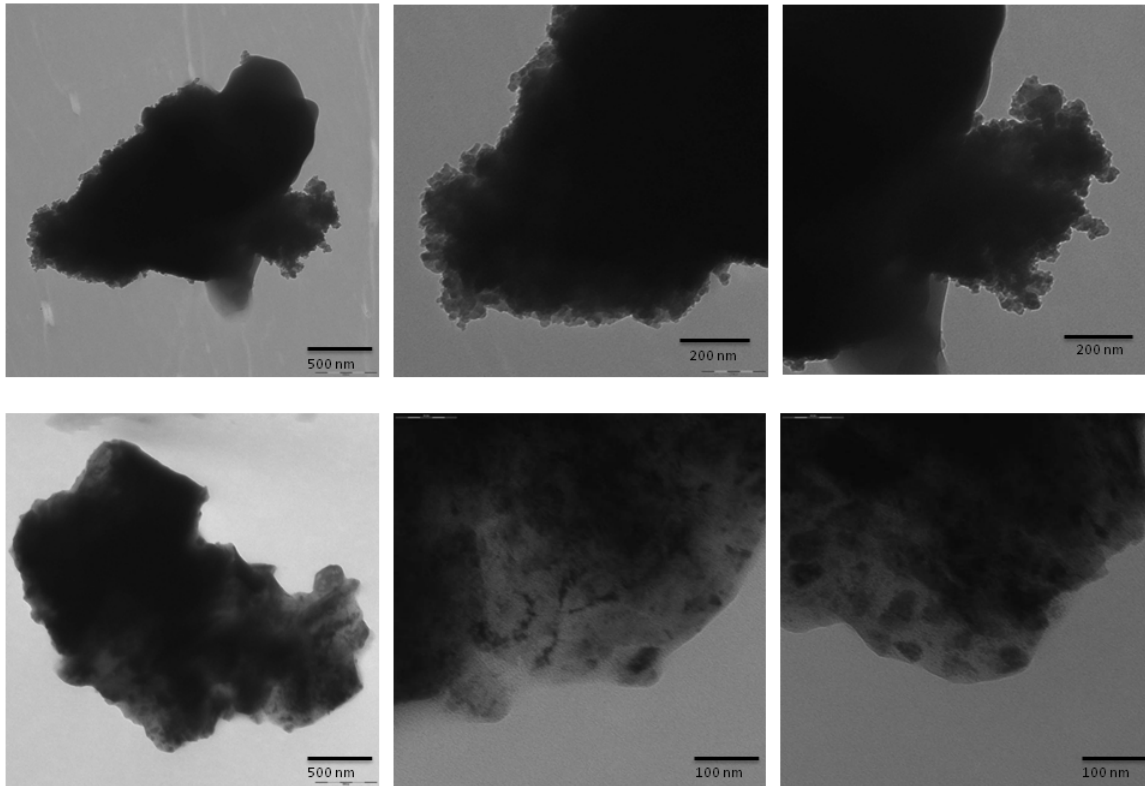


Figure D.2: In collaboration with Dr. Michaela Aichler, from the Institute of Pathology at the Helmholtz Zentrum München, we performed electron microscopy on some of the magnetic objects isolated from zebrafish in order to gain more information about these. Preparation of the samples was done by chemical extraction of the magnetic material in a sodium hypochlorite solution, following the protocol by (Mann et al., 1988). As the magnetic objects could reliably be found also in the Casper line, I used these fish to avoid pigments in the preparation. Objects isolated with chemical extraction was similar to those identified during the gentle dissociation (Figure D.1b). Two examples from TEM are shown (left). The objects were 1-2 μm in size, however when investigated more closely clearly also consisted of smaller structures with size in the order of 50 nm (right). The dark color indicates electron dense areas, however further investigation of the elemental composition was not possible.

D. Magnetic material in fishes

Extracellular magnetic material in salmon

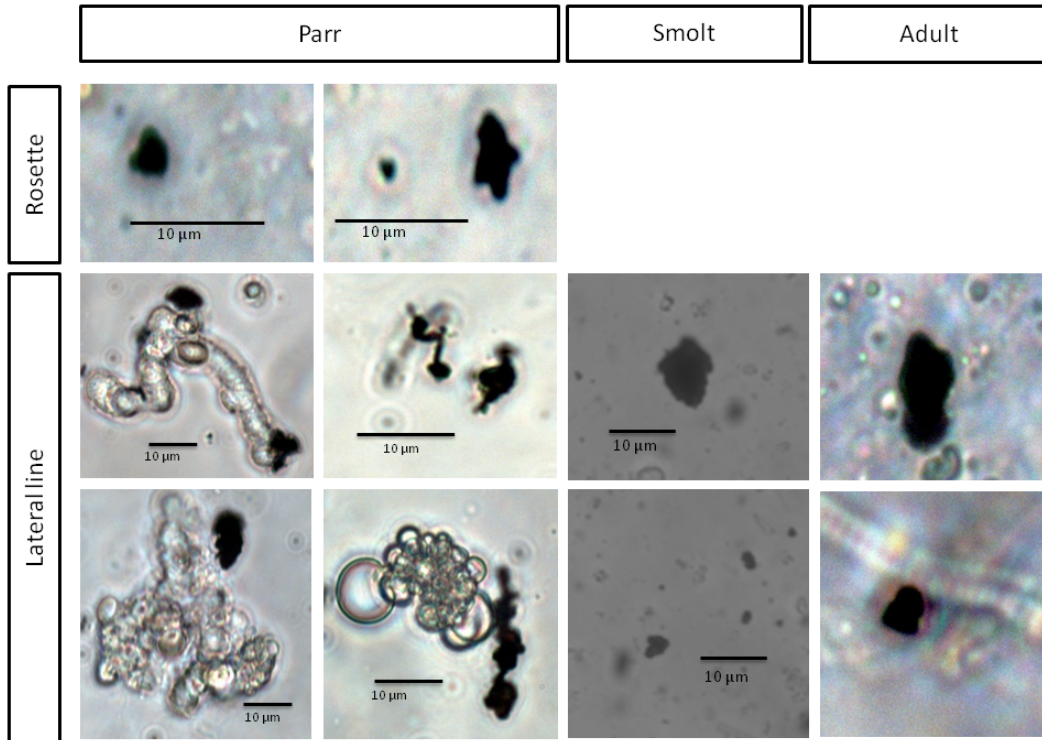


Figure D.3: Magnetic objects found in salmon tissues resembles those in zebrafish. Magnetic extracellular objects (black) were found in the lateral line in all stages of salmon and in the rosettes of parr. The objects turn with the applied magnetic field showing their permanent magnetization.

Table D.1: Magnetic material reported in fishes

Species	Location	Magnetite	Methods	Reference
Salmon				
<i>Oncorhynchus nerka</i>	Ethmoid tissue	SD	HRTEM, EDX	Mann et al. 1988
<i>Oncorhynchus nerka</i>	Frontal skull	SD	SQUID	Walker et al. 1988
<i>Oncorhynchus tshawytscha</i>	Dermethmoid tissue	SD	SQUID, TEM	Kirschvink et al. 1985
<i>Salmo salar</i> L.	Lateral line	SD	SQUID,	Moore et al. 1990
		MD	TEM, EDX	
Trout				
<i>Oncorhynchus mykiss</i>	Olfactory epithelium	SD	Reflection, TEM	Walker et al. 1997
<i>Oncorhynchus mykiss</i>	Olfactory epithelium	SD	AFM, MFM	Diebel et al. 2000
<i>Oncorhynchus mykiss</i>	Olfactory epithelium	SD	TEM, EDX	Eder et al. 2012
			Reflection	
			Rotation*	
Other fishes				
<i>Anguilla anguilla</i>	Lateral line	SD	TEM, EDX, SQUID	Moore & Riley 2009
<i>Thunnus albacares</i>	Dermethmoid bone	SD	SQUID, TEM	Walker et al. 1984

*see Figure 2.9

D. Magnetic material in fishes

Appendix E

Magnetization measurement of fish feed samples

E. Magnetization measurement of fish feed samples

Magnetization measurement of fish feed samples

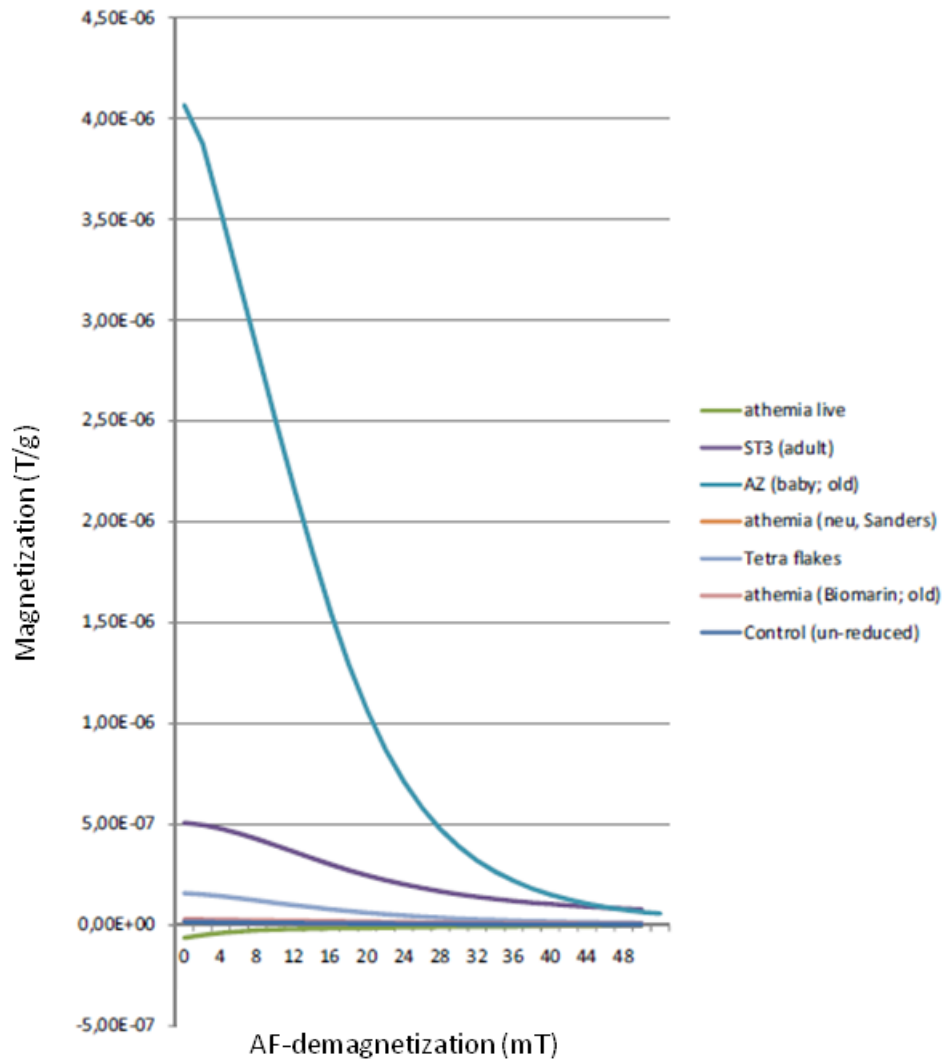


Figure E.1: SQUID magnetization measurements of fish feed samples. Fish that were used search for candidate magnetoreceptor cells were strictly kept on a diet of artemia to avoid magnetic contaminations. Measurements were performed by Dr. Stephan Eder.

Appendix F

Juvenile zebrafish and medaka in
an oscillating magnetic field

F. Juvenile zebrafish and medaka in an oscillating magnetic field

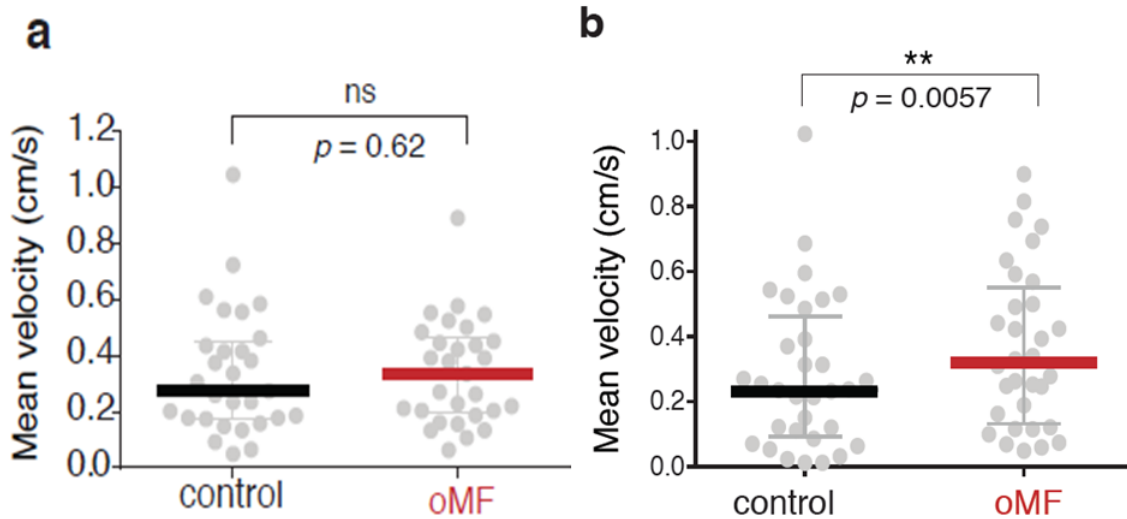


Figure F.1: Juvenile zebrafish (a) and medaka (b) in an oscillating magnetic field. The fish were observed in the presence of an oscillating magnetic field (oMF) and in the sham mode (control) produced by double wrapped coils. The fish were observed individually one minute before and one minute after the onset of the magnetic stimulus. A second group of fish experienced first the magnetic field for one minute before the stimulus was switched off. Zebrafish (AB) did not significantly alter the swimming velocity between the two conditions ($n = 29$, Wilcoxon signed rank test)(a). Medaka (CAB) showed a significant increase in mean swimming velocity in during the oMF phase compared to the control ($n = 32$, Wilcoxon signed rank test)(b). Plots represents median with the interquartile range. From Myklatun, Lauri et al. (2018)

Bibliography

- Adams, J. D., Kim, U., & Soh, H. T. (2008). Multitarget magnetic activated cell sorter. *Proceedings of the National Academy of Sciences*, **105**(47), 18165–18170.
- Ahrens, M. B., Li, J. M., Orger, M. B., Robson, D. N., Schier, A. F., Engert, F., & Portugues, R. (2012). Brain-wide neuronal dynamics during motor adaptation in zebrafish. *Nature*, **485**(7399), 471–477.
- Akerboom, J., Chen, T.-W., Wardill, T. J., Tian, L., Marvin, J. S., Mutlu, S., Calderón, N. C., Esposti, F., Borghuis, B. G., Sun, X. R., et al. (2012). Optimization of a gcamp calcium indicator for neural activity imaging. *Journal of Neuroscience*, **32**(40), 13819–13840.
- Alexandre, D. & Ghysen, A. (1999). Somatotopy of the lateral line projection in larval zebrafish. *Proceedings of the National Academy of Sciences*, **96**(13), 7558–7562.
- Anikeeva, P. & Jasanoff, A. (2016). Problems on the back of an envelope. *eLife*, **5**, e19569.
- Avni, R., Zadicario, P., & Eilam, D. (2006). Exploration in a dark open field: a shift from directional to positional progression and a proposed model of acquiring spatial information. *Behavioural Brain Research*, **171**(2), 313–323.
- Bainbridge, C., Rodriguez, A., Schuler, A., Cisneros, M., & Vidal-Gadea, A. G. (2016). Magnetic orientation in *c. elegans* relies on the integrity of the villi of the {AFD} magnetosensory neurons. *Journal of Physiology-Paris*.
- Batschelet, E. (1981). *Circular statistics in biology*. London: Academic Press.
- Bazalova, O., Kvicalova, M., Valkova, T., Slaby, P., Bartos, P., Netusil, R., Tomanova, K., Braeunig, P., Lee, H.-J., Sauman, I., Damulewicz, M., Provaznik, J., Pokorny, R., Dolezel, D., & Vacha, M. (2016). Cryptochrome 2 mediates directional magnetoreception in cockroaches. *Proceedings of the National Academy of Sciences*, **113**(6), 1660–1665.

BIBLIOGRAPHY

- Beason, R. & Semm, P. (1996). Does the avian ophthalmic nerve carry magnetic navigational information? *Journal of Experimental Biology*, **199**(5), 1241–1244.
- Beason, R., Dussourd, N., & Deutschlander, M. (1995). Behavioural evidence for the use of magnetic material in magnetoreception by a migratory bird. *Journal of Experimental Biology*, **198**(1), 141–146.
- Beason, R. C. & Semm, P. (1987). Magnetic responses of the trigeminal nerve system of the bobolink (*dolichonyx oryzivorus*). *Neuroscience Letters*, **80**(2), 229–234.
- Begall, S., Malkemper, E. P., Červený, J., Němec, P., & Burda, H. (2013). Magnetic alignment in mammals and other animals. *Mammalian Biology-Zeitschrift für Säugetierkunde*, **78**(1), 10–20.
- Blakemore, R. P. (1975). Magnetotactic bacteria. *Science*, **190**(4212), 377–379.
- Boles, L. C. & Lohmann, K. J. (2003). True navigation and magnetic maps in spiny lobsters. *Nature*, **421**(6918), 60–63.
- Boyden, E. S., Zhang, F., Bamberg, E., Nagel, G., & Deisseroth, K. (2005). Millisecond-timescale, genetically targeted optical control of neural activity. *Nature Neuroscience*, **8**(9), 1263–1268.
- Burger, T., Lucová, M., Moritz, R. E., Oelschläger, H. H., Druga, R., Burda, H., Wiltschko, W., Wiltschko, R., & Němec, P. (2010). Changing and shielded magnetic fields suppress c-fos expression in the navigation circuit: input from the magnetosensory system contributes to the internal representation of space in a subterranean rodent. *Journal of The Royal Society Interface*, **7**(50), 1275–1292.
- Chatani, M., Mantoku, A., Takeyama, K., Abduweli, D., Sugamori, Y., Aoki, K., Ohya, K., Suzuki, H., Uchida, S., Sakimura, T., et al. (2015). Microgravity promotes osteoclast activity in medaka fish reared at the international space station. *Scientific Reports*, **5**.
- Chaves, I., Pokorny, R., Byrdin, M., Hoang, N., Ritz, T., Brettel, K., Essen, L.-O., van der Horst, G. T. J., Batschauer, A., & Ahmad, M. (2011). The cryptochromes: Blue light photoreceptors in plants and animals. *Annual Review of Plant Biology*, **62**(1), 335–364. PMID: 21526969.
- Chung, S. H., Clark, D. A., Gabel, C. V., Mazur, E., & Samuel, A. D. (2006). The role of the *afd* neuron in *c. elegans* thermotaxis analyzed using femtosecond laser ablation. *BMC Neuroscience*, **7**(1), 30.
- Coronado, L. M., Nadovich, C. T., & Spadafora, C. (2014). Malarial hemozoin: from target to tool. *Biochimica et Biophysica Acta (BBA)-General Subjects*, **1840**(6), 2032–2041.

BIBLIOGRAPHY

- Cresci, A., De Rosa, R., Putman, N. F., & Agnisola, C. (2017). Earth-strength magnetic field affects the rheotactic threshold of zebrafish swimming in shoals. *Comparative Biochemistry and Physiology Part A: Molecular & Integrative Physiology*, **204**, 169–176.
- Davila, A., Fleissner, G., Winklhofer, M., & Petersen, N. (2003). A new model for a magnetoreceptor in homing pigeons based on interacting clusters of superparamagnetic magnetite. *Physics and Chemistry of the Earth, Parts A/B/C*, **28**(16–19), 647 – 652. *Paleo, Rock and Environmental Magnetism 2002*.
- Davila, A. F., Winklhofer, M., Shcherbakov, V. P., & Petersen, N. (2005). Magnetic pulse affects a putative magnetoreceptor mechanism. *Biophysical Journal*, **89**(1), 56 – 63.
- Deisseroth, K. (2011). Optogenetics. *Nature Methods*, **8**(1), 26–29.
- Diebel, C. E., Proksch, R., Green, C. R., Neilson, P., & Walker, M. M. (2000). Magnetite defines a vertebrate magnetoreceptor. *Nature*, **406**(6793), 299–302.
- Dommer, D. H., Gazzolo, P. J., Painter, M. S., & Phillips, J. B. (2008). Magnetic compass orientation by larval drosophila melanogaster. *Journal of Insect Physiology*, **54**(4), 719–726.
- Drew, R. E., Settles, M. L., Churchill, E. J., Williams, S. M., Balli, S., & Robison, B. D. (2012). Brain transcriptome variation among behaviorally distinct strains of zebrafish (danio rerio). *BMC Genomics*, **13**(1), 1.
- Edelman, N. B., Fritz, T., Nimpf, S., Pichler, P., Lauwers, M., Hickman, R. W., Papadaki-Anastasopoulou, A., Ushakova, L., Heuser, T., Resch, G. P., et al. (2015). No evidence for intracellular magnetite in putative vertebrate magnetoreceptors identified by magnetic screening. *Proceedings of the National Academy of Sciences*, **112**(1), 262–267.
- Eder, S. H., Cadiou, H., Muhamad, A., McNaughton, P. A., Kirschvink, J. L., & Winklhofer, M. (2012). Magnetic characterization of isolated candidate vertebrate magnetoreceptor cells. *Proceedings of the National Academy of Sciences*, **109**(30), 12022–12027.
- Engeszer, R. E., Patterson, L. B., Rao, A. A., & Parichy, D. M. (2007). Zebrafish in the wild: a review of natural history and new notes from the field. *Zebrafish*, **4**(1), 21–40.
- Ērglis, K., Wen, Q., Ose, V., Zeltins, A., Sharipo, A., Janmey, P. A., & Cēbers, A. (2007). Dynamics of magnetotactic bacteria in a rotating magnetic field. *Biophysical Journal*, **93**(4), 1402–1412.

BIBLIOGRAPHY

- Ernst, D. A. & Lohmann, K. J. (2016). Effect of magnetic pulses on caribbean spiny lobsters: implications for magnetoreception. *Journal of Experimental Biology*.
- Faivre, D. & Schüler, D. (2008). Magnetotactic bacteria and magnetosomes. *Chemical Reviews*, **108**(11), 4875–4898.
- Fedele, G., Green, E. W., Rosato, E., & Kyriacou, C. P. (2014). An electromagnetic field disrupts negative geotaxis in drosophila via a cry-dependent pathway. *Nature communications*, **5**.
- Fenko, L., Yizhar, O., & Deisseroth, K. (2011). The development and application of optogenetics. *Neuroscience*, **34**(1), 389.
- Fleissner, G., Holtkamp-Rötzler, E., Hanzlik, M., Winklhofer, M., Fleissner, G., Petersen, N., & Wiltschko, W. (2003). Ultrastructural analysis of a putative magnetoreceptor in the beak of homing pigeons. *Journal of Comparative Neurology*, **458**(4), 350–360.
- Foley, L. E., Gegear, R. J., & Reppert, S. M. (2011). Human cryptochrome exhibits light-dependent magnetosensitivity. *Nature Communications*, **2**, 356.
- Frankel, R. B., Blakemore, R. P., & Wolfe, R. S. (1979). Magnetite in freshwater magnetotactic bacteria. *Science*, **203**(4387), 1355–1356.
- Franken, L., Klein, M., Spasova, M., Elsukova, A., Wiedwald, U., Welz, M., Knolle, P., Farle, M., Limmer, A., & Kurts, C. (2015). Splenic red pulp macrophages are intrinsically superparamagnetic and contaminate magnetic cell isolates. *Scientific Reports*, **5**, 12940.
- Furutani-Seiki, M. & Wittbrodt, J. (2004). Medaka and zebrafish, an evolutionary twin study. *Mechanisms of Development*, **121**(7–8), 629 – 637.
- Gegear, R. J., Casselman, A., Waddell, S., & Reppert, S. M. (2008). Cryptochrome mediates light-dependent magnetosensitivity in drosophila. *Nature*, **454**(7207), 1014–1018.
- Gegear, R. J., Foley, L. E., Casselman, A., & Reppert, S. M. (2010). Animal cryptochromes mediate magnetoreception by an unconventional photochemical mechanism. *Nature*, **463**(7282), 804–807.
- Gould, J. L. (2004). Animal navigation. *Current Biology*, **14**(6), R221–R224.
- Gould, J. L., Kirschvink, J., & Deffeyes, K. (1978). Bees have magnetic remanence. *Science*, **201**(4360), 1026–1028.

BIBLIOGRAPHY

- Goya, G., Berquó, T. S., Fonseca, F. C., & Morales, M. (2003). Static and dynamic magnetic properties of spherical magnetite nanoparticles. *Journal of Applied Physics*, **94**(5), 3520–3528.
- Guryev, V., Koudijs, M. J., Berezikov, E., Johnson, S. L., Plasterk, R. H., Van Eeden, F. J., & Cuppen, E. (2006). Genetic variation in the zebrafish. *Genome research*, **16**(4), 491–497.
- Han, K.-H. & Frazier, A. B. (2004). Continuous magnetophoretic separation of blood cells in microdevice format. *Journal of Applied Physics*, **96**(10), 5797–5802.
- Han, K.-H. & Frazier, A. B. (2006). Paramagnetic capture mode magnetophoretic microseparator for high efficiency blood cell separations. *Lab on a Chip*, **6**(2), 265–273.
- Hansen, A. & Eckart, Z. (1998). The peripheral olfactory organ of the zebrafish, danio rerio: an ultrastructural study. *Chemical senses*, **23**(1), 39–48.
- Hanzlik, M., Winklhofer, M., & Petersen, N. (1996). Spatial arrangement of chains of magnetosomes in magnetotactic bacteria. *Earth and Planetary Science Letters*, **145**(1-4), 125–134.
- Hanzlik, M., Heunemann, C., Holtkamp-Rötzler, E., Winklhofer, M., Petersen, N., & Fleissner, G. (2000). Superparamagnetic magnetite in the upper beak tissue of homing pigeons. *Biometals*, **13**(4), 325–331.
- Hejazian, M., Li, W., & Nguyen, N.-T. (2015). Lab on a chip for continuous-flow magnetic cell separation. *Lab on a Chip*, **15**(4), 959–970.
- Hikosaka, O. (2010). The habenula: from stress evasion to value-based decision-making. *Nature reviews neuroscience*, **11**(7), 503–513.
- Hore, P. J. & Mouritsen, H. (2016). The radical-pair mechanism of magnetoreception. *Annual Review of Biophysics*, **45**(1), 299–344. PMID: 27216936.
- Huang, H., Delikanli, S., Zeng, H., Ferkey, D. M., & Pralle, A. (2010). Remote control of ion channels and neurons through magnetic-field heating of nanoparticles. *Nature nanotechnology*, **5**(8), 602–606.
- Hyodo-Taguchi, Y. & Egami, N. (1985). Establishment of inbred strains of the medaka *oryzias latipes* and the usefulness of the strains for biomedical research. *Zoological science*, **2**(3), 305–316.
- Irwin, W. P. & Lohmann, K. J. (2005). Disruption of magnetic orientation in hatchling loggerhead sea turtles by pulsed magnetic fields. *Journal of Comparative Physiology A*, **191**(5), 475–480.

BIBLIOGRAPHY

- Ivanov, A. O. & Kuznetsova, O. B. (2001). Magnetic properties of dense ferrofluids: an influence of interparticle correlations. *Physical Review E*, **64**(4), 041405.
- Kalmijn, A. J. & Blakemore, R. P. (1978). The magnetic behavior of mud bacteria. In *Animal migration, navigation, and homing*, pages 354–355. Springer.
- Kalueff, A. V., Gebhardt, M., Stewart, A. M., Cachat, J. M., Brimmer, M., Chawla, J. S., Craddock, C., Kyzar, E. J., Roth, A., Landsman, S., et al. (2013). Towards a comprehensive catalog of zebrafish behavior 1.0 and beyond. *Zebrafish*, **10**(1), 70–86.
- Kasahara, M., Naruse, K., Sasaki, S., Nakatani, Y., Qu, W., Ahsan, B., Yamada, T., Nagayasu, Y., Doi, K., Kasai, Y., et al. (2007). The medaka draft genome and insights into vertebrate genome evolution. *Nature*, **447**(7145), 714–719.
- Kim, T., Moore, D., & Fussenegger, M. (2012). Genetically programmed superparamagnetic behavior of mammalian cells. *Journal of biotechnology*, **162**(2), 237–245.
- Kimchi, T., Etienne, A. S., & Terkel, J. (2004). A subterranean mammal uses the magnetic compass for path integration. *Proceedings of the National Academy of Sciences of the United States of America*, **101**(4), 1105–1109.
- Kimura, K. D., Miyawaki, A., Matsumoto, K., & Mori, I. (2004). The c. elegans thermosensory neuron afd responds to warming. *Current Biology*, **14**(14), 1291–1295.
- Kinkhabwala, A., Riley, M., Koyama, M., Monen, J., Satou, C., Kimura, Y., Higashijima, S.-i., & Fetcho, J. (2011). A structural and functional ground plan for neurons in the hindbrain of zebrafish. *Proceedings of the National Academy of Sciences*, **108**(3), 1164–1169.
- Kirschvink, J., Walker, M., Chang, S.-B., Dizon, A., & Peterson, K. (1985). Chains of single-domain magnetite particles in chinook salmon, *oncorhynchus tshawytscha*. *Journal of Comparative Physiology A*, **157**(3), 375–381.
- Kirschvink, J. L. (1989). Magnetite biomineralization and geomagnetic sensitivity in higher animals: an update and recommendations for future study. *Bioelectromagnetics*, **10**(3), 239–259.
- Kirschvink, J. L. (1992). Uniform magnetic fields and double-wrapped coil systems: improved techniques for the design of bioelectromagnetic experiments. *Bioelectromagnetics*, **13**(5), 401–411.

BIBLIOGRAPHY

- Kirschvink, J. L. & Gould, J. L. (1981). Biogenic magnetite as a basis for magnetic field detection in animals. *Biosystems*, **13**(3), 181 – 201.
- Kirschvink, J. L., Walker, M. M., & Diebel, C. E. (2001). Magnetite-based magnetoreception. *Current opinion in neurobiology*, **11**(4), 462–467.
- Kirschvink, J. L., Winklhofer, M., & Walker, M. M. (2010). Biophysics of magnetic orientation: strengthening the interface between theory and experimental design. *Journal of The Royal Society Interface*, page rsif20090491.
- Kishkinev, D., Chernetsov, N., Pakhomov, A., Heyers, D., & Mouritsen, H. (2015). Eurasian reed warblers compensate for virtual magnetic displacement. *Current Biology*, **25**(19), R822–R824.
- Kobayashi, A. K., Kirschvink, J. L., & Nesson, M. H. (1995). Ferromagnetism and emfs. *Nature*, **374**(6518), 123–123.
- Krylov, V., Osipova, E., Pavlova, V., & Batrakova, A. (2016). Influence of magnetic field on the spatial orientation in zebrafish (*danio rerio*)(cyprinidae) and roach (*rutilus rutilus*)(cyprinidae). *Journal of Ichthyology*, **56**(3).
- Kuterbach, D. A., Walcott, B., Reeder, R. J., & Frankel, R. B. (1982). Iron-containing cells in the honey bee (*apis mellifera*). *Science*, **218**(4573), 695.
- Landler, L., Nimpf, S., Hochstoeger, T., Nordmann, G. C., Papadaki-Anastasopoulou, A., & Keays, D. A. (2018). Comment on” magnetosensitive neurons mediate geomagnetic orientation in *caenorhabditis elegans*”. *eLife*, **7**, e30187.
- Le Sage, D., Arai, K., Glenn, D., DeVience, S., Pham, L., Rahn-Lee, L., Lukin, M., Yacoby, A., Komeili, A., & Walsworth, R. (2013). Optical magnetic imaging of living cells. *Nature*, **496**(7446), 486–489.
- Lee, W. & Yang, K.-L. (2014). Using medaka embryos as a model system to study biological effects of the electromagnetic fields on development and behavior. *Ecotoxicology and Environmental Safety*, **108**, 187–194.
- Light, P., Salmon, M., & Lohmann, K. J. (1993). Geomagnetic orientation of loggerhead sea turtles: Evidence for an inclination compass. *Journal of Experimental Biology*, **182**(1), 1–10.
- Lin, Y. A., Wong, T.-S., Bhardwaj, U., Chen, J.-M., McCabe, E., & Ho, C.-M. (2007). Formation of high electromagnetic gradients through a particle-based microfluidic approach. *Journal of Micromechanics and Microengineering*, **17**(7), 1299.

BIBLIOGRAPHY

- Liu, C., Lagae, L., Wirix-Speetjens, R., & Borghs, G. (2007). On-chip separation of magnetic particles with different magnetophoretic mobilities. *Journal of Applied Physics*, **101**(2), 024913.
- Liu, X., Lopez, P. A., Giessen, T. W., Giles, M., Way, J. C., & Silver, P. A. (2016). Engineering genetically-encoded mineralization and magnetism via directed evolution. *Scientific Reports*, **6**.
- Lohmann, K., Pentcheff, N., Nevitt, G., Stetten, G., Zimmer-Faust, R., Jarrard, H., & Boles, L. (1995). Magnetic orientation of spiny lobsters in the ocean: experiments with undersea coil systems. *Journal of Experimental Biology*, **198**(10), 2041–2048.
- Lohmann, K. J. & Lohmann, C. F. (1993). A light-independent magnetic compass in the leatherback sea turtle. *The Biological Bulletin*, **185**(1), 149–151.
- Makhlouf, S. A., Parker, F., & Berkowitz, A. (1997). Magnetic hysteresis anomalies in ferritin. *Physical Review B*, **55**(22), R14717.
- Malkemper, E. P., Eder, S. H., Begall, S., Phillips, J. B., Winklhofer, M., Hart, V., & Burda, H. (2015). Magnetoreception in the wood mouse (*apodemus sylvaticus*): influence of weak frequency-modulated radio frequency fields. *Scientific Reports*, **4**, 9917.
- Malkemper, E. P., Painter, M. S., & Landler, L. (2016). Shifted magnetic alignment in vertebrates: Evidence for neural lateralization? *Journal of Theoretical Biology*, **399**, 141–147.
- Mann, S., Sparks, N., Walker, M. M., & Kirschvink, J. L. (1988). Ultrastructure, morphology and organization of biogenic magnetite from sockeye salmon, *oncorhynchus nerka*: implications for magnetoreception. *Journal of Experimental Biology*, **140**(1), 35–49.
- Marhold, S., Wiltschko, W., & Burda, H. (1997). A magnetic polarity compass for direction finding in a subterranean mammal. *Naturwissenschaften*, **84**(9), 421–423.
- Meister, M. (2016). Physical limits to magnetogenetics. *eLife*, **5**, e17210.
- Melville, D., Paul, F., & Roath, S. (1975). Direct magnetic separation of red cells from whole blood. *Nature*.
- Miltenyi, S., Müller, W., Weichel, W., & Radbruch, A. (1990). High gradient magnetic cell separation with macs. *Cytometry*, **11**(2), 231–238.

BIBLIOGRAPHY

- Moore, A. & Riley, W. (2009). Magnetic particles associated with the lateral line of the european eel *anguilla anguilla*. *Journal of Fish Biology*, **74**(7), 1629–1634.
- Moore, A., Freake, S., & Thomas, I. (1990). Magnetic particles in the lateral line of the atlantic salmon (*salmo salar* l.). *Philosophical Transactions of the Royal Society of London B: Biological Sciences*, **329**(1252), 11–15.
- Mori, I. (1999). Genetics of chemotaxis and thermotaxis in the nematode *caenorhabditis elegans*. *Annual review of genetics*, **33**(1), 399–422.
- Mori, I. & Ohshima, Y. (1995). Neural regulation of thermotaxis in *caenorhabditis elegans*. *Nature*, **376**(6538), 344.
- Mouritsen, H., Janssen-Bienhold, U., Liedvogel, M., Feenders, G., Stalleicken, J., Dirks, P., & Weiler, R. (2004). Cryptochromes and neuronal-activity markers colocalize in the retina of migratory birds during magnetic orientation. *Proceedings of the National Academy of Sciences of the United States of America*, **101**(39), 14294–14299.
- Muheim, R., Bäckman, J., & Åkesson, S. (2002). Magnetic compass orientation in european robins is dependent on both wavelength and intensity of light. *Journal of Experimental Biology*, **205**(24), 3845–3856.
- Muheim, R., Edgar, N. M., Sloan, K. A., & Phillips, J. B. (2006). Magnetic compass orientation in *c57bl/6j* mice. *Learning & Behavior*, **34**(4), 366–373.
- Munro, U., Munro, J., Phillips, J., Wiltschko, R., & Wiltschko, W. (1997). Evidence for a magnetite-based navigational “map” in birds. *Naturwissenschaften*, **84**(1), 26–28.
- Myklatun, A., Cappetta, M., Winklhofer, M., Ntziachristos, V., & Westmeyer, G. G. (2017). Microfluidic sorting of intrinsically magnetic cells under visual control. *accepted in Scientific Reports*.
- Myklatun, Lauri, Eder, S. H., Cappetta, M., Shcherbakov, D., Wurst, W., Winklhofer, M., & Westmeyer, G. G. (2018). Zebrafish and medaka offer insights into the neurobehavioral correlates of vertebrate magnetoreception. *Nature communications*, **9**(1), 802.
- Nam, J., Huang, H., Lim, H., Lim, C., & Shin, S. (2013). Magnetic separation of malaria-infected red blood cells in various developmental stages. *Analytical Chemistry*, **85**(15), 7316–7323.
- Němec, P., Altmann, J., Marhold, S., Burda, H., & Oelschläger, H. H. A. (2001). Neuroanatomy of magnetoreception: The superior colliculus involved in magnetic orientation in a mammal. *Science*, **294**(5541), 366–368.

BIBLIOGRAPHY

- Nießner, C. & Winklhofer, M. (2017). Radical-pair-based magnetoreception in birds: radio-frequency experiments and the role of cryptochrome. *Journal of Comparative Physiology A*, pages 1–9.
- Nießner, C., Denzau, S., Peichl, L., Wiltschko, W., & Wiltschko, R. (2014). Magnetoreception in birds: I. immunohistochemical studies concerning the cryptochrome cycle. *Journal of Experimental Biology*, **217**(23), 4221–4224.
- Osipova, E. A., Pavlova, V. V., Nepomnyashchikh, V. A., & Krylov, V. V. (2016). Influence of magnetic field on zebrafish activity and orientation in a plus maze. *Behavioural Processes*, **122**, 80–86.
- Painter, M. S., Dommer, D. H., Altizer, W. W., Muheim, R., & Phillips, J. B. (2013). Spontaneous magnetic orientation in larval drosophila shares properties with learned magnetic compass responses in adult flies and mice. *Journal of Experimental Biology*, **216**(7), 1307–1316.
- Pamme, N. (2006). Magnetism and microfluidics. *Lab on a Chip*, **6**(1), 24–38.
- Phillips, J. B. (1986). Two magnetoreception pathways in a migratory salamander. *Science*, **233**(4765), 765–767.
- Phillips, J. B. & Borland, S. C. (1992a). Behavioural evidence for use of a light-dependent magnetoreception mechanism by a vertebrate. *Nature*, **359**(6391), 142–144.
- Phillips, J. B. & Borland, S. C. (1992b). Magnetic compass orientation is eliminated under near-infrared light in the eastern red-spotted newt *Notophthalmus viridescens*. *Animal Behaviour*, **44**(4), 796–797.
- Phillips, J. B. & Sayeed, O. (1993). Wavelength-dependent effects of light on magnetic compass orientation in *Drosophila melanogaster*. *Journal of Comparative Physiology A*, **172**(3), 303–308.
- Putman, N. F., Lohmann, K. J., Putman, E. M., Quinn, T. P., Klimley, A. P., & Noakes, D. L. (2013). Evidence for geomagnetic imprinting as a homing mechanism in Pacific salmon. *Current Biology*, **23**(4), 312–316.
- Qin, S., Yin, H., Yang, C., Dou, Y., Liu, Z., Zhang, P., Yu, H., Huang, Y., Feng, J., Hao, J., et al. (2016). A magnetic protein biocompass. *Nature Materials*, **15**(2), 217–226.
- Quinn, T. P., Merrill, R. T., & Brannon, E. L. (1981). Magnetic field detection in sockeye salmon. *Journal of Experimental Zoology*, **217**(1), 137–142.

BIBLIOGRAPHY

- Randlett, O., Wee, C. L., Naumann, E. A., Nnaemeka, O., Schoppik, D., Fitzgerald, J. E., Portugues, R., Lacoste, A. M., Riegler, C., Engert, F., et al. (2015). Whole-brain activity mapping onto a zebrafish brain atlas. *Nature Methods*, **12**(11), 1039–1046.
- Rey, S., Boltana, S., Vargas, R., Roher, N., & MacKenzie, S. (2013). Combining animal personalities with transcriptomics resolves individual variation within a wild-type zebrafish population and identifies underpinning molecular differences in brain function. *Molecular Ecology*, **22**(24), 6100–6115.
- Ritz, T., Adem, S., & Schulten, K. (2000). A model for photoreceptor-based magnetoreception in birds. *Biophysical Journal*, **78**(2), 707 – 718.
- Ritz, T., Thalau, P., Phillips, J. B., Wiltschko, R., & Wiltschko, W. (2004). Resonance effects indicate a radical-pair mechanism for avian magnetic compass. *Nature*, **429**(6988), 177–180.
- Rosensweig, R. E. (2002). Heating magnetic fluid with alternating magnetic field. *Journal of magnetism and magnetic materials*, **252**, 370–374.
- Sackerman, J., Donegan, J. J., Cunningham, C. S., Nguyen, N. N., Lawless, K., Long, A., Benno, R. H., & Gould, G. G. (2010). Zebrafish behavior in novel environments: effects of acute exposure to anxiolytic compounds and choice of danio rerio line. *International journal of comparative psychology/ISCP; sponsored by the International Society for Comparative Psychology and the University of Calabria*, **23**(1), 43.
- Salas, C., Broglio, C., & Rodríguez, F. (2003). Evolution of forebrain and spatial cognition in vertebrates: conservation across diversity. *Brain, Behavior and Evolution*, **62**(2), 72–82.
- Scherer, C. & Figueiredo Neto, A. M. (2005). Ferrofluids: properties and applications. *Brazilian Journal of Physics*, **35**(3A), 718–727.
- Schleifer, K. H., Schüler, D., Spring, S., Weizenegger, M., Amann, R., Ludwig, W., & Köhler, M. (1991). The genus magnetospirillum gen. nov. description of magnetospirillum gryphiswaldense sp. nov. and transfer of aquaspirillum magnetotacticum to magnetospirillum magnetotacticum comb. nov. *Systematic and Applied Microbiology*, **14**(4), 379–385.
- Schüler, D. (2008). Genetics and cell biology of magnetosome formation in magnetotactic bacteria. *FEMS Microbiology Reviews*, **32**(4), 654–672.

BIBLIOGRAPHY

- Schüler, D., Uhl, R., & Bäuerlein, E. (1995). A simple light scattering method to assay magnetism in magnetospirillum gryphiswaldense. *FEMS Microbiology Letters*, **132**(1-2), 139–145.
- Schulten, K., Swenberg, C. E., & Weller, A. (1978). A biomagnetic sensory mechanism based on magnetic field modulated coherent electron spin motion. *Zeitschrift für Physikalische Chemie*, **111**(1), 1–5.
- Schwarze, S., Steenken, F., Thiele, N., Kobylkov, D., Lefeldt, N., Dreyer, D., Schneider, N.-L., & Mouritsen, H. (2016a). Migratory blackcaps can use their magnetic compass at 5 degrees inclination, but are completely random at 0 degrees inclination. *Scientific Reports*, **6**.
- Schwarze, S., Schneider, N.-L., Reichl, T., Dreyer, D., Lefeldt, N., Engels, S., Baker, N., Hore, P., & Mouritsen, H. (2016b). Weak broadband electromagnetic fields are more disruptive to magnetic compass orientation in a night-migratory songbird (*erithacus rubecula*) than strong narrow-band fields. *Frontiers in Behavioral Neuroscience*, **10**.
- Semm, P. (1983). Neurobiological investigations on the magnetic sensitivity of the pineal gland in rodents and pigeons. *Comparative Biochemistry and Physiology Part A: Physiology*, **76**(4), 683–689.
- Semm, P. & Beason, R. C. (1990). Responses to small magnetic variations by the trigeminal system of the bobolink. *Brain research bulletin*, **25**(5), 735–740.
- Shaw, J., Boyd, A., House, M., Woodward, R., Mathes, F., Cowin, G., Saunders, M., & Baer, B. (2015). Magnetic particle-mediated magnetoreception. *Journal of The Royal Society Interface*, **12**(110).
- Shcherbakov, D., Winklhofer, M., Petersen, N., Steidle, J., Hilbig, R., & Blum, M. (2005). Magnetosensation in zebrafish. *Current Biology*, **15**(5), R161–R162.
- Shcherbakov, D., Knörzer, A., Espenhahn, S., Hilbig, R., Haas, U., & Blum, M. (2013). Sensitivity differences in fish offer near-infrared vision as an adaptable evolutionary trait. *PLoS ONE*, **8**(5), 1–11.
- Shcherbakov, V. P. & Winklhofer, M. (1999). The osmotic magnetometer: a new model for magnetite-based magnetoreceptors in animals. *European Biophysics Journal*, **28**(5), 380–392.
- Siegel, A. C., Shevkopyas, S. S., Weibel, D. B., Bruzewicz, D. A., Martinez, A. W., & Whitesides, G. M. (2006). Cofabrication of electromagnets and microfluidic systems in poly (dimethylsiloxane). *Angewandte Chemie*, **118**(41), 7031–7036.

BIBLIOGRAPHY

- Skauli, K. S., Reitan, J. B., & Walther, B. T. (2000). Hatching in zebrafish (*danio rerio*) embryos exposed to a 50 hz magnetic field. *Bioelectromagnetics*, **21**(5), 407–410.
- Stanley, S. A., Gagner, J. E., Damanpour, S., Yoshida, M., Dordick, J. S., & Friedman, J. M. (2012). Radio-wave heating of iron oxide nanoparticles can regulate plasma glucose in mice. *Science*, **336**(6081), 604–608.
- Stanley, S. A., Sauer, J., Kane, R. S., Dordick, J. S., & Friedman, J. M. (2015). Remote regulation of glucose homeostasis in mice using genetically encoded nanoparticles. *Nature Medicine*, **21**(1), 92–98.
- Stewart, A., Cachat, J., Wong, K., Gaikwad, S., Gilder, T., DiLeo, J., Chang, K., Utterback, E., & Kalueff, A. V. (2010). Homebase behavior of zebrafish in novelty-based paradigms. *Behavioural Processes*, **85**(2), 198 – 203.
- Stewart, A., Cachat, J. M., Wong, K., Wu, N., Grossman, L., Suci, C., Goodspeed, J., Elegante, M. F., Bartels, B. K., Elkhayat, S. I., et al. (2011). Phenotyping of zebrafish homebase behaviors in novelty-based tests. *Zebrafish Neurobehavioral Protocols*, pages 143–155.
- Stewart, A. M., Gaikwad, S., Kyzar, E., & Kalueff, A. V. (2012). Understanding spatio-temporal strategies of adult zebrafish exploration in the open field test. *Brain Research*, **1451**, 44–52.
- Sun, C., Hassanisaber, H., Yu, R., Ma, S., Verbridge, S. S., & Lu, C. (2016). Paramagnetic structures within a microfluidic channel for enhanced immunomagnetic isolation and surface patterning of cells. *Scientific Reports*, **6**.
- Sun, L., Zborowski, M., Moore, L. R., & Chalmers, J. J. (1998). Continuous, flow-through immunomagnetic cell sorting in a quadrupole field. *Cytometry*, **33**(4), 469–475.
- Takebe, A., Furutani, T., Wada, T., Koinuma, M., Kubo, Y., Okano, K., & Okano, T. (2012). Zebrafish respond to the geomagnetic field by bimodal and group-dependent orientation. *Scientific Reports*, **2**, 727.
- Thalau, P., Ritz, T., Stapput, K., Wiltschko, R., & Wiltschko, W. (2005). Magnetic compass orientation of migratory birds in the presence of a 1.315 mhz oscillating field. *Naturwissenschaften*, **92**(2), 86–90.
- Thapa, D., Palkar, V., Kurup, M., & Malik, S. (2004). Properties of magnetite nanoparticles synthesized through a novel chemical route. *Materials Letters*, **58**(21), 2692–2694.

BIBLIOGRAPHY

- Treiber, C. D., Salzer, M. C., Riegler, J., Edelman, N., Sugar, C., Breuss, M., Pichler, P., Cadiou, H., Saunders, M., Lythgoe, M., et al. (2012). Clusters of iron-rich cells in the upper beak of pigeons are macrophages not magnetosensitive neurons. *Nature*, **484**(7394), 367–370.
- Uebe, R. & Schüler, D. (2016). Magnetosome biogenesis in magnetotactic bacteria. *Nature Reviews Microbiology*, **14**(10), 621–637.
- Vidal-Gadea, A., Ward, K., Beron, C., Ghorashian, N., Gokce, S., Russell, J., Truong, N., Parikh, A., Gadea, O., Ben-Yakar, A., & Pierce-Shimomura, J. (2015). Magnetosensitive neurons mediate geomagnetic orientation in *Caenorhabditis elegans*. *eLife*, **4**, e07493.
- Walcott, C., Gould, J. L., & Kirschvink, J. (1979). Pigeons have magnets. *Science*, **205**(4410), 1027–1029.
- Walker, M. M., Kirschvink, J. L., Chang, S.-B. R., & Dizon, A. E. (1984). A candidate magnetic sense organ in the yellowfin tuna, *thunnus albacares*. *Science*, **224**(4650), 751–753.
- Walker, M. M., Quinn, T. P., Kirschvink, J. L., & Groot, C. (1988). Production of single-domain magnetite throughout life by sockeye salmon, *oncorhynchus nerka*. *Journal of Experimental Biology*, **140**(1), 51–63.
- Walker, M. M., Diebel, C. E., Haugh, C. V., Pankhurst, P. M., Montgomery, J. C., & Green, C. R. (1997). Structure and function of the vertebrate magnetic sense. *Nature*, **390**(6658), 371–376.
- Wang, Y., Pan, Y., Parsons, S., Walker, M., & Zhang, S. (2007). Bats respond to polarity of a magnetic field. *Proceedings of the Royal Society of London B: Biological Sciences*, **274**(1627), 2901–2905.
- Ward, B. K., Tan, G. X., Roberts, D. C., Della Santina, C. C., Zee, D. S., & Carey, J. P. (2014). Strong static magnetic fields elicit swimming behaviors consistent with direct vestibular stimulation in adult zebrafish. *PloS one*, **9**(3), e92109.
- Wheeler, M. A., Smith, C. J., Ottolini, M., Barker, B. S., Purohit, A. M., Grippo, R. M., Gaykema, R. P., Spano, A. J., Beenhakker, M. P., Kucenas, S., et al. (2016). Genetically targeted magnetic control of the nervous system. *Nature Neuroscience*, **19**(5), 756–761.
- Wilson, C. A., High, S. K., McCluskey, B. M., Amores, A., Yan, Y.-l., Titus, T. A., Anderson, J. L., Batzel, P., Carvan, M. J., Schartl, M., et al. (2014). Wild sex in zebrafish: loss of the natural sex determinant in domesticated strains. *Genetics*, pages genetics–114.

BIBLIOGRAPHY

- Wiltschko, R. & Wiltschko, W. (2014). Sensing magnetic directions in birds: radical pair processes involving cryptochrome. *Biosensors*, **4**(3), 221–242.
- Wiltschko, R., Stapput, K., Bischof, H.-J., & Wiltschko, W. (2007a). Light-dependent magnetoreception in birds: increasing intensity of monochromatic light changes the nature of the response. *Frontiers in Zoology*, **4**(1), 1.
- Wiltschko, R., Stapput, K., Ritz, T., Thalau, P., & Wiltschko, W. (2007b). Magnetoreception in birds: different physical processes for two types of directional responses. *HFSP J*, **1**(1), 41–48.
- Wiltschko, R., Gehring, D., Denzau, S., Nießner, C., & Wiltschko, W. (2014). Magnetoreception in birds: II. behavioural experiments concerning the cryptochrome cycle. *Journal of Experimental Biology*, **217**(23), 4225–4228.
- Wiltschko, R., Thalau, P., Gehring, D., Nießner, C., Ritz, T., & Wiltschko, W. (2015). Magnetoreception in birds: the effect of radio-frequency fields. *Journal of The Royal Society Interface*, **12**(103), 20141103.
- Wiltschko, R., Ahmad, M., Nießner, C., Gehring, D., & Wiltschko, W. (2016). Light-dependent magnetoreception in birds: the crucial step occurs in the dark. *Journal of The Royal Society Interface*, **13**(118), 20151010.
- Wiltschko, W. (1978). Further analysis of the magnetic compass of migratory birds. In *Animal Migration, Navigation, and Homing*, pages 302–310. Springer.
- Wiltschko, W. & Wiltschko, R. (1972). Magnetic compass of european robins. *Science*, **176**(4030), 62–64.
- Wiltschko, W. & Wiltschko, R. (1996). Magnetic orientation in birds. *Journal of Experimental Biology*, **199**(1), 29–38.
- Wiltschko, W. & Wiltschko, R. (2001). Light-dependent magnetoreception in birds: the behaviour of european robins, *erithacus rubecula*, under monochromatic light of various wavelengths and intensities. *Journal of Experimental Biology*, **204**(19), 3295–3302.
- Wiltschko, W. & Wiltschko, R. (2005). Magnetic orientation and magnetoreception in birds and other animals. *Journal of Comparative Physiology A*, **191**(8), 675–693.
- Wiltschko, W., Munro, U., Ford, H., & Wiltschko, R. (1993). Red light disrupts magnetic orientation of migratory birds. *Nature*, **364**(6437), 525–527.

BIBLIOGRAPHY

- Wiltschko, W., Munro, U., Beason, R., Ford, H., & Wiltschko, R. (1994). A magnetic pulse leads to a temporary deflection in the orientation of migratory birds. *Cellular and Molecular Life Sciences*, **50**(7), 697–700.
- Wiltschko, W., Munro, U., Ford, H., & Wiltschko, R. (1998). Effect of a magnetic pulse on the orientation of silvereyes, *zosterops l. lateralis*, during spring migration. *Journal of Experimental Biology*, **201**(23), 3257–3261.
- Wiltschko, W., Möller, A., Gesson, M., Noll, C., & Wiltschko, R. (2004). Light-dependent magnetoreception in birds: analysis of the behaviour under red light after pre-exposure to red light. *Journal of Experimental Biology*, **207**(7), 1193–1202.
- Wiltschko, W., Freire, R., Munro, U., Ritz, T., Rogers, L., Thalau, P., & Wiltschko, R. (2007c). The magnetic compass of domestic chickens, *gallus gallus*. *Journal of Experimental Biology*, **210**(13), 2300–2310.
- Winklhofer, M. & Kirschvink, J. L. (2010). A quantitative assessment of torque-transducer models for magnetoreception. *Journal of The Royal Society Interface*, **7**(Suppl 2), S273–S289.
- Winklhofer, M. & Mouritsen, H. (2016). A magnetic protein compass? *bioRxiv*, page 094607.
- Winklhofer, M., Holtkamp-Rötzler, E., Hanzlik, M., Fleissner, G., & Petersen, N. (2001). Clusters of superparamagnetic magnetite particles in the upper-beak skin of homing pigeons. *European Journal of Mineralogy*, **13**(4), 659–669.
- Winklhofer, M., Dylida, E., Thalau, P., Wiltschko, W., & Wiltschko, R. (2013). Avian magnetic compass can be tuned to anomalously low magnetic intensities. *Proceedings of the Royal Society of London B: Biological Sciences*, **280**(1763), 20130853.
- Wittbrodt, J., Shima, A., & Scharl, M. (2002). Medaka—a model organism from the far east. *Nature Reviews Genetics*, **3**(1), 53–64.
- Wu, L.-Q. & Dickman, J. D. (2011). Magnetoreception in an avian brain in part mediated by inner ear lagena. *Current Biology*, **21**(5), 418–423.
- Xia, N., Hunt, T. P., Mayers, B. T., Alsberg, E., Whitesides, G. M., Westervelt, R. M., & Ingber, D. E. (2006). Combined microfluidic-micromagnetic separation of living cells in continuous flow. *Biomedical Microdevices*, **8**(4), 299–308.
- Yorke, E. D. (1979). A possible magnetic transducer in birds. *Journal of Theoretical Biology*, **77**(1), 101 – 105.

-
- Yoshii, T., Ahmad, M., & Helfrich-Förster, C. (2009). Cryptochrome mediates light-dependent magnetosensitivity of *Drosophila*'s circadian clock. *PLoS Biol*, **7**(4), 1–7.
- Zadicario, P., Avni, R., Zadicario, E., & Eilam, D. (2005). ‘looping’—an exploration mechanism in a dark open field. *Behavioural brain research*, **159**(1), 27–36.
- Zborowski, M. & Chalmers, J. J. (2011). Rare cell separation and analysis by magnetic sorting. *Analytical Chemistry*, **83**(21), 8050–8056. PMID: 21812408.
- Zborowski, M., Sun, L., Moore, L. R., Williams, P. S., & Chalmers, J. J. (1999). Continuous cell separation using novel magnetic quadrupole flow sorter. *Journal of Magnetism and Magnetic Materials*, **194**(1), 224–230.
- Zhou, R. & Wang, C. (2016). Microfluidic separation of magnetic particles with soft magnetic microstructures. *Microfluidics and Nanofluidics*, **20**(3), 1–11.



Acknowledgments

I would like to thank my supervisor, Prof. Gil Westmeyer, for this challenging and very exciting project. Thank you also to all the former and present members of the Westmeyer lab who have shared this unforgettable time with me. Some people deserve special mentioning, since my time as a PhD student would not have been the same without them.

Dr. Antonella Lauri, thank you for being such a great friend and mentor for me through this time, both scientifically and in life. The project would not have reached so far without you.

Sheryl Roberts, thank you for being a friend and fellow PhD student through the years. All your support, the hours in the library and all the discussions during dinners and coffee breaks have been really inspiring.

Dr. Michele Cappetta, thank you for being there to support me in my projects and in life.

Anja Stelzl, thank you for taking care, not only of the fish, but also all of everyone in the lab.

Felix Sigmund, thank you for your kindness during difficult times.

Dr. Stephan Eder, thank you for a great collaboration, both in the behavioral studies and in establishing the setups.

Prof. Michael Winklhofer, thank you for the valuable discussions and feedback on all of my projects.

Anne Gro Refsland, thank you for being a good friend, always ready to listen.

And finally, I would like to thank my dear family for always being there for me, even when I am far away.